Copy No. 120

~~RESTRICTED~~

RM No. A7H28

NACA RM No. A7H28

TECH LIBRARY KAFB, NM
0069286

NACA

RESEARCH MEMORANDUM

AN INVESTIGATION AT LOW SPEED OF A LARGE-SCALE TRIANGULAR WING OF ASPECT RATIO TWO.- II. THE EFFECT OF AIRFOIL SECTION MODIFICATIONS AND THE DETERMINATION OF THE WAKE DOWNWASH

By Adrien E. Anderson

Ames Aeronautical Laboratory
Moffett Field, Calif.

Declassified by Authority of LARC Security Classification Officer (SCO) letter dated June 16, 1983
Marvin T. Hammer

~~CLASSIFIED~~

This document contains classified information affecting the National Defense of the United States within the meaning of the Espionage Act, USC 50:31 and 32. Its transmission or the revelation of its contents in any manner to an unauthorized person is prohibited by law. Information so classified may be imparted only to persons in the military and naval services of the United States, appropriate civilian officers and employees of the Federal Government who have a legitimate interest therein, and to United States citizens of known loyalty and discretion who of necessity must be informed thereof.

AFMDC
TECHNICAL L
AFL 2811

NATIONAL ADVISORY COMMITTEE FOR AERONAUTICS

WASHINGTON

December 10, 1947

~~RESTRICTED~~

319.98/13

TECH LIBRARY KAFB, NM
0069286

NATIONAL ADVISORY COMMITTEE FOR AERONAUTICS

RESEARCH MEMORANDUM

AN INVESTIGATION AT LOW SPEED OF A LARGE-SCALE TRIANGULAR WING OF ASPECT RATIO TWO. – II. THE EFFECT OF AIRFOIL SECTION MODIFICATIONS AND THE DETERMINATION OF THE WAKE DOWNWASH

By Adrien E. Anderson

SUMMARY

This report extends the study of the characteristics of a large-scale triangular wing to include the effects of section modifications. The characteristics shown in part I of this investigation, NACA RM No. A7F06, are for a triangular wing having a symmetrical sharp-edged double-wedge airfoil section; whereas, those in the subject report are for a wing of identical plan form, but having various degrees of rounding of the wing leading edge and of the wing maximum thickness. In addition, data were obtained on the dynamic pressure and downwash angle at three stations aft of the wing trailing edge (0.48, 0.72, and 0.96 M.A.C.) in the extended chord plane of the wing. Photographs were obtained of the condensation trails resulting from vortices formed at the leading edge of the wing at high angles of attack.

In general it was found that the effects of rounding the airfoil section were small. Rounding the maximum thickness line resulted in negligible changes; rounding the leading edge to 0.0025 chord removed most of the breaks in the force and moment characteristics of the wing without flaps but otherwise showed small effect; additional rounding of the leading edge had no further effects.

The condensation trails indicated the presence of two vortices springing from the apex of the triangle and trailing downstream above the upper surface of the wing and inboard of the tips. These trails first appeared at about the angle of attack at which the breaks appeared in the force and moment characteristics, became shortened with increased angles of attack. and disappeared at maximum lift.

At low angles of attack there was an approximately linear variation of downwash angle with angle of attack (0.65). At higher

angles of attack the rate of change decreased with angle of attack and became negative prior to maximum lift. It was concluded that this serves to indicate a breakdown in normal flow and the establishment of partially separated flow conditions.

INTRODUCTION

A general study of triangular plan-form wings has been undertaken to determine their characteristics throughout as wide a Mach number and Reynolds number range as possible. The selection of a symmetrical double-wedge airfoil section made possible a theoretical analysis of the supersonic characteristics of the wing and thus allowed a choice of plan form and section which appeared good from the supersonic standpoint. It was recognized, however, that at both supersonic and subsonic speeds certain improvements might be expected as a result of rounding the leading edge and maximum thickness line.

Beyond this approach it was desired to determine the effect of airfoil section modifications on certain specific characteristics found during the earlier low-speed investigation. Reference 1 showed that at some lift coefficient, depending on the flap deflection and angle of sideslip, all of the wing characteristics underwent a marked change. This was believed to indicate the existence of a different type of flow over the wing at high and low lift coefficients.

During the subject investigation, therefore, it was desired to find, not only the effects of airfoil section modifications on the low-speed longitudinal characteristics of the wing, but to find more evidence of the two flow types. And in particular to determine the effects of nose radius and Reynolds number on the formation of the strongly separated type of flow and the accompanying change in force characteristics. Finally, it was desired to obtain some indication of the problems associated with the use of a tail as a longitudinal control for a triangular wing airplane, through a limited survey of the downwash and the dynamic pressure in the wing wake.

SYMBOLS AND COEFFICIENTS

The standard NACA coefficients and symbols used within this report are defined below and in figure 1:

A aspect ratio (b^2/S)

α free-stream angle of attack, degrees

α_T increment of angle of attack due to wind-tunnel wall interference, degrees

b wing span, feet

c wing chord, measured parallel to air stream, feet

$\bar{c}$ mean aerodynamic chord, measured parallel to air stream, feet

C wind-tunnel test-section area, normal to air stream, square feet

C_L lift coefficient (lift/qS)

C_D drag coefficient (drag/qS)

C_{D_T} increment of drag coefficient due to wind-tunnel-wall interference

C_m pitching-moment coefficient (pitching moment/$qS\bar{c}$)

ϵ downwash angle, degrees

ϵ_T increment of downwash angle due to wind-tunnel-wall interference, degrees

δ_f split-flap deflection, measured perpendicular to hinge line, degrees

δ_w wind-tunnel-wall-interference correction factor at position of wing

δ_t wind-tunnel-wall-interference correction factor at position of survey apparatus

ν kinematic viscosity, square feet per second

q dynamic pressure, pounds per square foot

q_w dynamic pressure in wake of wing, pounds per square foot

R Reynolds number $(V\bar{c}/\nu)$

S wing area, square feet

V free-stream velocity, feet per second

EQUIPMENT

The plan form of the wing was that of an isosceles triangle with an apex angle of 53.13°, which made the angle of sweepback of the leading edge 63.43° and the aspect ratio two. The basic wing design had a symmetrical double-wedge airfoil section with a maximum thickness of 5 percent at 20 percent chord.

The split flaps were of constant chord (16 percent of the M.A.C.) with the hinge line located parallel to the trailing edge of the wing. The span was terminated at the line of maximum airfoil section thickness (86 percent of the wing span) thus establishing a flap area equal to 18.5 percent of the wing area.

Figure 2 is a line drawing describing the general arrangement of the basic wing, while the modifications are shown in the photographs and sketches of figure 3. Part (a) of figure 3 shows the basic wing with the split flaps deflected. The rounded maximum thickness, part (b), consisted of an arc of sufficient radius to be tangent to the surface of the double-wedge section at 15 and 25 percent chord. Both the top and bottom surfaces of the wing were rounded. To this configuration was added a 0.0025c nose radius in the chordwise plane (part (c)). The resultant rounding reduced the wing chord, and hence reduced the wing area approximately 1.7 percent.

The partial-span sharp leading edges were simulated by placing dural caps over the 0.0025c nose radius so that the airfoil section varied from the original double-wedge section at the apex of the triangle to the 0.0025c radius nose at 25 percent of the span in one case and 50 percent in the other (fig. 3(d)).

The two large-radius leading edges were constructed by building up the front wedge rather than by cutting back on the wedge as was done in the case of the small nose radius. Hence the wing with the 1-percent nose radius in the chordwise plane and the 1.1-percent nose radius normal to the leading edge (part (e) of the figures) has the same wing area as the basic wing. For convenience in construction in these two cases the maximum thickness was not rounded; that is, the sharp double-wedge maximum thickness contour was restored to the wing profile.

The instrumentation used in making the downwash and dynamic-pressure surveys in the wake of the wing consisted of a survey rake comprising eight combined pitch, yaw, and pitot-static tubes. Details of a tube and the orientation of the rake are described in the line drawing figure 4, while figure 5 shows a close-up of the rake. It will be noted from figure 4 that the survey rake was mounted on an extension of the tail boom, hence, it pitched with the wing as the angle of attack varied.

TESTS

Force and moment data were obtained through the angle-of-attack range at zero angle of sideslip for the plain wing and the various split flap configurations. The force-test investigation was conducted at dynamic pressures between 5 and 40 pounds per square foot which corresponds to a Reynolds number range of approximately 6×10^6 to 19×10^6 as based on the mean aerodynamic chord. Downwash surveys were obtained at a dynamic pressure of 25 pounds per square foot for stations 0.48, 0.72, and 0.96 M.A.C. behind the trailing edge of the wing with symmetrical double-wedge airfoil section. An additional run was made at 15 pounds per square foot pressure with the survey apparatus in the middle position and with the split flaps deflected 22°.

RESULTS

The data are presented about the stability axes with their origin located at 50 percent of the root chord, which corresponds to the quarter-chord station of the mean aerodynamic chord of the basic plan form.

All of the force data have been corrected for air-stream inclination and for wind-tunnel-wall effect, the latter correction being that for a wing of the same span but with rectangular plan forms. The following corrections, based on the theory of reference 2 for a wind tunnel with oval cross section, were applied:

$$\alpha_T = \delta_w \frac{S}{C} \times 57.3 = 0.732\ C_L \qquad (1)$$

$$C_{D_T} = \delta_w \frac{S}{C} C_L^2 = 0.01277\ C_L^2 \qquad (2)$$

where

$$\delta_w = 0.1167$$

and

$$C = 2856 \text{ square feet}$$

Consideration of the forces acting on the tail boom indicated that its tare effect would be negligible. Drag and pitching-moment tares resulting from strut interference, based on tares obtained with a rectangular wing, were applied to the data. Any alterations to the plan-form area except changes in moment centers were also taken into account in computing the coefficients.

Corrections were applied to the downwash data for wind-tunnel-wall effect. Equation (1) above was used to correct the angle of attack, C_L being based on the values obtained from the force tests of the wing. In the same manner the downwash angle ϵ was corrected by the following equation:

$$\epsilon_T = \delta_t \frac{S}{C} C_L \times 57.3 \qquad (3)$$

This correction varied with the three different positions behind the wing as follows:

M.A.C.'s behind trailing edge of wing	δ_t	ϵ_T
0.48	0.1658	1.040 C_L
.72	.1853	1.162 C_L
.96	.2022	1.268 C_L

The values of ϵ were adjusted to go through zero at zero angle of attack ($C_L = 0$) to account for a slight misalinement of the directional pitot tubes. For the case with the flaps deflected the corresponding increment of ϵ from the flap zero run at $\alpha = 0^\circ$ was applied to the values of ϵ.

The value of free-stream dynamic pressure used in the wake survey investigation was based on a survey (without the presence of the wing) of that portion of the test section occupied by the survey rake.

The basic results of the investigation of the effect of airfoil section modification are presented in figures 6 to 15 and are summarized in figures 16 to 18; figure 19 is concerned with the visual study of vortices on the wing, while figures 20 to 22 are concerned with the downwash data. Table I, a summary of the configurations investigated, should also serve as an index to the figures containing the basic results.

DISCUSSION

Effects of Airfoil Section Modifications

Negligible changes in the force characteristics of the wing were measured following modification of the wing to have a rounded maximum thickness line. Comparison of figure 6 (characteristics of the basic wing reproduced from reference 1) with figure 7 shows that the only discernible effect was a slight reduction in the abruptness of the force break with the flaps undeflected. It was concluded, therefore, that the maximum thickness rounding was not an important parameter from the standpoint of low-speed force characteristics and no further investigation of its effects was made.

The effects on the longitudinal-force characteristics of rounding the section leading edge to a radius equal to 0.0025 of the local streamwise chord are shown through comparison of figures 6 and 8. This modification produced a small change in the force characteristics. However, the change in the moment characteristics of the wing was appreciable at lift coefficients greater than that for which the breaks appeared in the basic wing characteristics. The magnitude of the break was reduced, resulting in almost complete elimination for the flap undeflected case, and it appeared at slightly lower values of lift coefficient. Further, the stability of the wing as measured by dC_m/dC_L showed less variation through the lift range than was found with the sharp leading edge installed. With the flaps undeflected this parameter varied from −0.12 to −0.09 for the sharp-edged wing; whereas with the round leading edge the variation was only from −0.14 to −0.12 for the same C_L range.

This change in aerodynamic characteristics brought about by the change in nose radius supported the conjecture that the break in the force curves was related to a change in the type of flow over the wing possibly induced by a sudden increase in the separation of the flow around the leading edge. It was believed that if this were true and in view of the fact that Reynolds number as well as nose radius affects the force characteristics of unswept wings in which separated flow exists (reference 3), a variation in Reynolds number should have a powerful effect on the force characteristics. Hence data were obtained throughout the Reynolds number range for which it was possible, structurally, to cover a lift-coefficient range including the break. However, as is shown by figure 9 a threefold variation in the Reynolds number of test had no appreciable or systematic effect on the force or moment characteristics.

To determine to what spanwise extent the leading edge must be rounded, tests were made with the leading edge rounded over portions of the span. (See description under equipment.) Figures 10 and 11 show that as the sharpness was progressively restored across the span, the wing characteristics reverted to those of the wholly sharp-edged wing. It can be inferred from this that the breaks in

the force characteristics result from the flow conditions at the root sections of the wing and that the installation of a fuselage will have a great effect on wing characteristics. A summary of the effects of these modifications on the wing pitching moment is given in figure 16.

Since a small nose radius produced some change in the force and moment characteristics, it was felt that a larger nose radius would produce further change. The leading edge of the subject wing was thus modified to have a 0.010c radius in the streamwise direction and then a 0.011c radius normal to the leading edge. The results of these modifications are shown in figures 12, 13, 14, and 15. Their effect on the pitching-moment and force characteristics is summarized in figures 17 and 18. These data show that the very large amount of leading-edge roundness produced no greater effect than the smallest on pitching-moment characteristics and that, as before, a threefold change in Reynolds number had no significant effect on the wing characteristics. It is noteworthy that, although there was no significant reduction in $C_{L_{max}}$, there was a reduction in the drag due to lift as the nose radius was increased. These results would seem to indicate, therefore, that the large amounts of rounding did not produce a marked change in the flow around the leading edge. It is possible however, that the lack of further effect of leading-edge rounding may be due to the very thin airfoil section.

Visible Trailing Vortices

During the investigation of the wing with the sharp leading edge, condensation trails appeared revealing the presence of two vortices originating at the apex of the triangle and extending downstream above the upper surface of the wing and inboard of the tips.

Figure 19(a) is a sketch showing the orientation of the vortices, while parts (b) and (c) are photographs of the vortices. They first became visible at angles of attack slightly above that at which the breaks in the force and moment characteristics appeared. The trails then decreased in length with increasing angle of attack until they disappeared at the angle for maximum lift. It was noted that, as they shortened, the trails appeared to maintain the same direction of flow over the upper surface of the wing when considered in plan view and an angle approximately equal to one-third the angle of attack above the surface when viewed from the side.

No condensation trails were ever noted at the lower angles of attack, although rather humid atmospheric conditions existed during some of the tests. In contrast, condensation trails were always

noted at the higher angles of attack even when the tunnel had been running for several hours with consequent unfavorable air conditions for the formation of condensation trails. With the flaps deflected these trails also appeared but their initial appearance was so indefinite that it could not be determined whether they appeared at an earlier or later angle of attack than that for the case of the plain wing, that is, as to whether their appearance was a function of angle of attack or circulation. No evidence of the existence of these trails was seen with the rounded leading edges. However, it was not known to what extent this was a function of atmospheric conditions.

A possible reason for the existence of the vortices over the wing may be seen from an analysis of the type of flow around a triangular wing. According to the theory of reference 4 the components of flow in planes normal to the axis of symmetry of a low-aspect-ratio wing can be considered two-dimensional. However, in accounting for the type of flow over the actual wing, certain variations to this theory are believed to exist. The two-dimensional flow about the section is altered, according to Messrs. Wilson and Lovell (reference 5) to the form shown in figure 19(d) because of the boundary-layer separation around the sharp leading edge. When the longitudinal component of velocity is added to the transverse components, the trailing vortices result. (See fig. 19(e).)

As previously stated, no condensation trails were ever noticed at the lower angles of attack. This lack of trails does not necessarily indicate the nonexistence of the two vortices, but rather that they were much weaker and of a much more limited extent than at the higher angles of attack.

Furthermore, the over-all flow pattern is not believed to be the same throughout the angle-of-attack range. At the low angles of attack, the flow pattern is characterized by laminar separation at the leading edge followed by transition to turbulent flow which reattaches to the surface; whereas at higher angles the separation is of such intensity and extent that the flow reattachment did not occur over part of the wing. This failure of the separated flow at the leading edge to reattach to the wing could account for the force and moment curve breaks and the change in the variation of force and moments above the break. At present these theories concerning the flow phenomenon lack experimental verification.

Surveys in Extended Chord Plane

Downwash angle and total-head surveys were made at three positions in the extended chord plane -0.48, 0.72, and 0.96 M.A.C. aft of the wing trailing edge. The results are presented in figures 20 and 21 and the downwash angle measurement summarized in figure 22.

An almost linear variation of downwash angle with angle of attack was found to exist up to angles of attack from 14° to 16°. The slope of the linear portion of these curves is summarized in figure 22 where it can be seen that for almost all of the longitudinal and spanwise stations, the value of $d\epsilon/d\alpha$ lay between 0.6 and 0.7. For a wing of aspect ratio two, Prandtl's wing theory would give a value of 1.00 for $d\epsilon/d\alpha$.

Above angles of attack of 14° to 16° it was found that the value of $d\epsilon/d\alpha$ decreased rapidly and, before $C_{L_{max}}$ was reached, became negative. It was also found that, above 16° angle of attack, the total head returned to and remained close to the value for free-stream total head, while the downwash angle began to decrease. In the case of a rectangular wing it would be expected that the downwash angle would increase up to the stall. The fact that both the downwash angle and the total head change at approximately the same angle of attack and, in this case, at an angle of attack considerably below that for $C_{L_{max}}$ is indicative of a breakdown in the normal flow pattern. It would also appear that these results concur with the force tests wherein breaks appear in the force and moment curves at approximately 16° angle of attack. If this is so then the flow at higher angles of attack may be partially separated as noted under the discussion of the condensation trails. It becomes pertinent, therefore, to question the possibility of obtaining acceptable flight characteristics where such flow exists to any extent. Further research into this problem is indicated to determine whether the characteristics of low-aspect-ratio wings at high lift coefficients warrant further study or are of academic interest only.

CONCLUSIONS

From the results of the investigations reported herein the following observations can be made:

1. Rounding the maximum thickness line of the double-wedge section had no significant effect on wing characteristics.

2. Rounding the wing leading edge to a value of 0.0025 of the local chord removed the breaks in the force curves with flaps undeflected but not with flaps deflected.

3. Restoring the leading-edge sharpness at the wing root resulted in restoring the breaks in the force curves.

4. Increasing the leading-edge radius from 0.0025 to 0.011 of the local chord had no significant effect.

5. At points 0.48, 0.72, and 0.96 M.A.C. behind the wing trailing edge, the rate of change of downwash with angle of attack was about 0.65 at low lift coefficients.

6. The change in downwash angle with angle of attack at high lift coefficients below $C_{L_{max}}$ indicates a breakdown in the normal flow pattern.

Ames Aeronautical Laboratory,
National Advisory Committee for Aeronautics,
Moffett Field, Calif.

REFERENCES

1. Anderson, Adrien E.: An Investigation at Low Speed of a Large-Scale Triangular Wing of Aspect Ratio Two. – I. Characteristics of a Wing Having a Symmetrical Double-Wedge Airfoil Section With Maximum Thickness at 20-Percent Chord. NACA RRM No. A7F06, 1946.

2. Tani, Itiro, Sanuki, Matao: The Wall Interference of a Wind Tunnel of Elliptic Cross Section. NACA TM No. 1075, 1944.

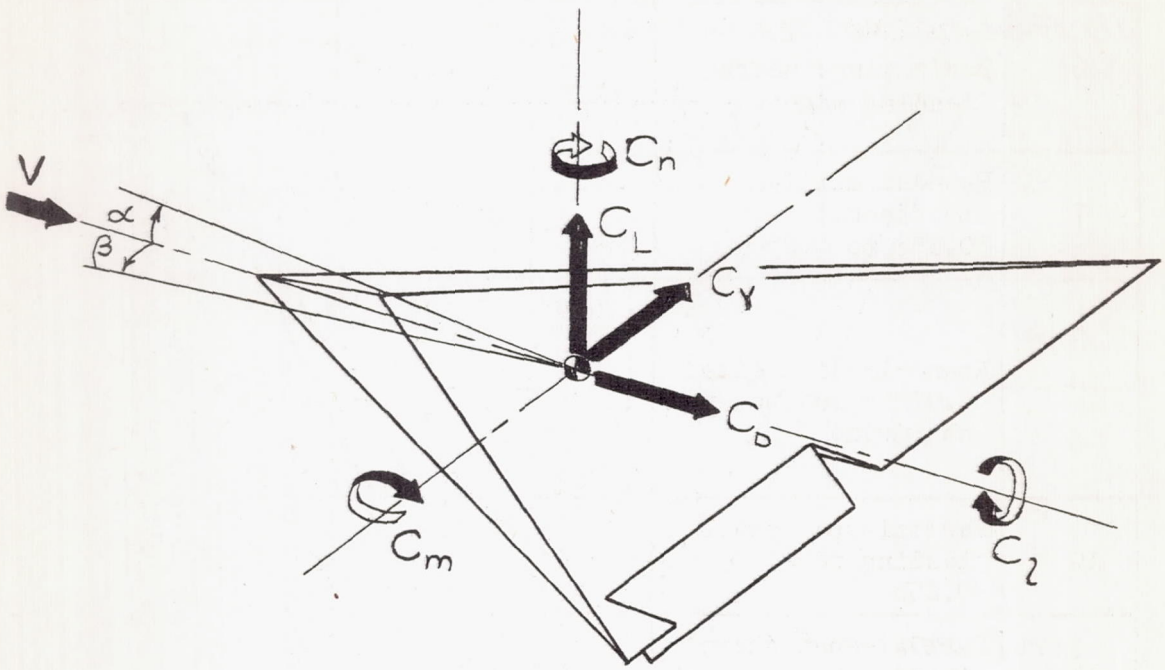
3. Jacobs, Eastman N., and Sherman, Albert: Airfoil Section Characteristics as Affected by Variations of the Reynolds Number. NACA TR No. 586, 1936.

4. Jones, Robert T.: Properties of Low-Aspect-Ratio Pointed Wings at Speeds Below and Above the Speed of Sound. NACA TN No. 1032, 1946.

5. Wilson, Herbert A., Jr., and Lovell, J. Calvin: Full-Scale Investigation of the Maximum Lift and Flow Characteristics of An Airplane Having Approximately Triangular Plan Form. NACA RRM No. L6K20, 1946.

TABLE I.- SUMMARY OF CONFIGURATIONS INVESTIGATED

Figure	Configuration	Split flaps	Reynolds number	Data Presented
6	Basic wing: sharp leading edge	-22.0° 0.0° 22.0° 44.5°	15.4×10^6	C_L vs α C_D C_m
7	Rounded maximum thickness: 0.15c to 0.25c	0.0° 22.0° 44.5°	14.0×10^6	
8	Round leading edge: 0.0025c radius chordwise	0.0° 22.0° 44.5°	14.6×10^6	
9		0.0°	6.8×10^6 to 19.0×10^6	
10	Partial-span sharp leading edge: 0.25b	0.0°	9.3×10^6 to 18.3×10^6	
11	Partial-span sharp leading edge: 0.50b	0.0°	14.7×10^6	
12	Round leading edge: 0.010c radius chordwise	0.0° 22.0° 44.5°	14.5×10^6	
13		0.0°	6.2×10^6 to 17.6×10^6	
14	Round leading edge: 0.011c radius normal to leading edge	-22.0° 0.0° 22.0° 44.5°	14.6×10^6	
15		0.0°	6.3×10^6 to 17.7×10^6	
20	Downwash survey behind wing	0.0° 22.0°		ϵ vs α
21				q_w/q vs α



NATIONAL ADVISORY
COMMITTEE FOR AERONAUTICS

FIGURE 1. - SIGN CONVENTION FOR THE STANDARD NACA COEFFICIENTS. ALL FORCES, MOMENTS, ANGLES, AND CONTROL SURFACE DEFLECTION ARE SHOWN AS POSITIVE.

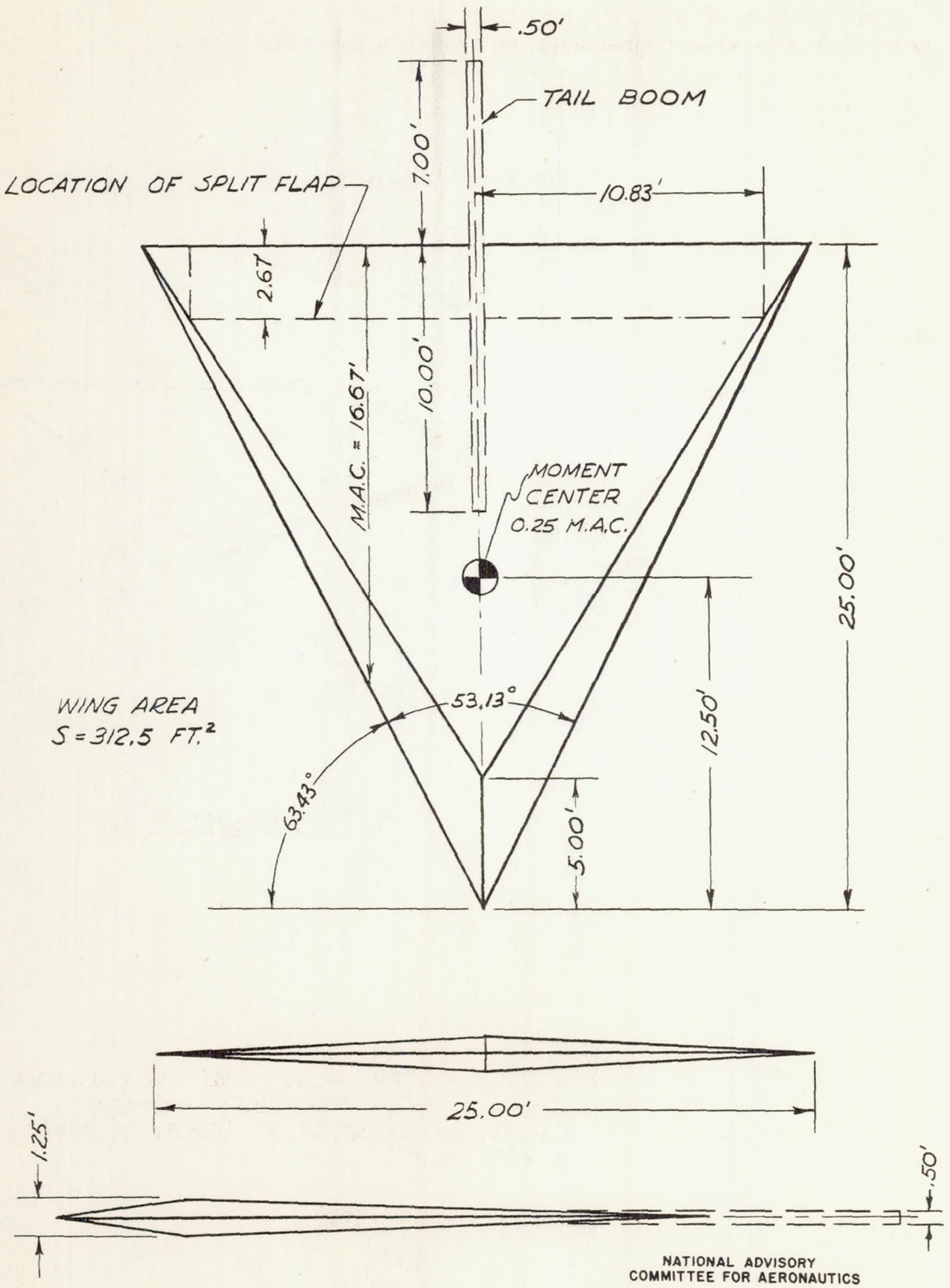
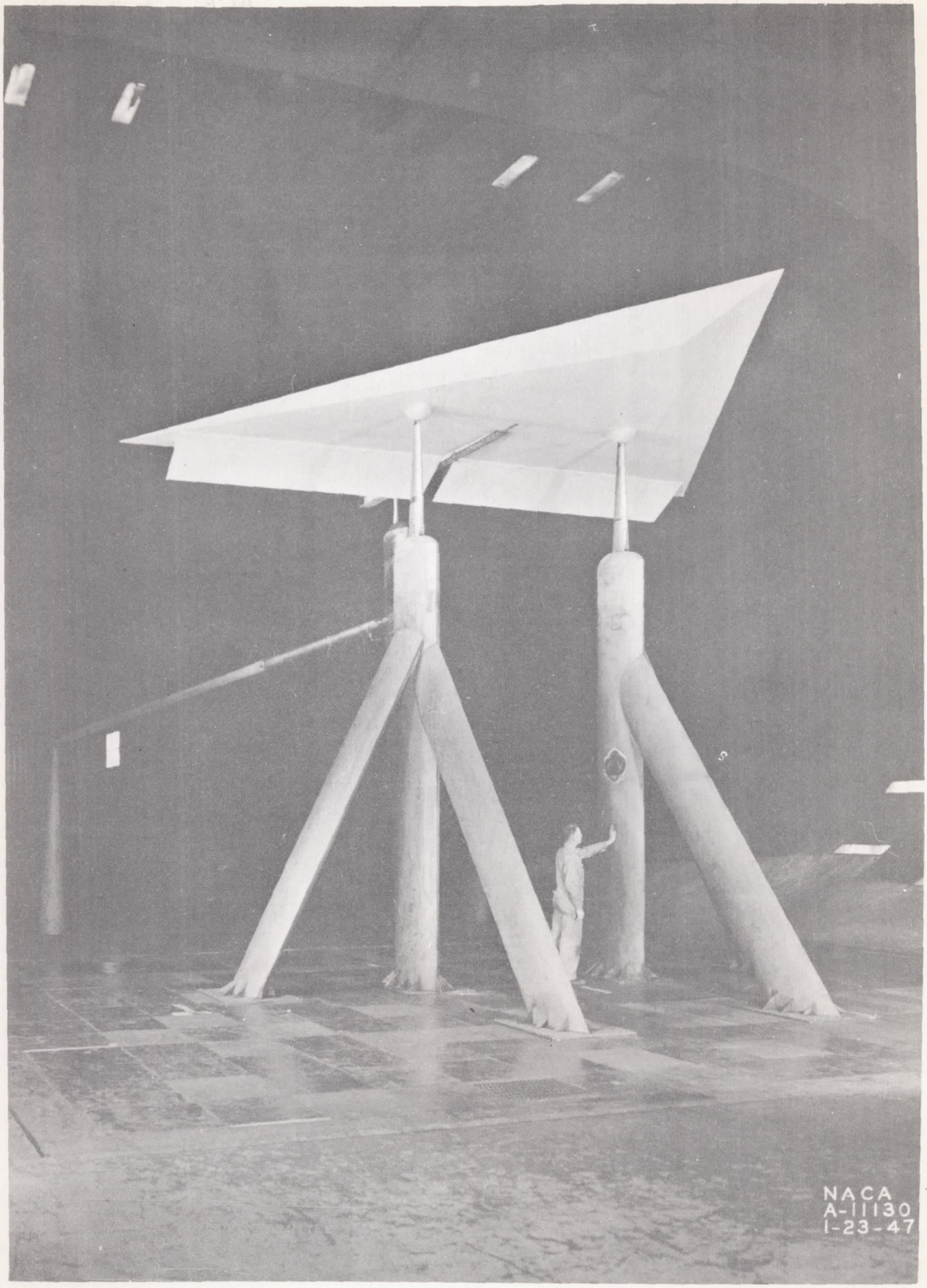
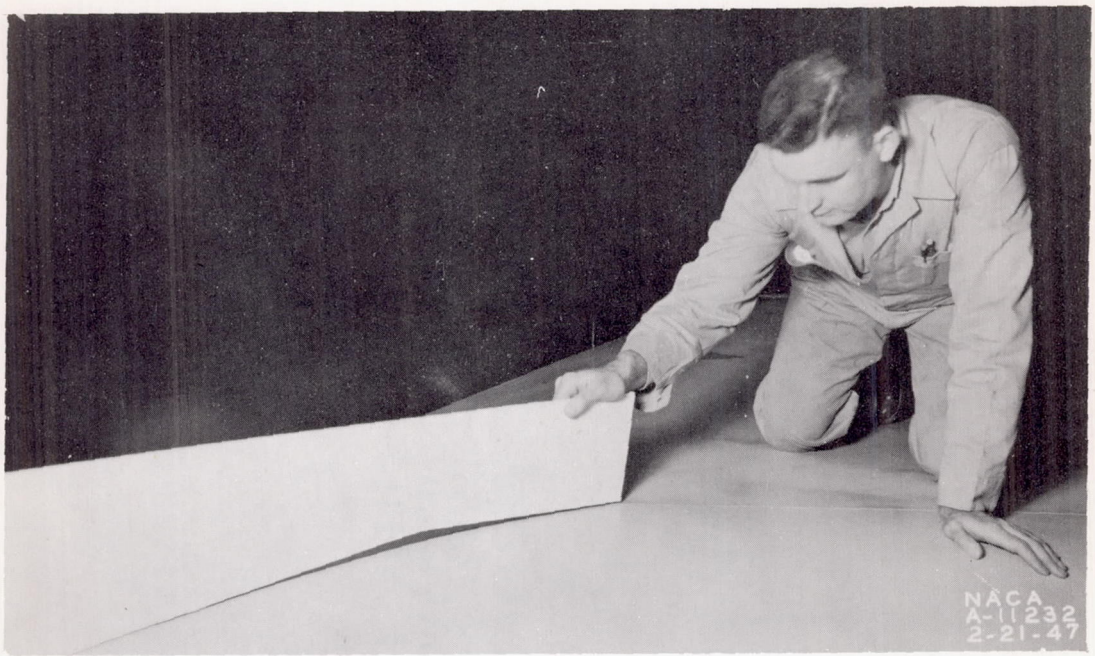


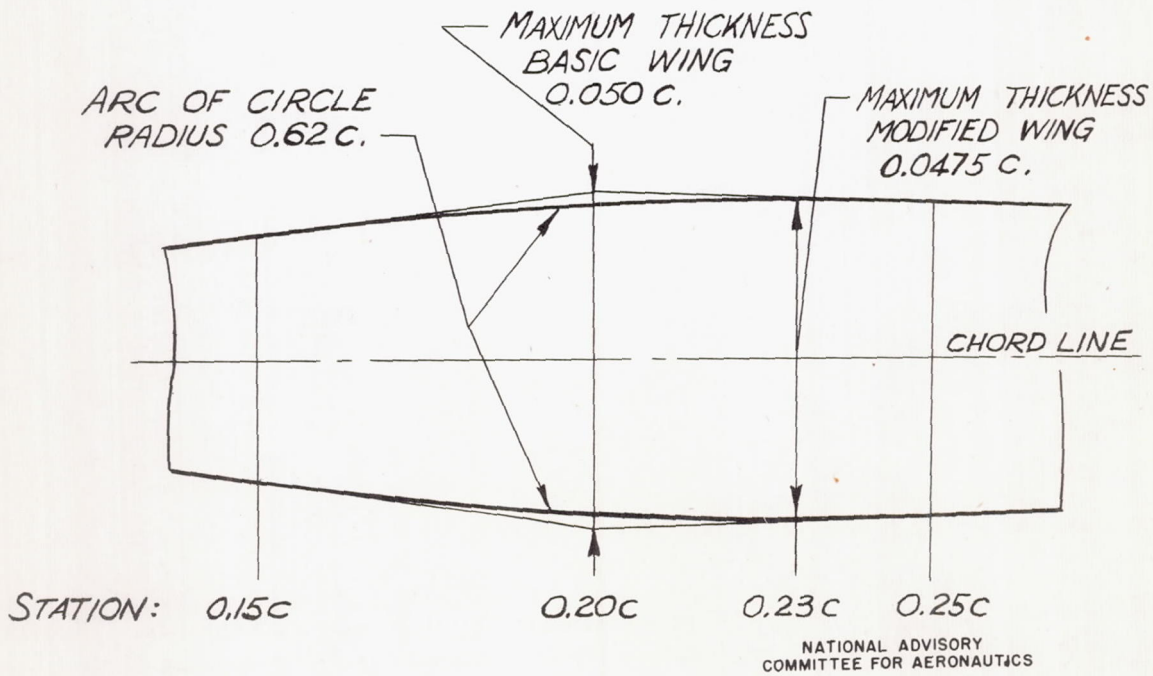
FIGURE 2.- GENERAL ARRANGEMENT OF BASIC WING DESIGN.



(a) Basic wing with split flaps deflected 29.5°.

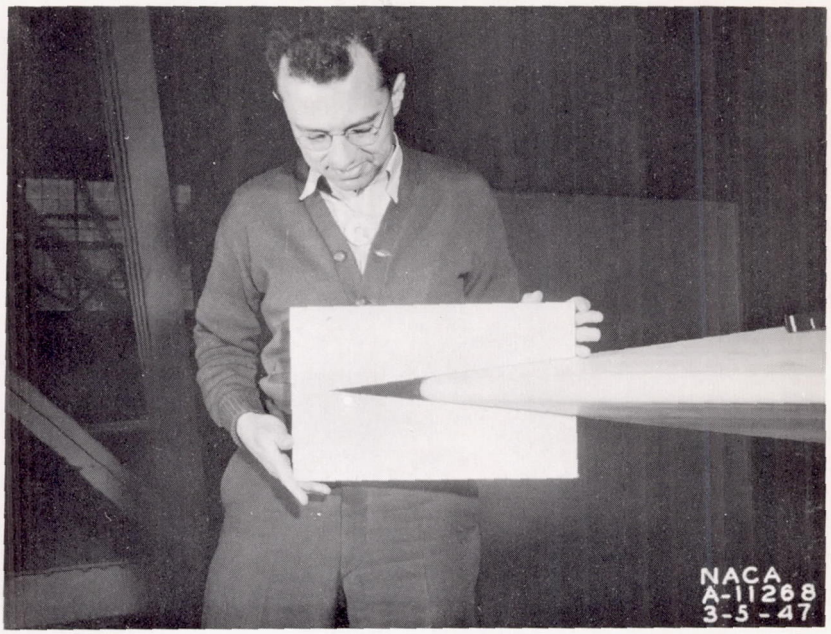
Figure 3.- Modifications to the airfoil section.

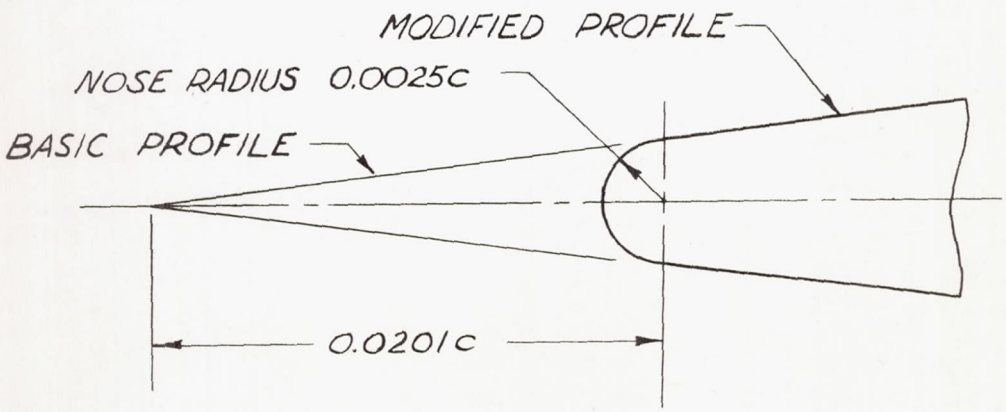




(b) THE ROUNDING OF THE MAXIMUM THICKNESS

FIGURE 3 - CONTINUED.

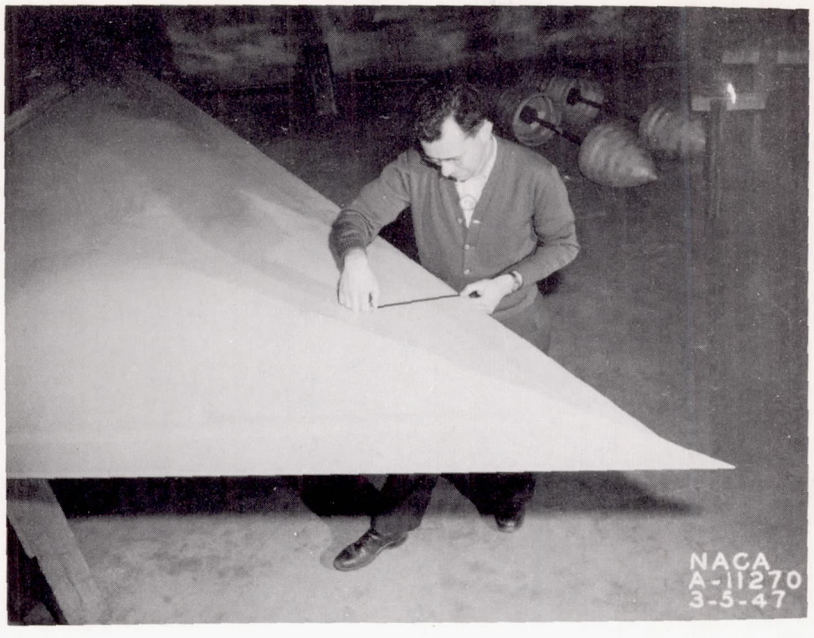


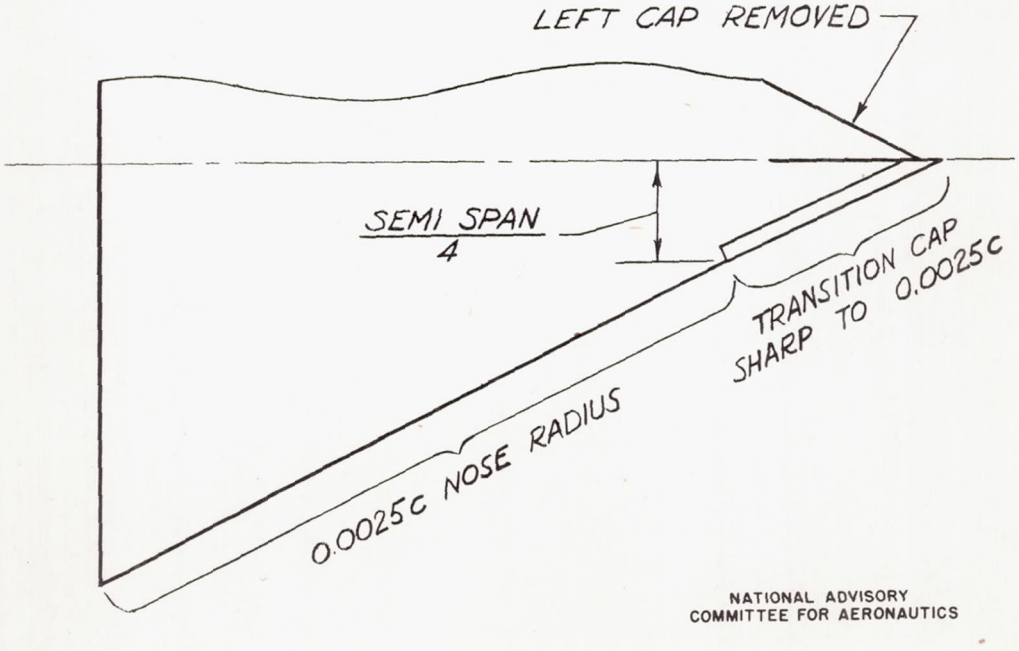


NATIONAL ADVISORY
COMMITTEE FOR AERONAUTICS

(c) THE 0.0025 CHORD ROUNDING OF THE NOSE.

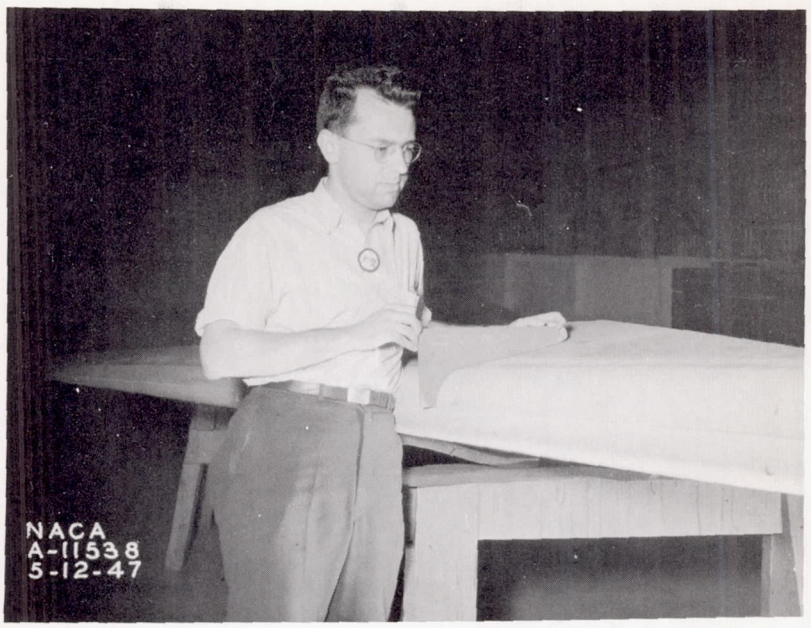
FIGURE 3.- CONTINUED.

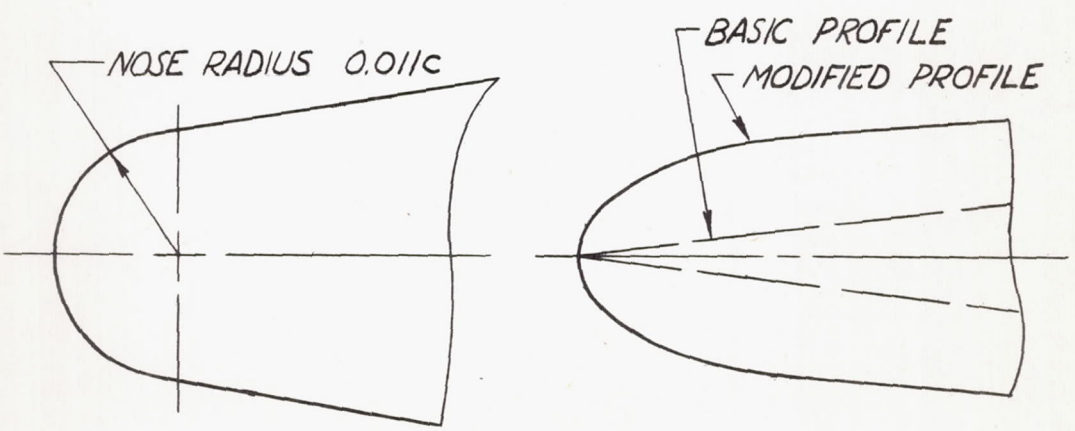




(d) THE APEX OF THE WING WITH THE LEFT HALF OF THE 25-PERCENT SPAN TRANSITION LEADING-EDGE CAP REMOVED.

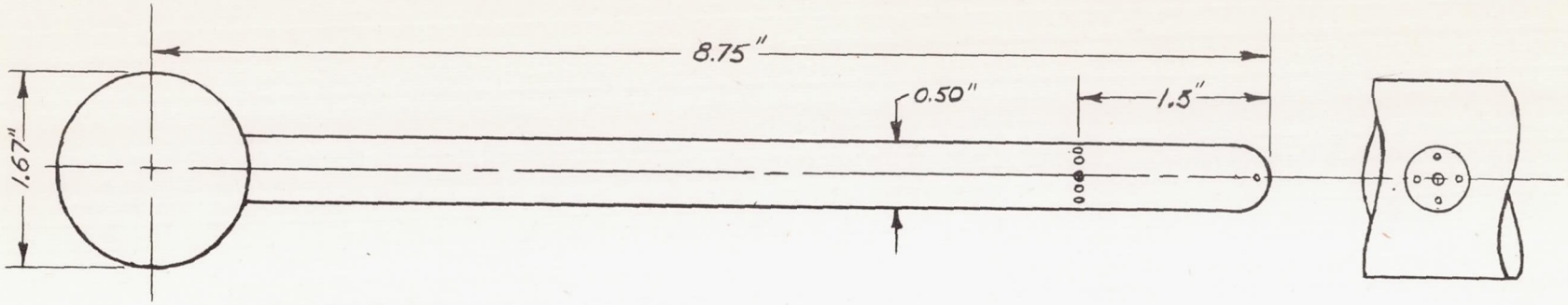
FIGURE 3.- CONTINUED.



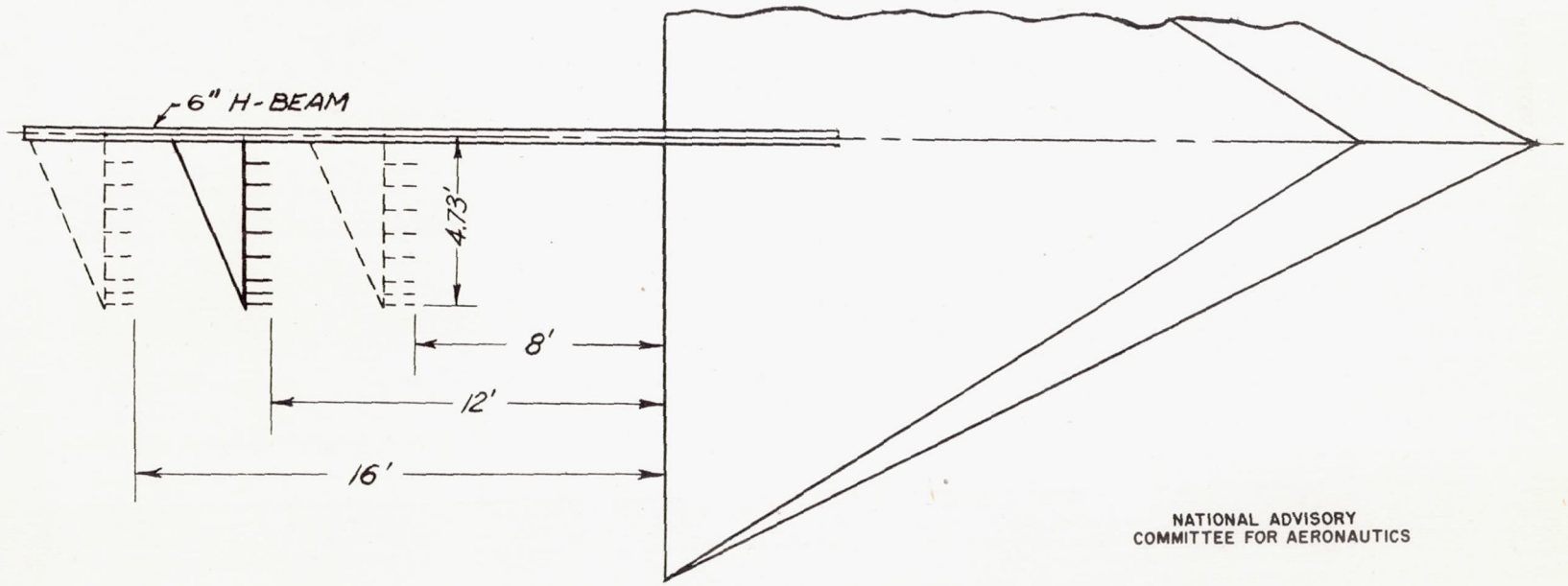


(e) THE 0.011c RADIUS NOSE NORMAL TO LEADING EDGE.

FIGURE 3. - CONCLUDED.



(a) COMBINED PITCH, YAW, AND PITOT-STATIC TUBE



(b) LOCATION OF SURVEY RAKE BEHIND WING.

FIGURE 4.- INSTRUMENTATION USED IN MAKING THE DYNAMIC-PRESSURE AND THE DOWNWASH SURVEYS.

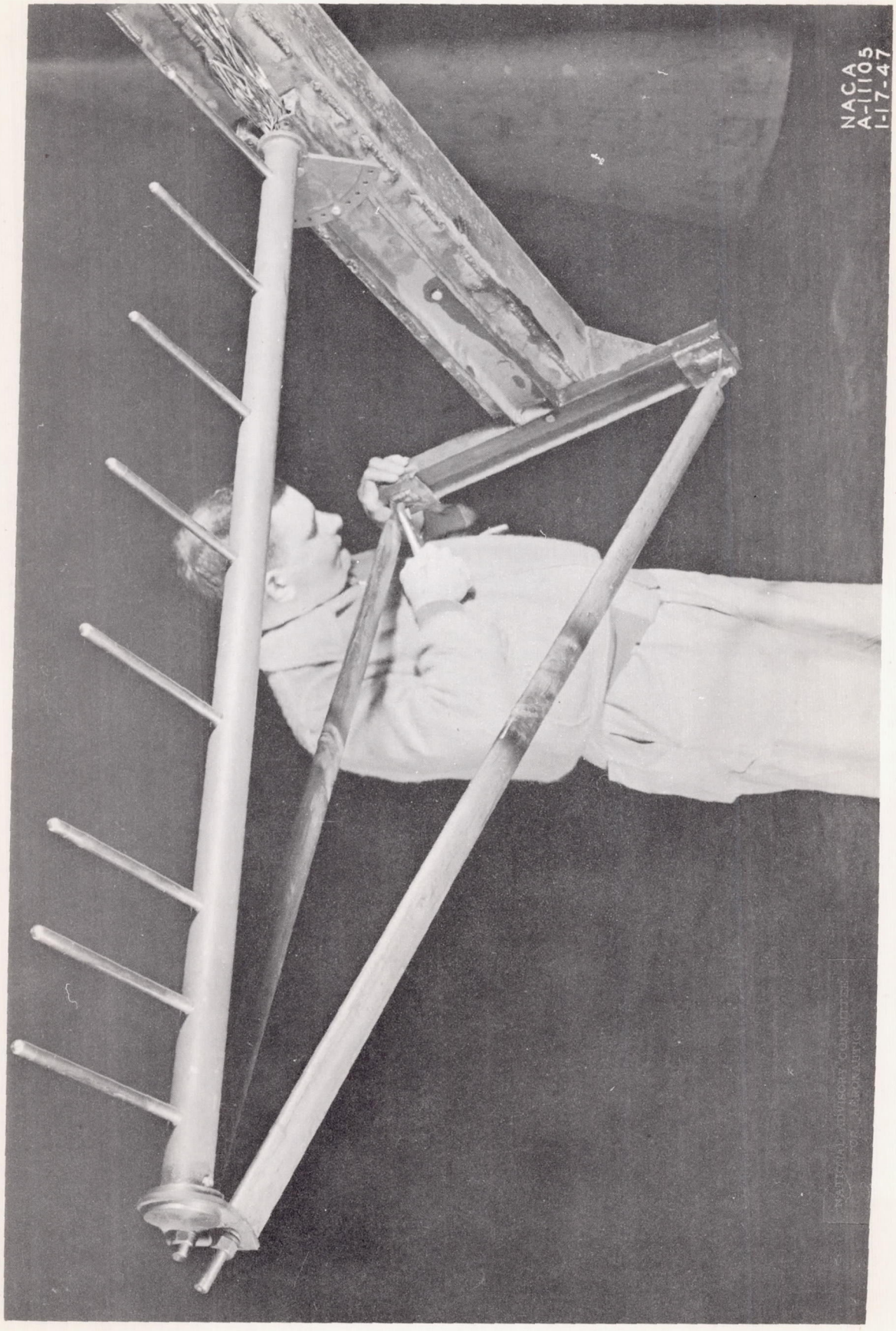
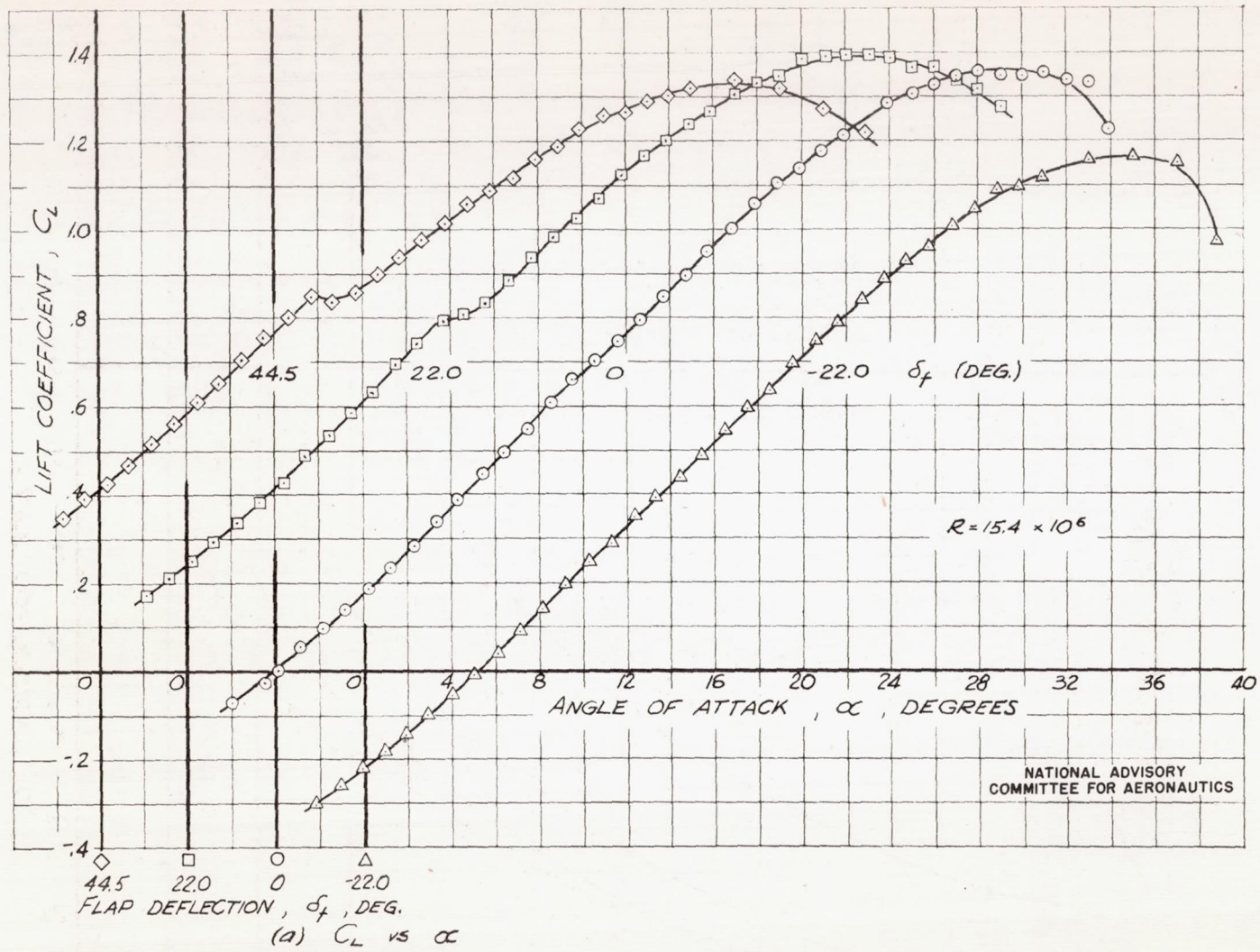
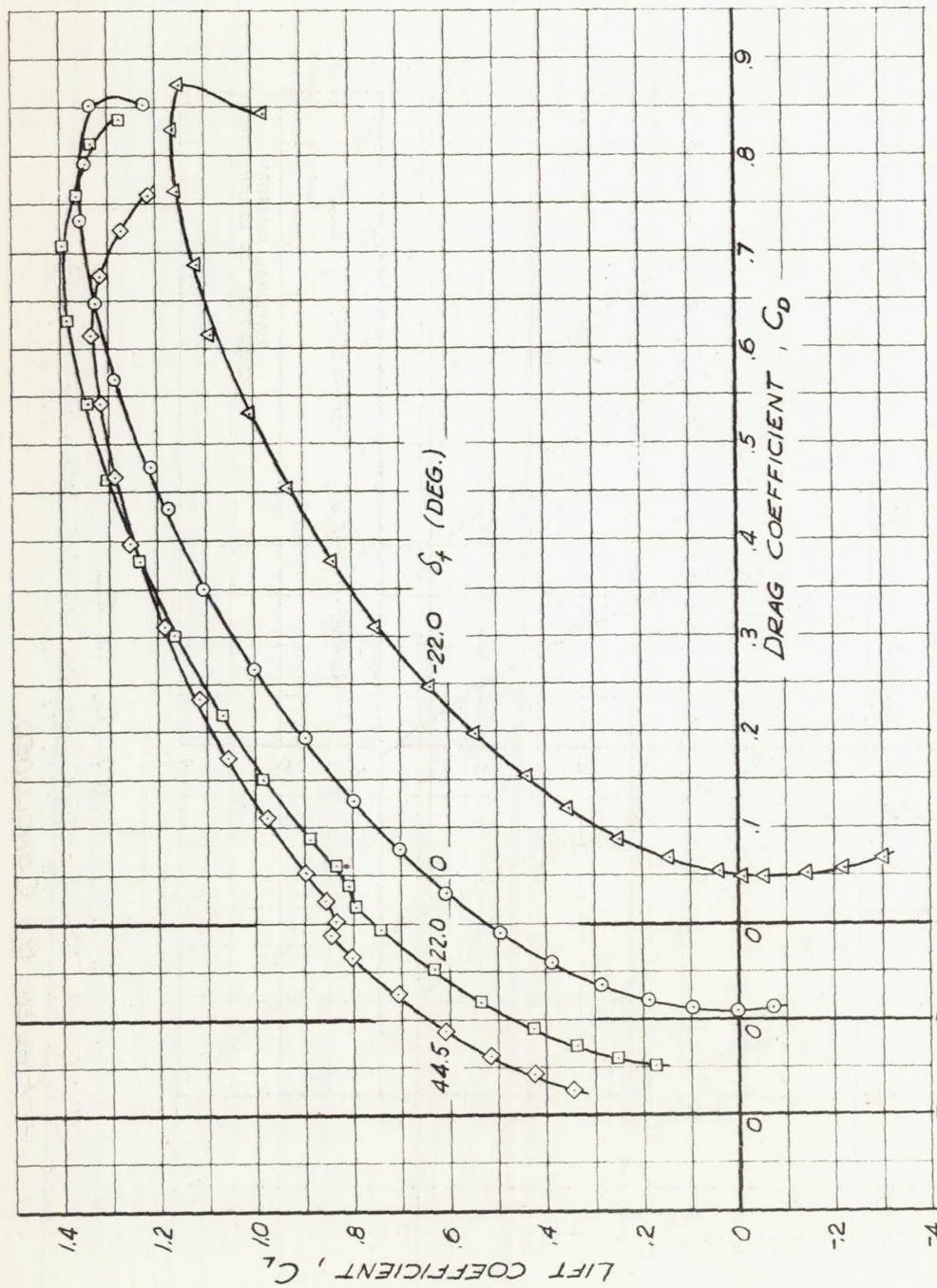


Figure 5.- Survey rake used in dynamic pressure and downwash surveys.



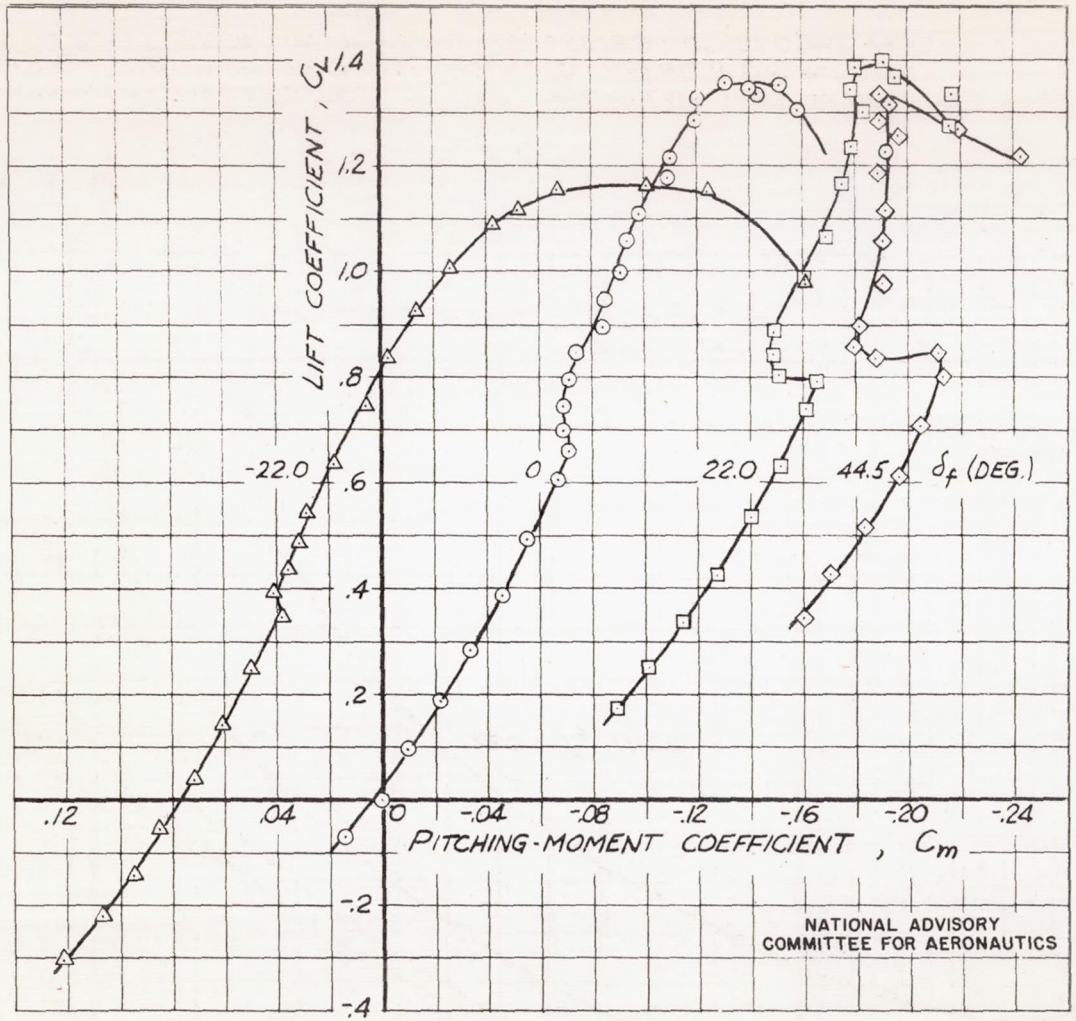
(a) C_L vs α

FIGURE 6.- AERODYNAMIC CHARACTERISTICS OF THE TRIANGULAR WING WITH SYMMETRICAL DOUBLE-WEDGE AIRFOIL SECTION AND WITH 18.5-PERCENT AREA SPLIT FLAPS DEFLECTED -22.0°, 0°, 22.0° AND 44.5°. DATA FROM REFERENCE 1.



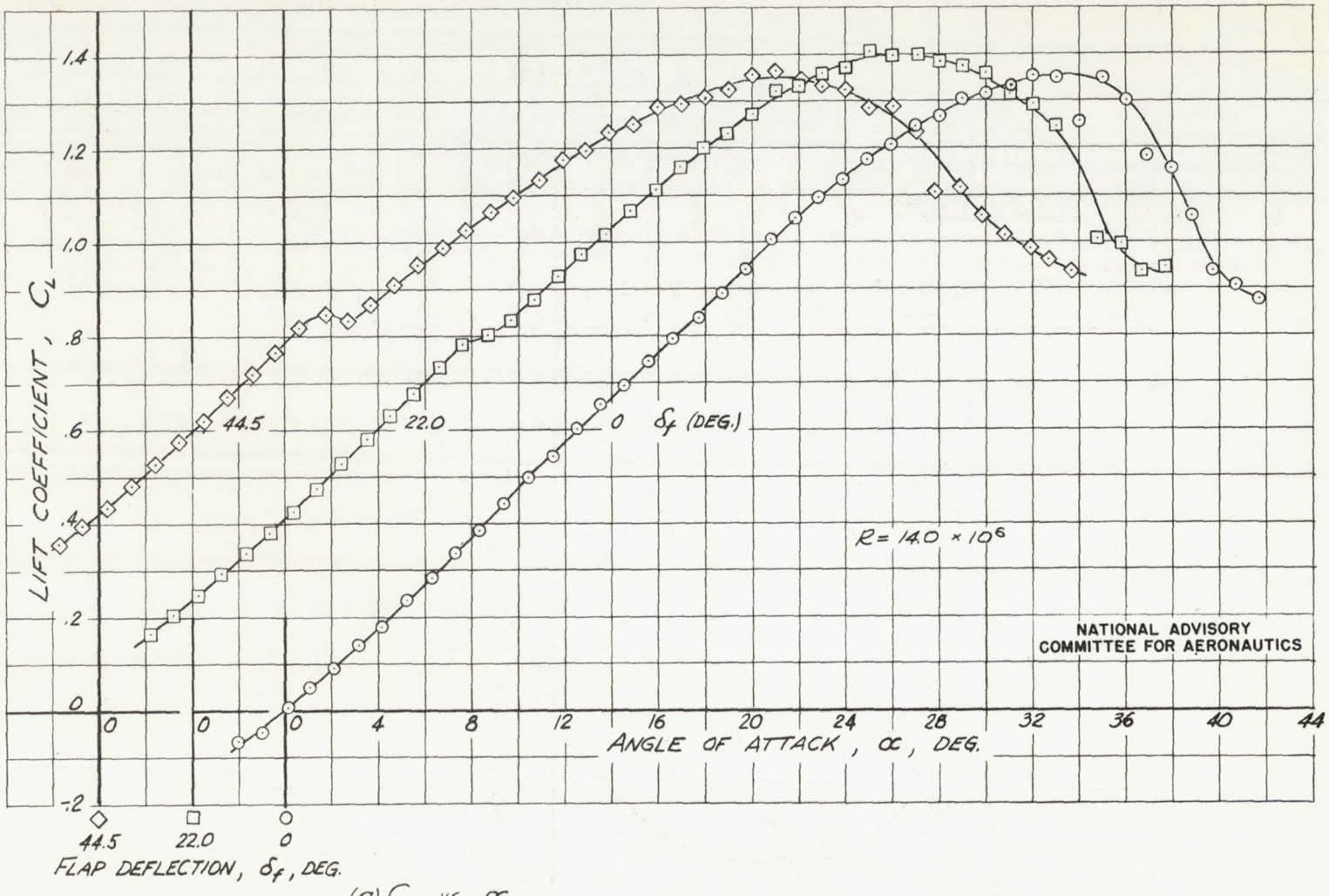
(b) C_L vs C_D

FIGURE 6.- CONTINUED.



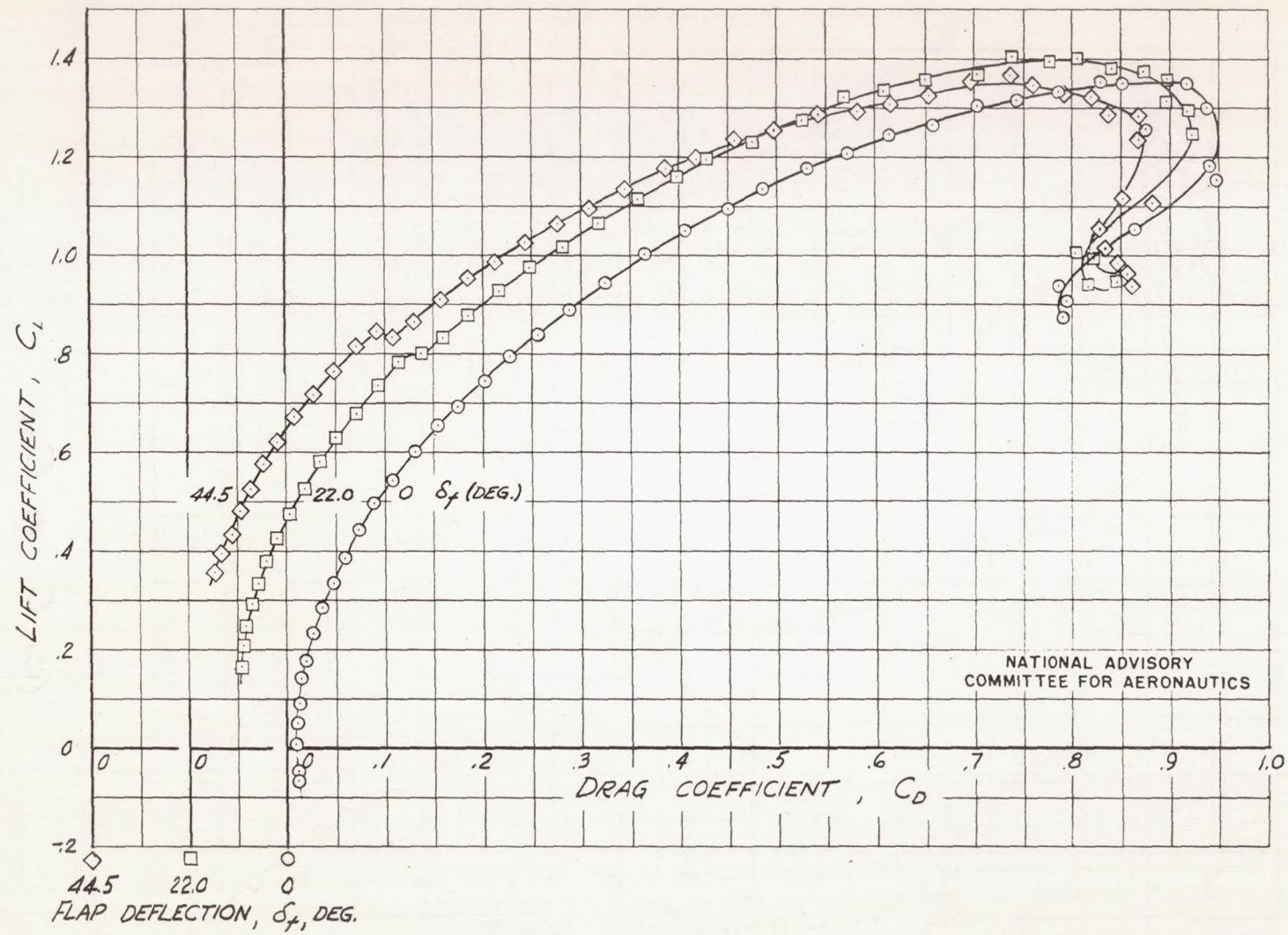
(c) C_L vs C_m

FIGURE 6.- CONCLUDED.



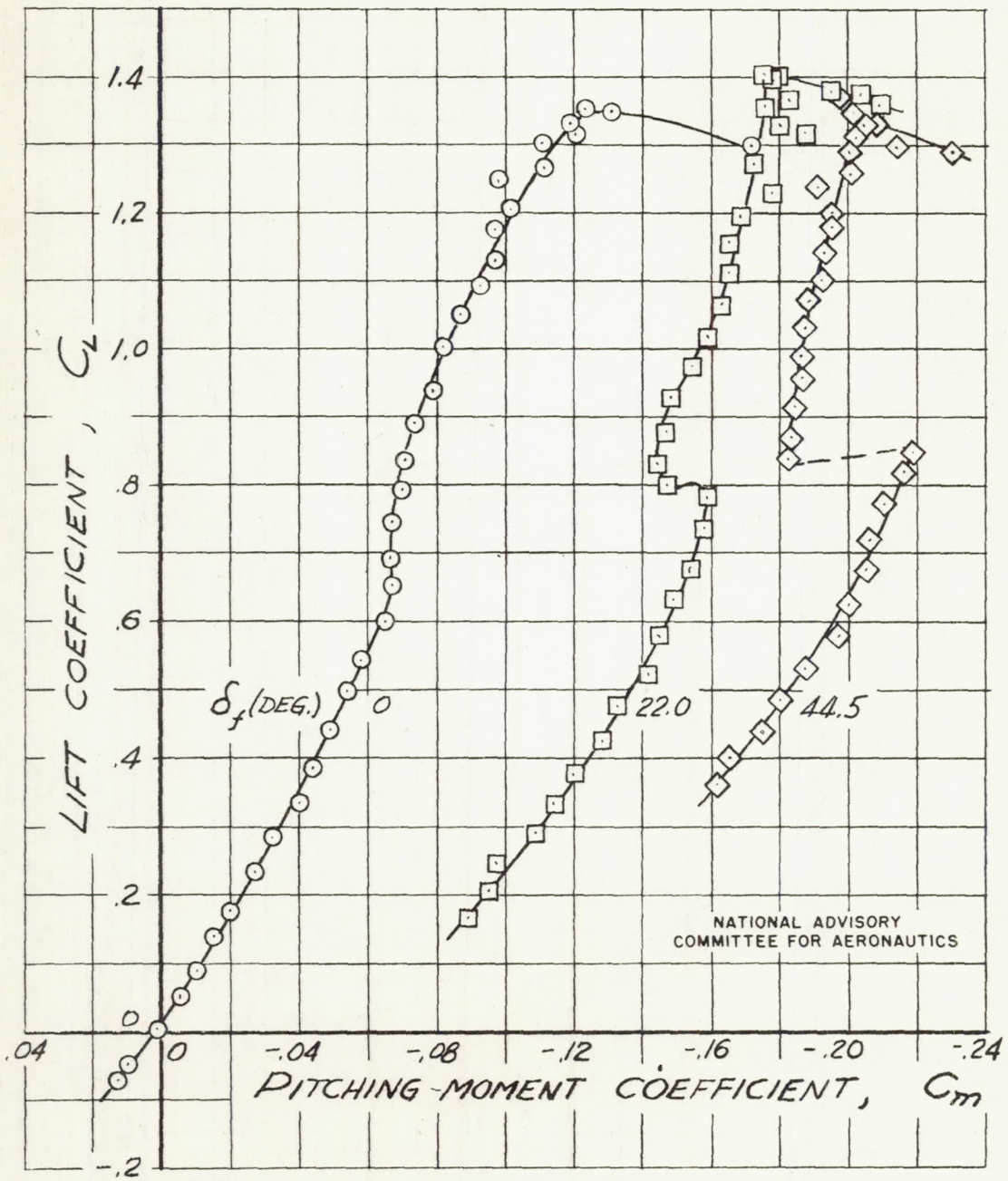
(a) C_L vs α

FIGURE 7.- AERODYNAMIC CHARACTERISTICS OF THE TRIANGULAR WING WITH THE AIRFOIL SECTION MAXIMUM THICKNESS ROUNDED BETWEEN 0.15 AND 0.25C AND WITH 18.5-PERCENT AREA SPLIT FLAPS DEFLECTED 0°, 22.0°, AND 44.5°.



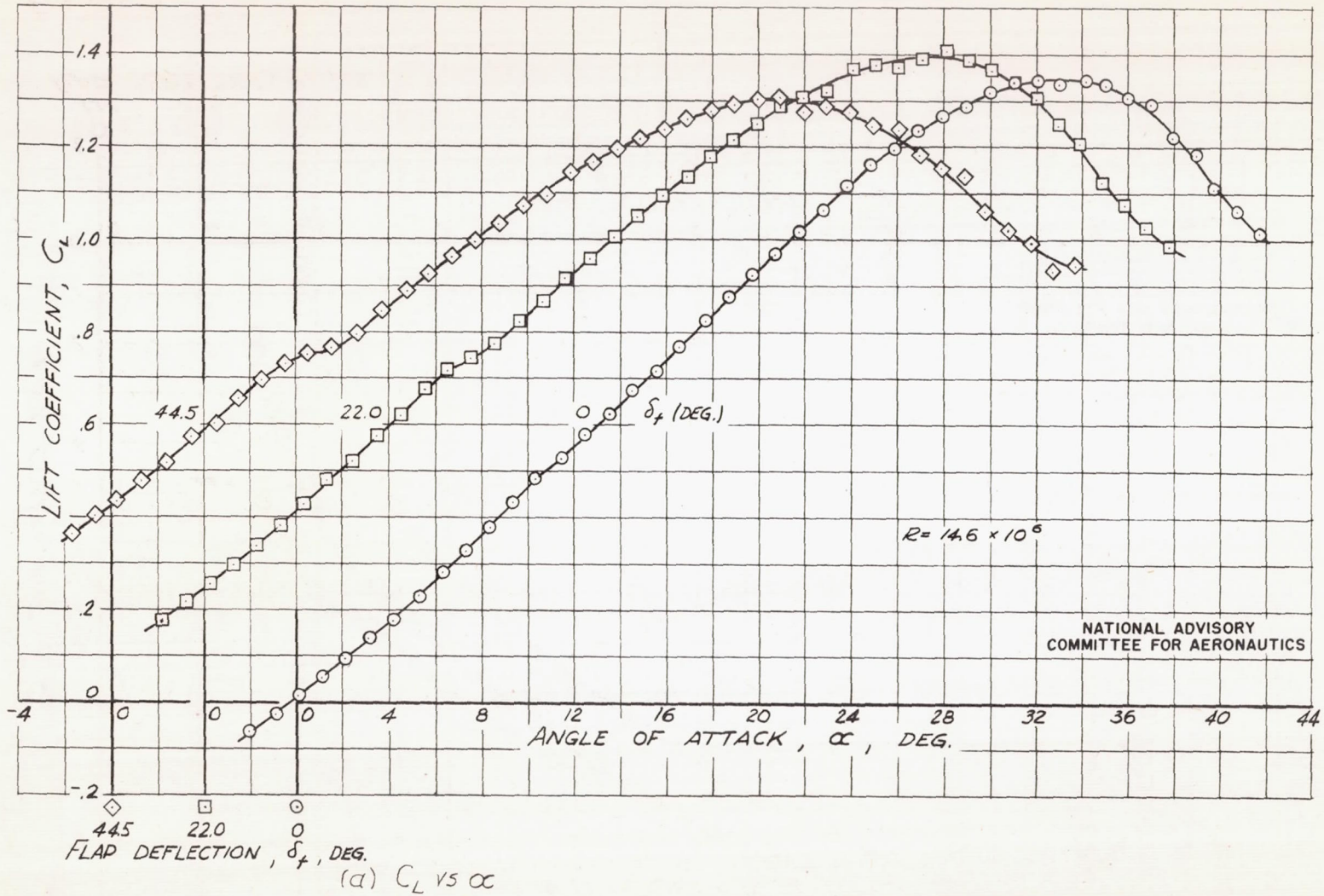
(b) C_L vs C_D

FIGURE 7.- CONTINUED.



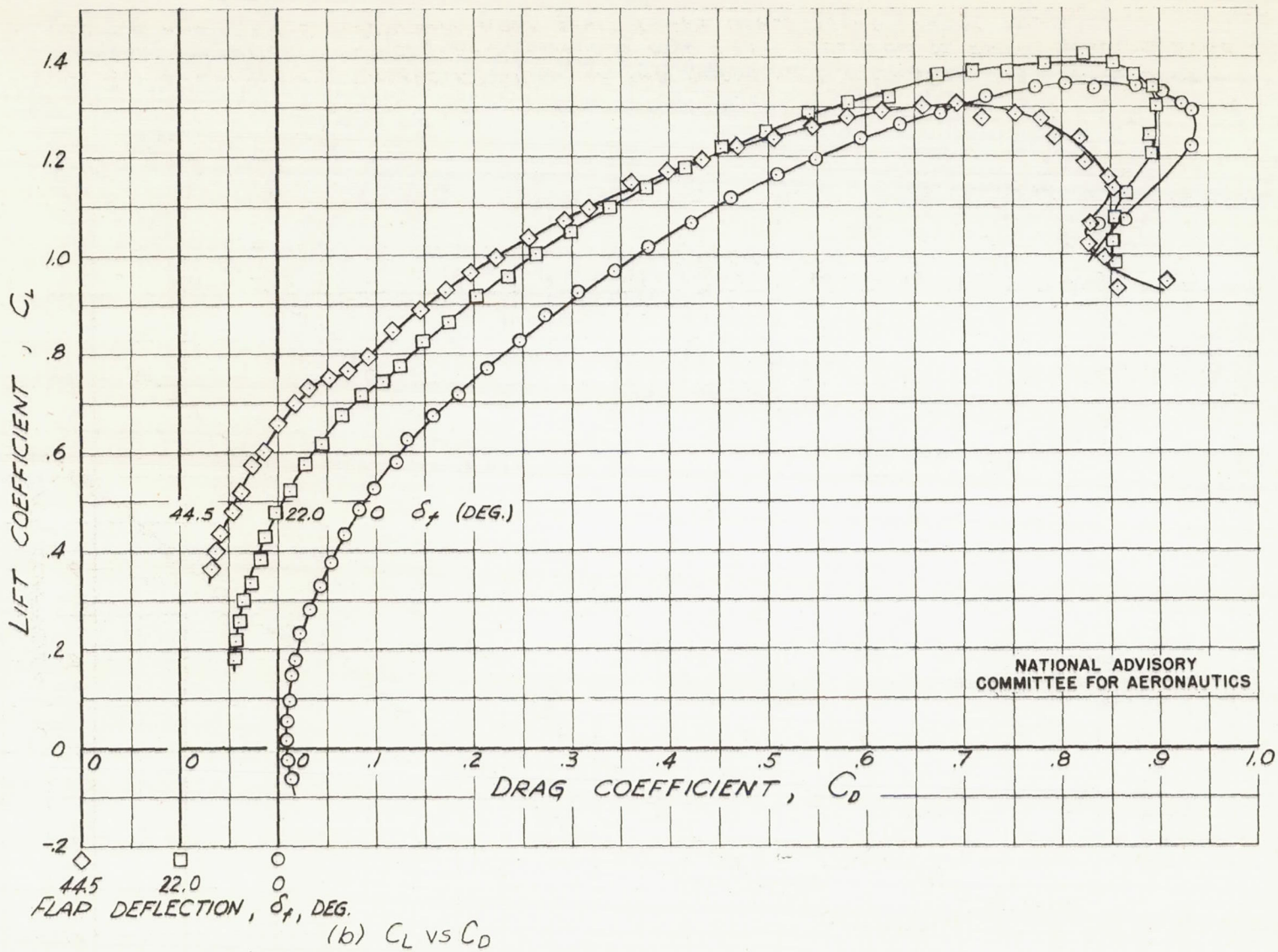
(c) C_L vs C_m

FIGURE 7.- CONCLUDED.



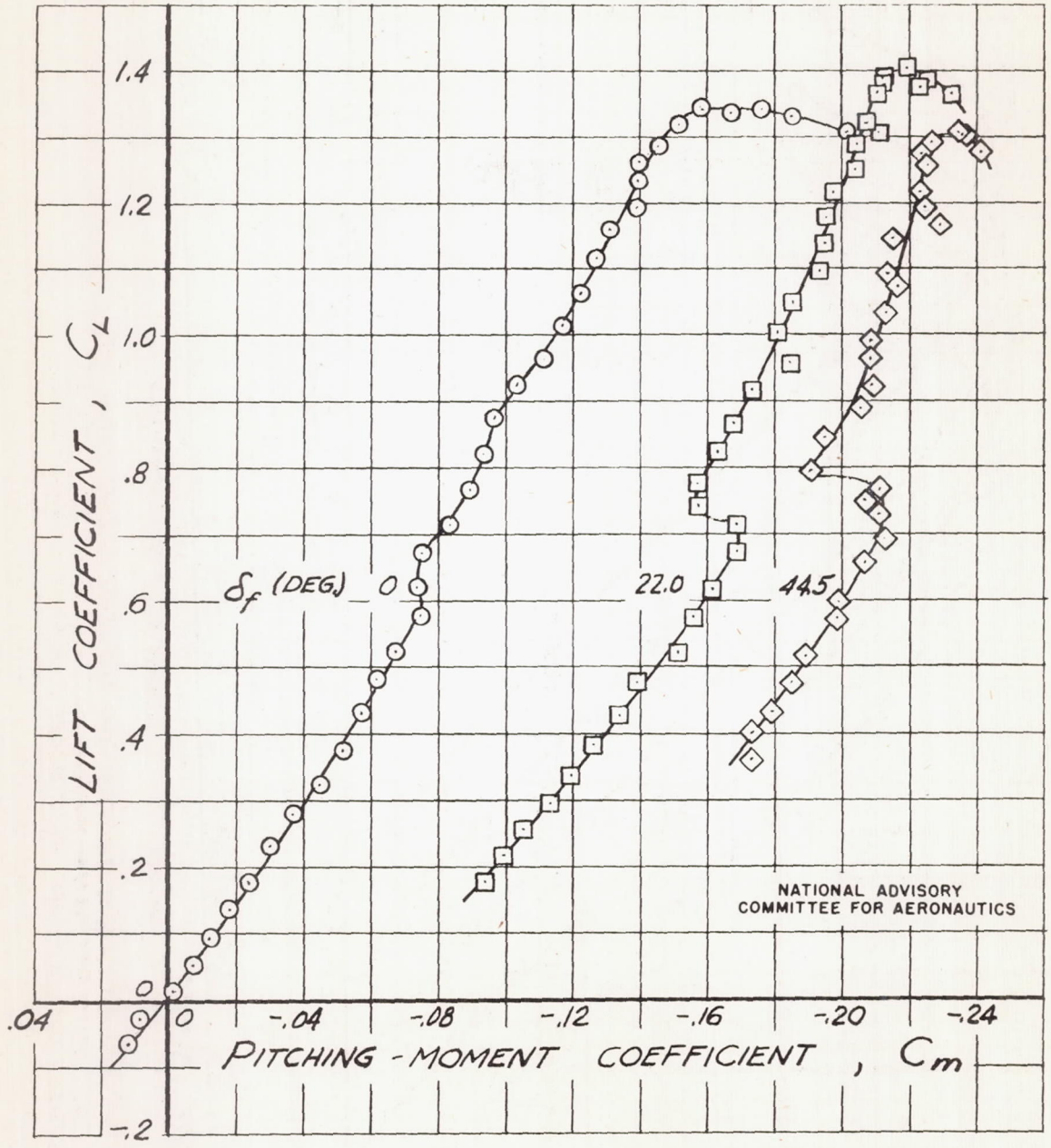
(a) C_L vs α

FIGURE 8. - AERODYNAMIC CHARACTERISTICS OF THE TRIANGULAR WING WITH THE AIRFOIL SECTION MAXIMUM THICKNESS ROUNDED BETWEEN 0.15 AND 0.25C PLUS 0.0025C RADIUS LEADING EDGE PROFILE AND WITH 18.5-PERCENT AREA SPLIT FLAPS DEFLECTED 0°, 22.0°, AND 44.5°.



(b) C_L vs C_D

FIGURE 8.- CONTINUED.



(c) C_L vs C_m

FIGURE 8.- CONCLUDED.

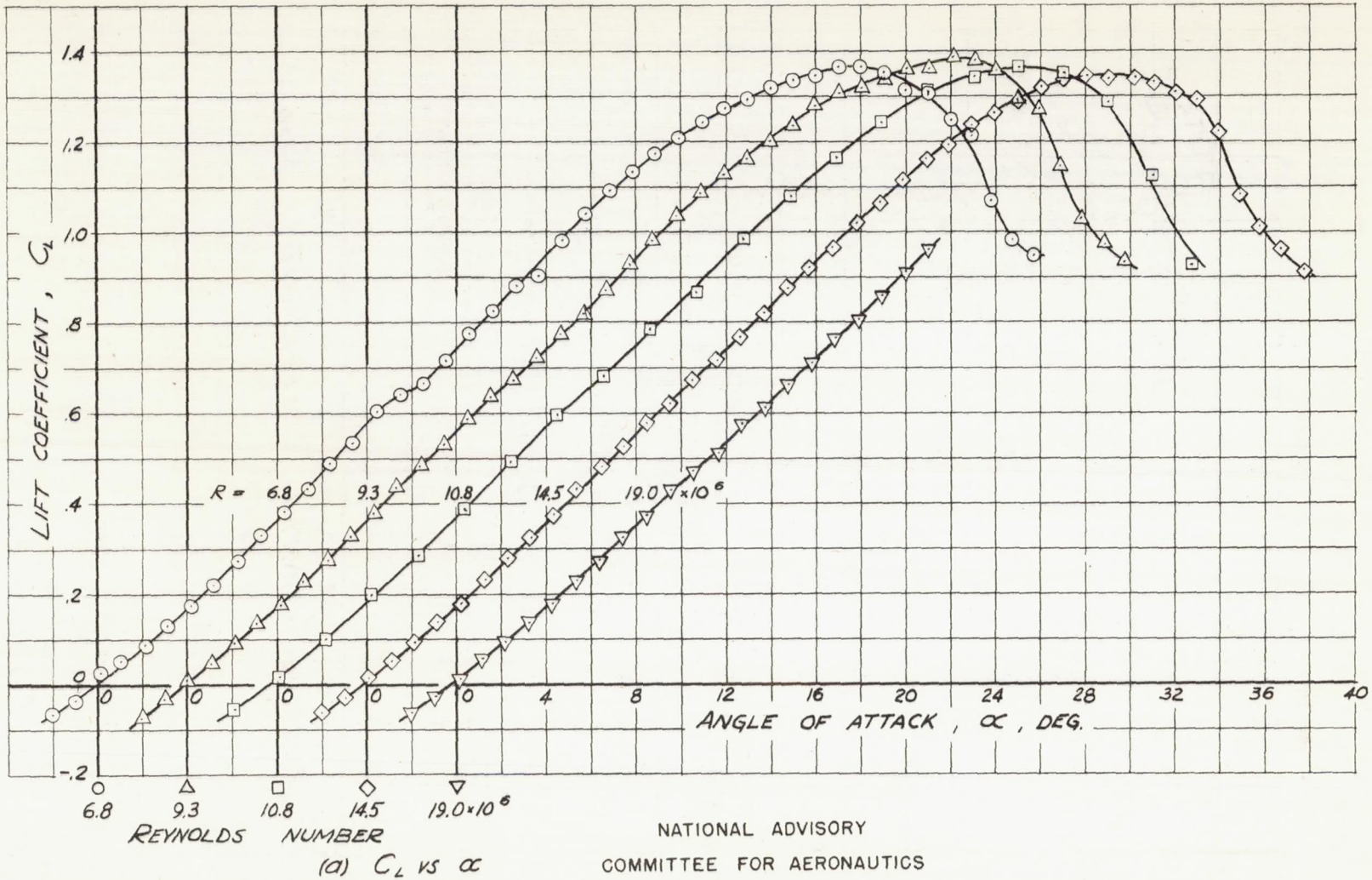
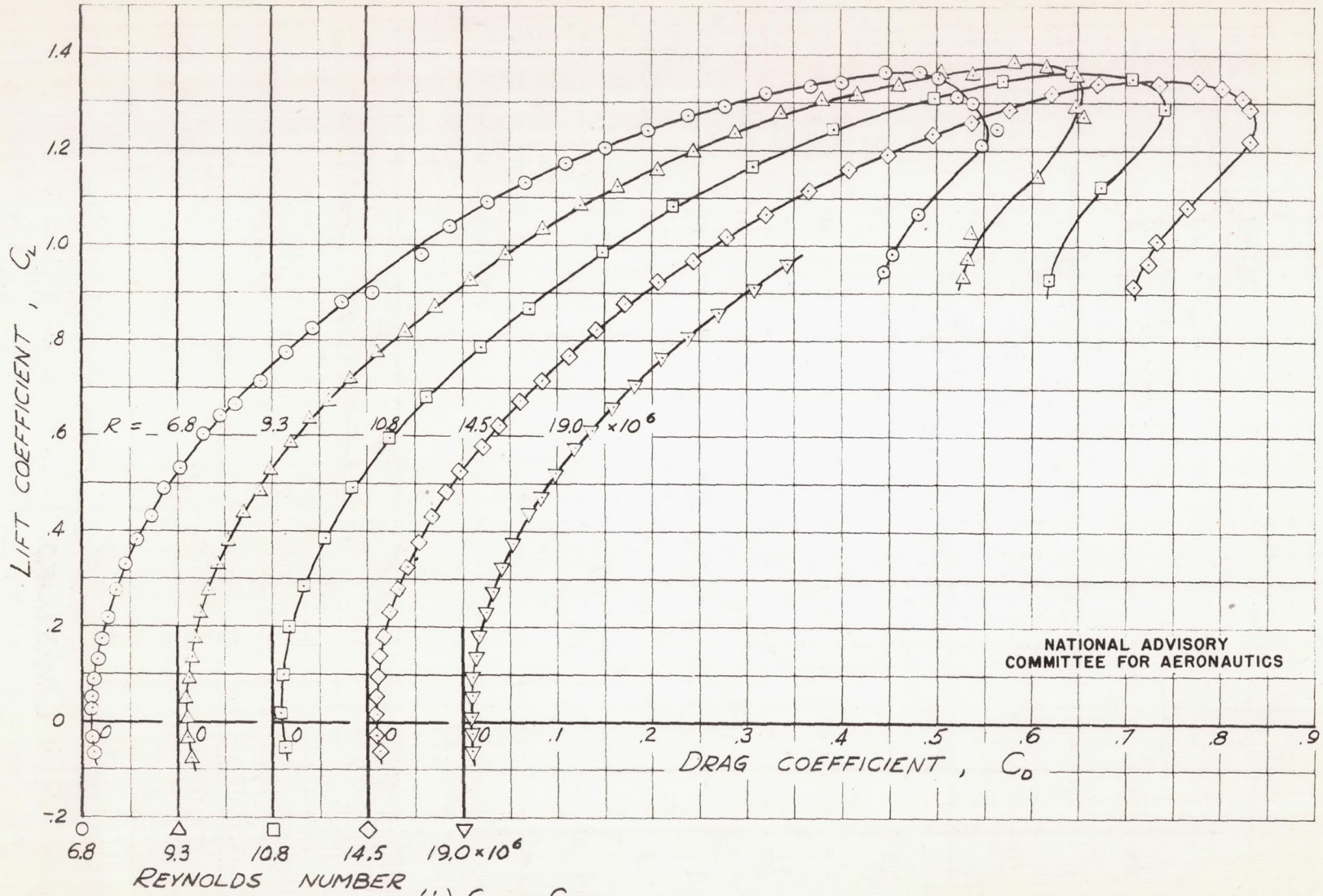
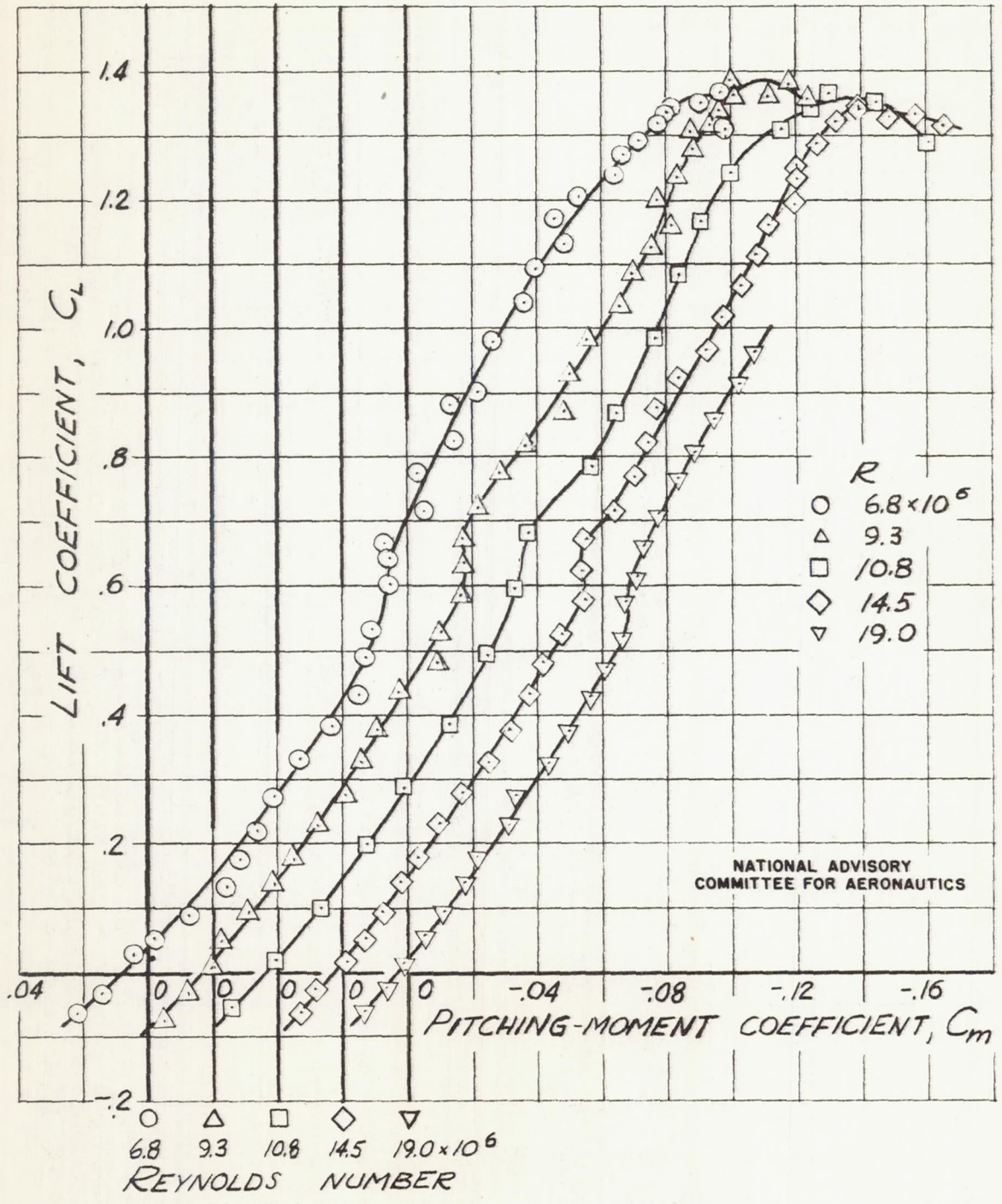


FIGURE 9.- AERODYNAMIC CHARACTERISTICS OF THE TRIANGULAR WING AT FIVE REYNOLDS NUMBERS WITH AIRFOIL SECTION MAXIMUM THICKNESS ROUNDED BETWEEN 0.15 AND 0.25C PLUS 0.0025 C RADIUS LEADING-EDGE PROFILE.



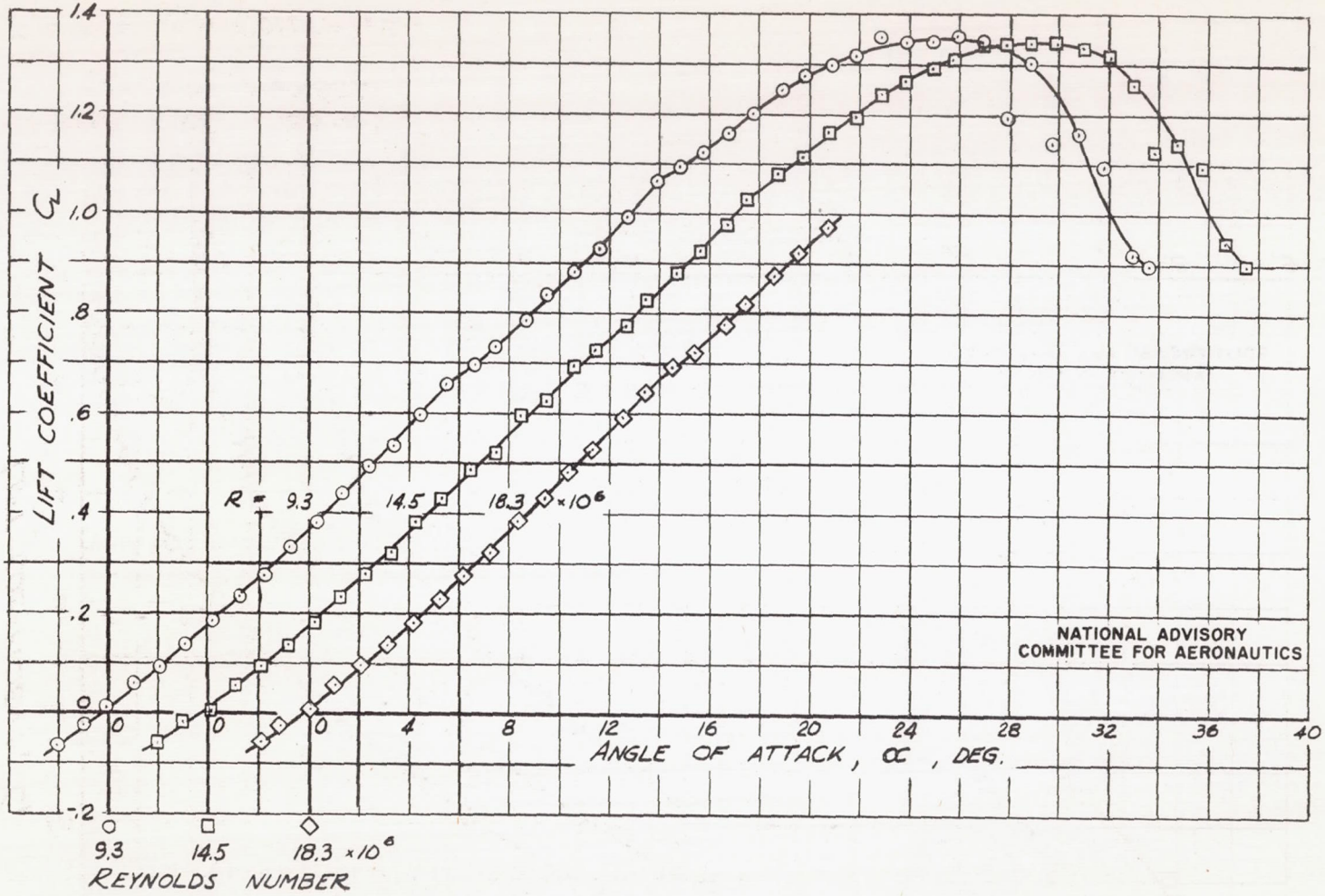
(b) C_L vs C_D

FIGURE 9.- CONTINUED.



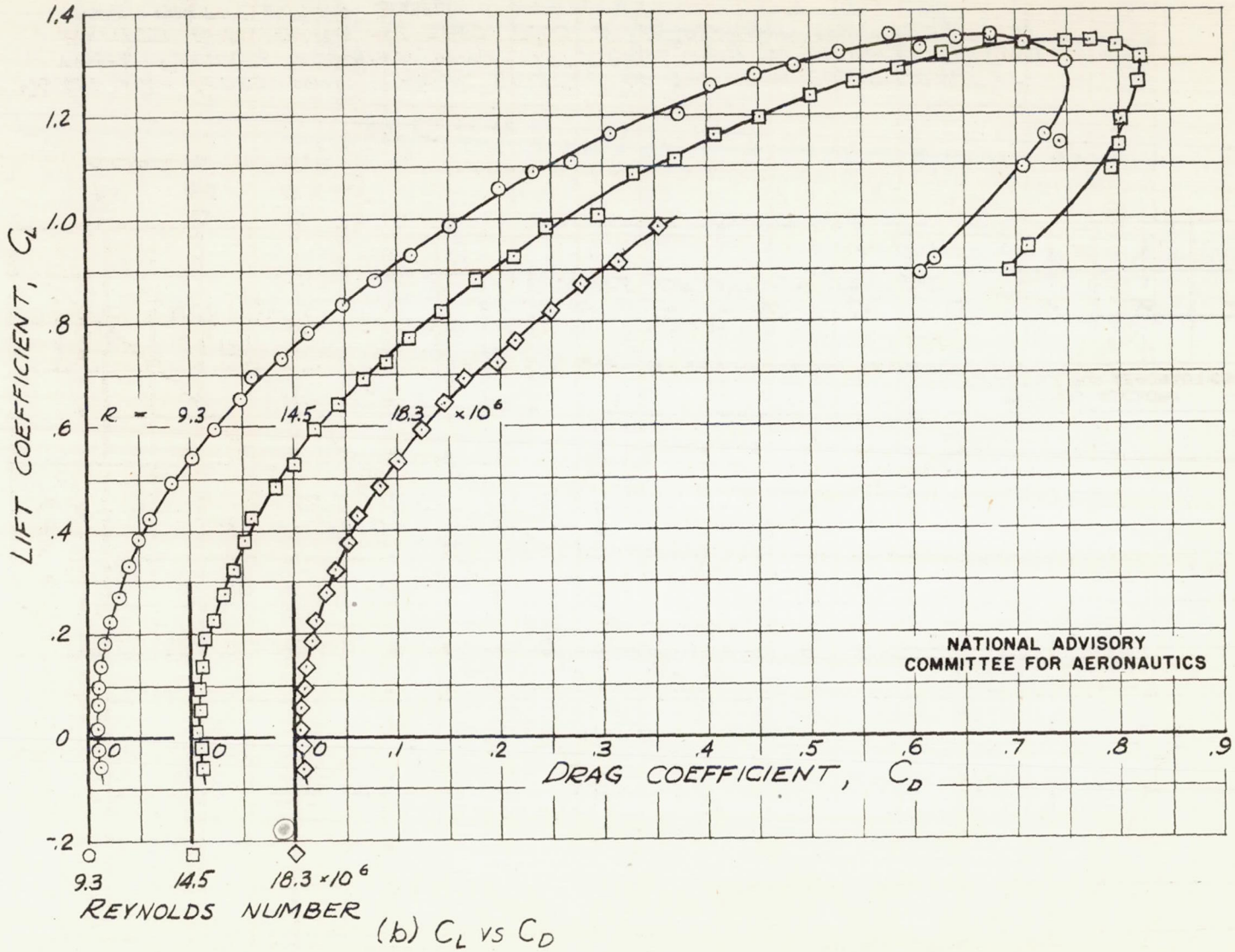
(c) C_L vs C_m

FIGURE 9.- CONCLUDED.



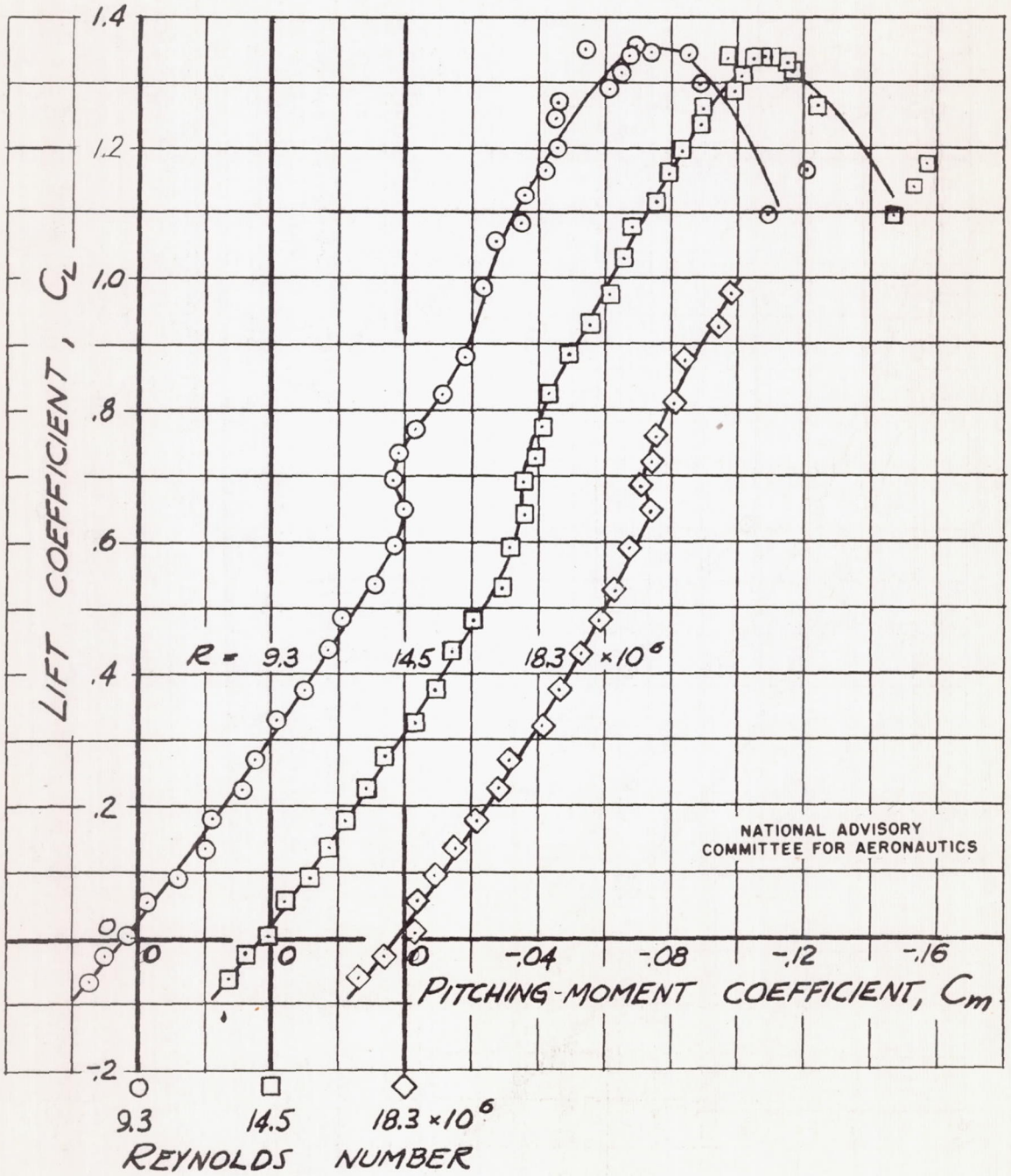
(a) C_L vs α

FIGURE 10.- AERODYNAMIC CHARACTERISTICS OF THE TRIANGULAR WING AT THREE REYNOLDS NUMBERS WITH THE AIRFOIL SECTION MAXIMUM THICKNESS ROUNDED BETWEEN 0.15 AND 0.25C PLUS A 25-PERCENT SPAN TRANSITION TYPE SHARP LEADING EDGE.



(b) C_L vs C_D

FIGURE 10. - CONTINUED.



(c) C_L vs C_m

FIGURE 10.- CONCLUDED.

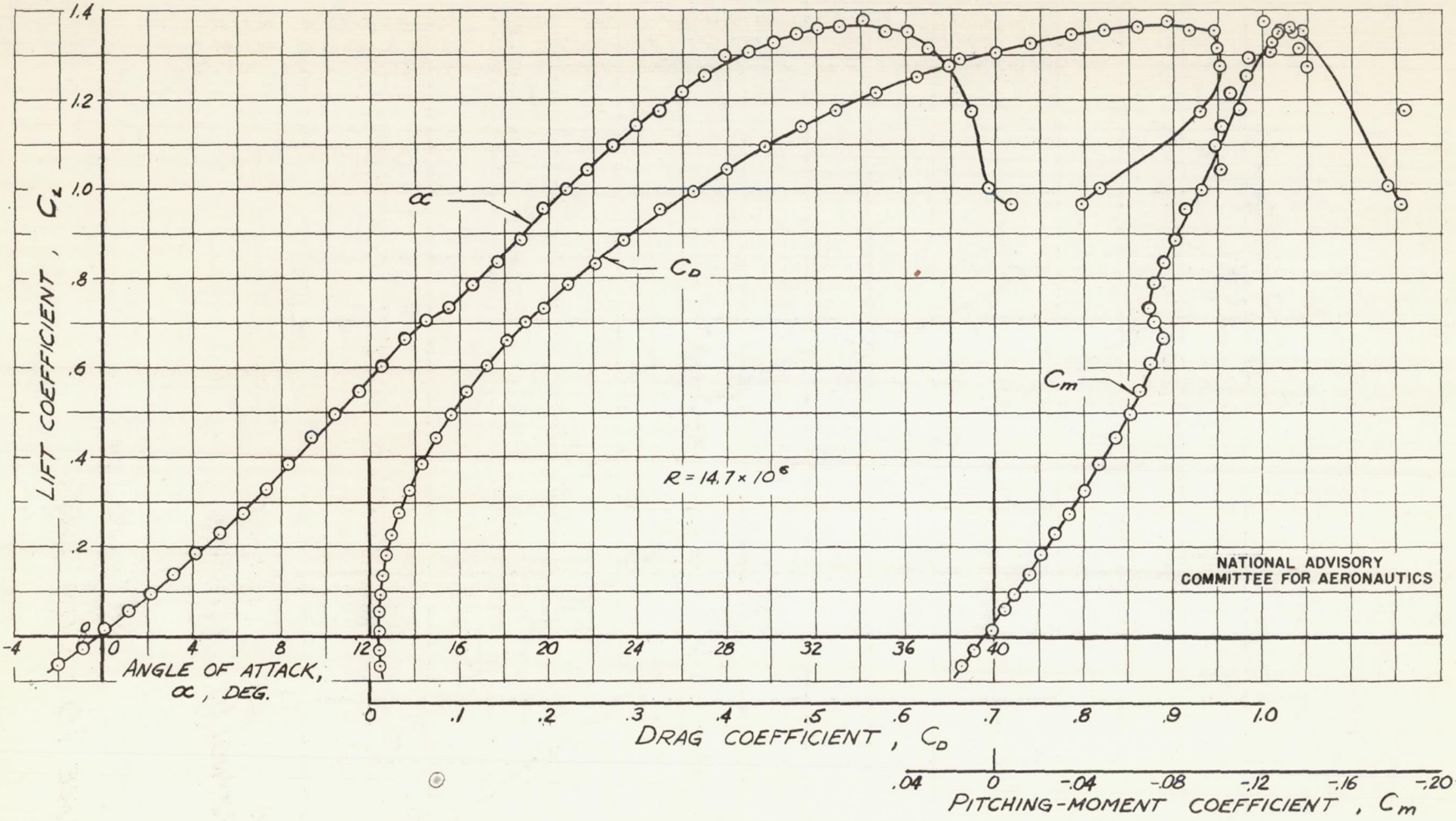
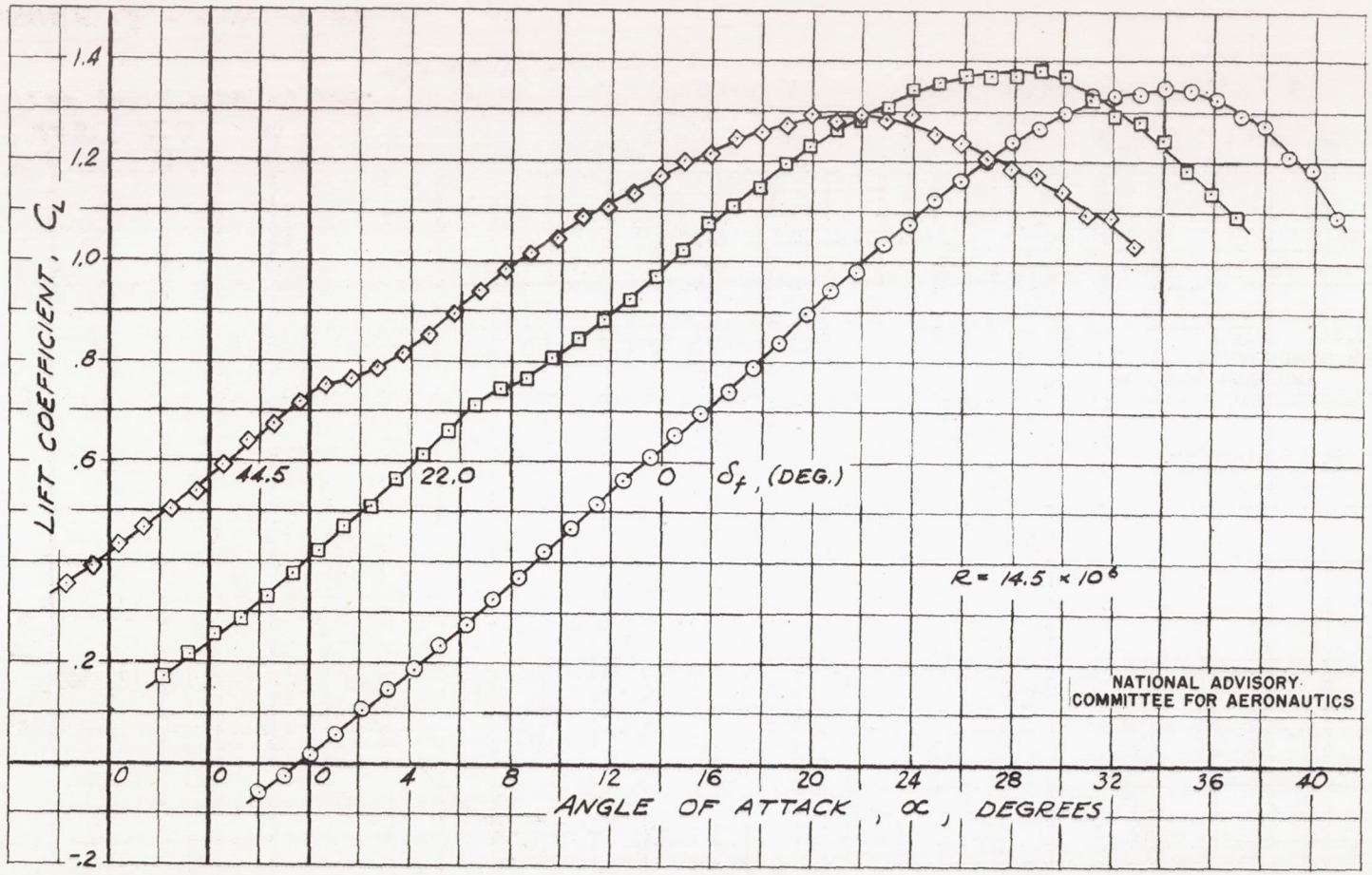
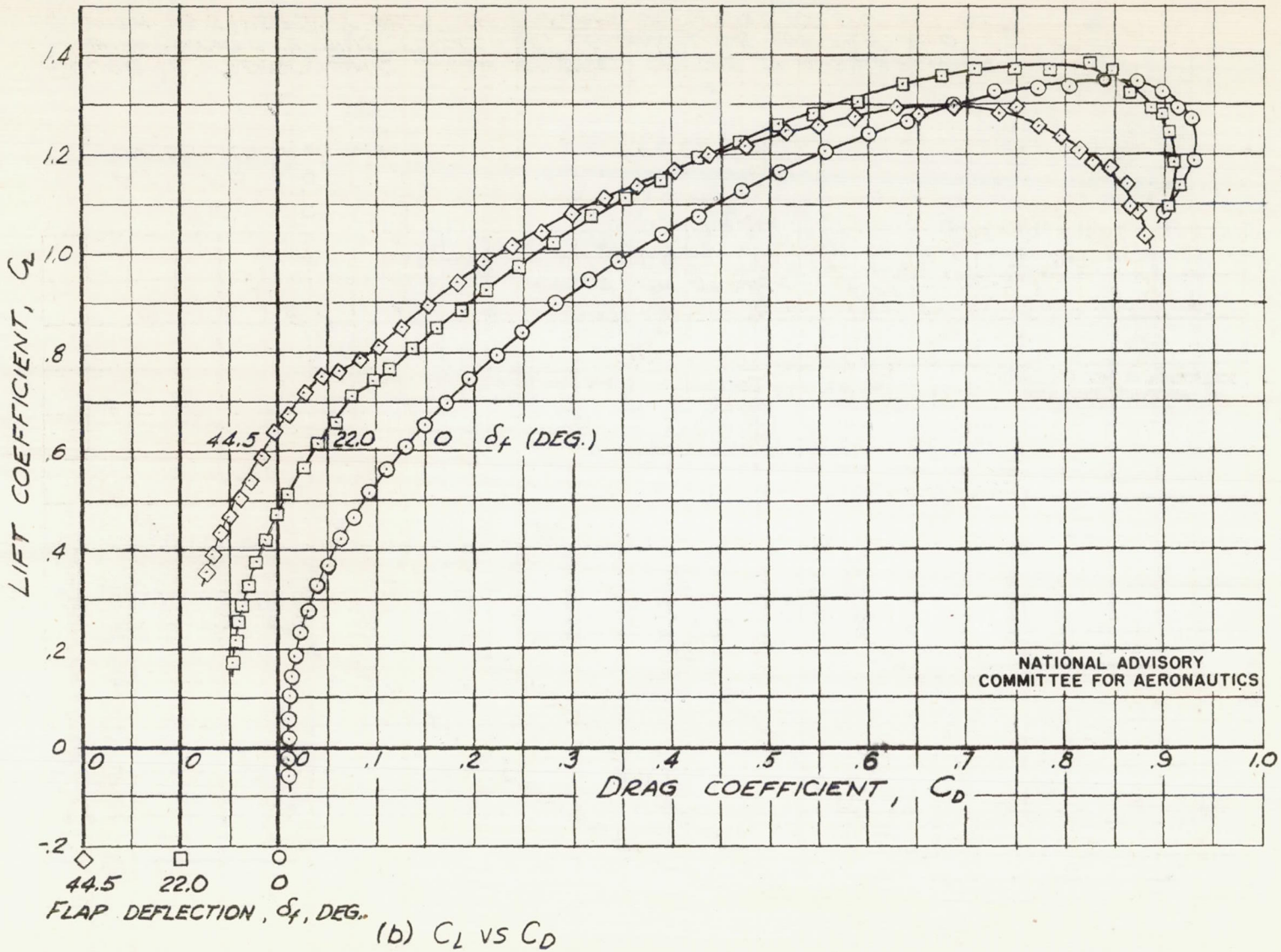


FIGURE 11.- AERODYNAMIC CHARACTERISTICS OF THE TRIANGULAR WING WITH THE AIRFOIL SECTION MAXIMUM THICKNESS ROUNDED BETWEEN 0.15 AND 0.25c PLUS A 50-PERCENT SPAN TRANSITION TYPE SHARP LEADING EDGE.



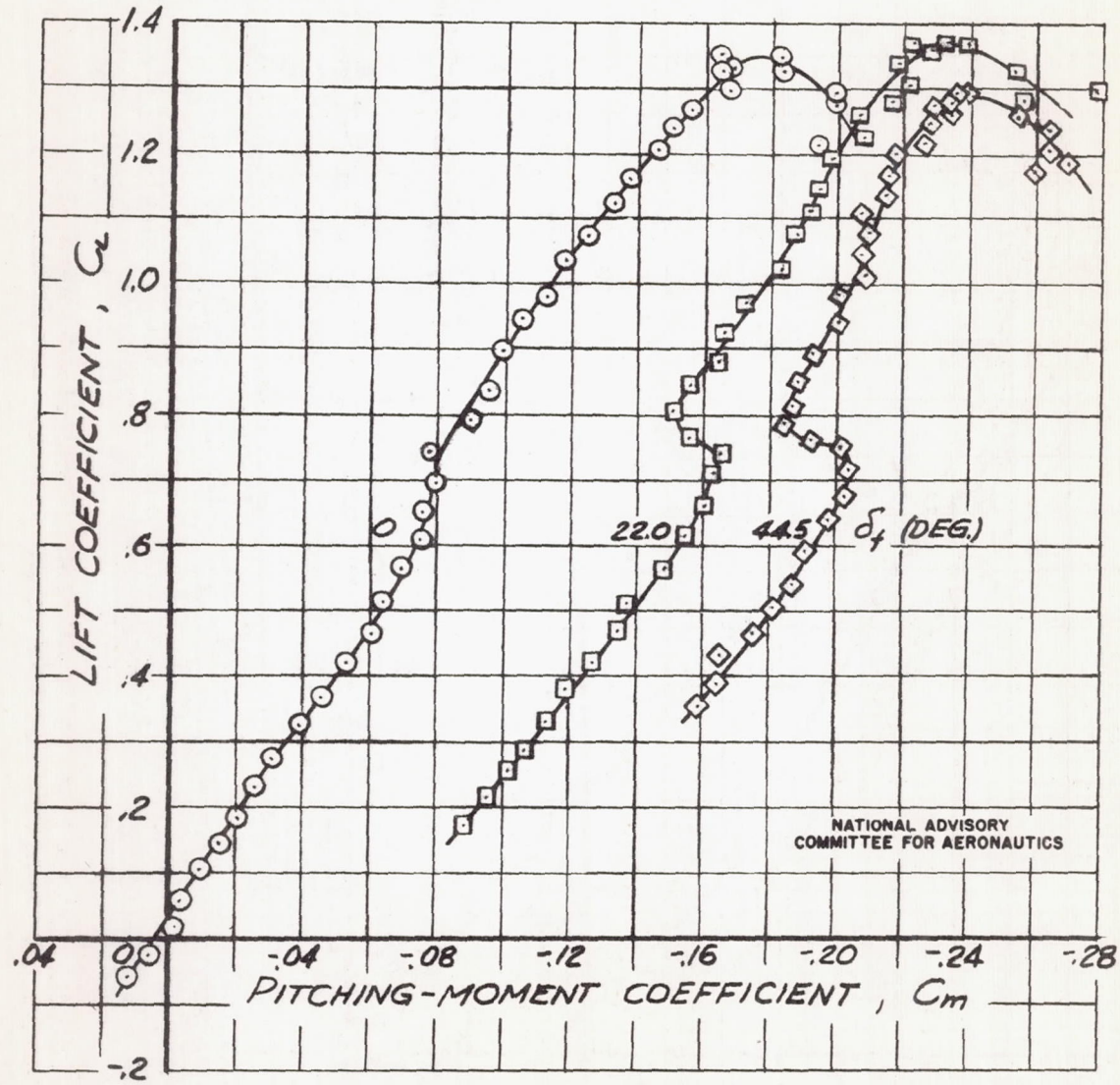
(a) C_L vs α

FIGURE 12. - AERODYNAMIC CHARACTERISTICS OF THE TRIANGULAR WING WITH 0.010 C RADIUS (CHORDWISE) LEADING-EDGE PROFILE AND WITH 18.5-PERCENT AREA SPLIT FLAPS DEFLECTED 0°, 22.0° AND 44.5°.



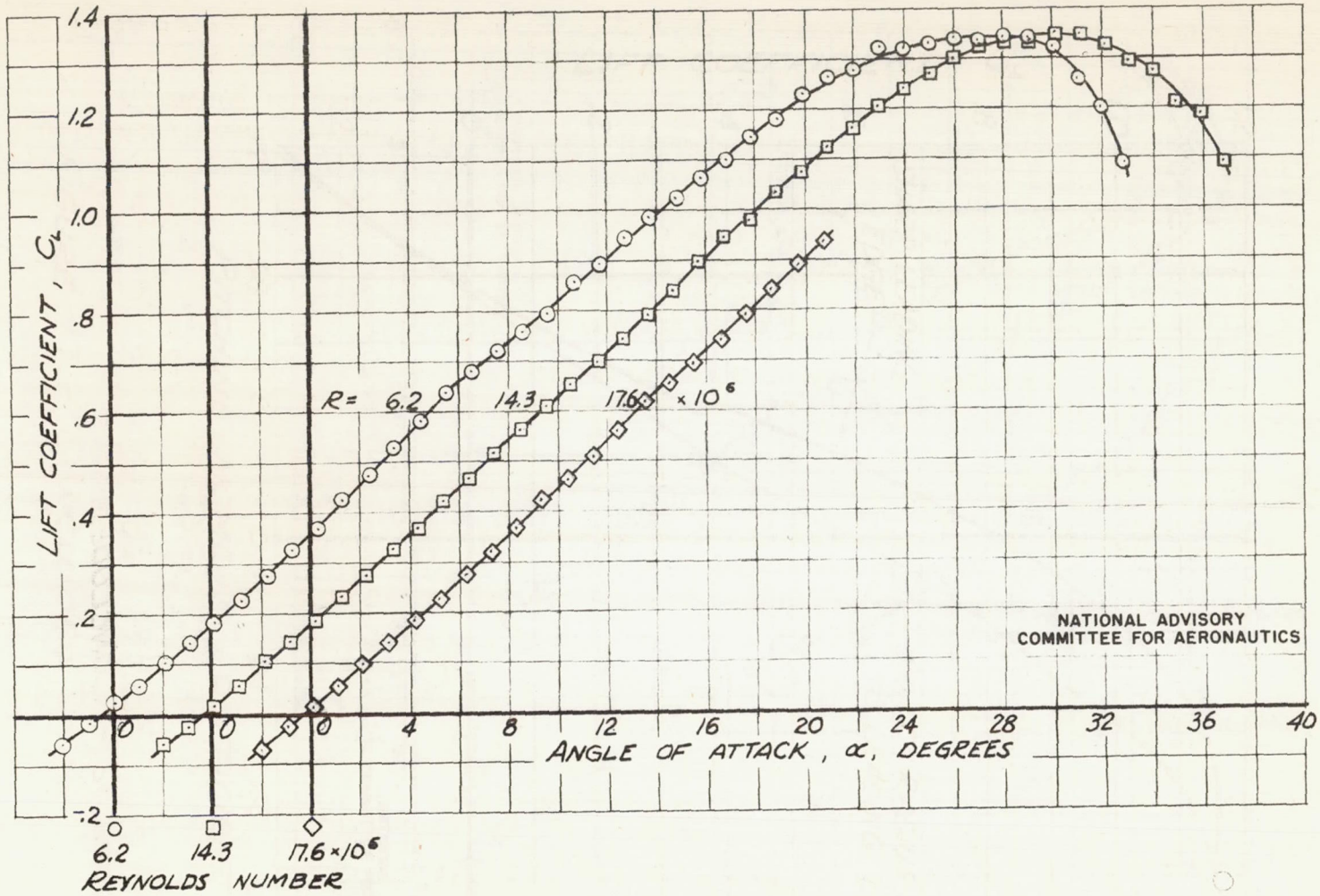
(b) C_L vs C_D

FIGURE 12.- CONTINUED.



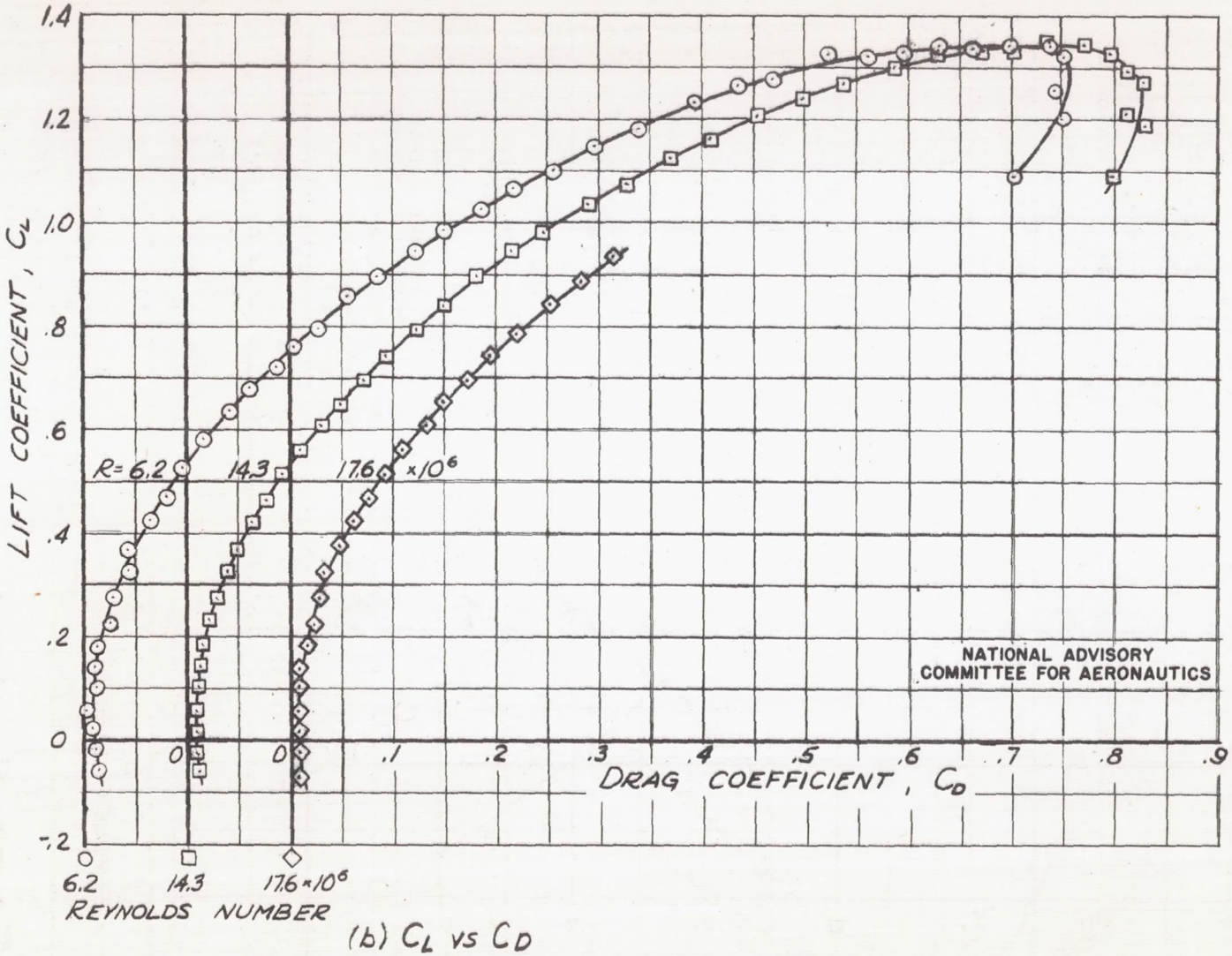
(c) C_L vs C_m

FIGURE 12.- CONCLUDED.



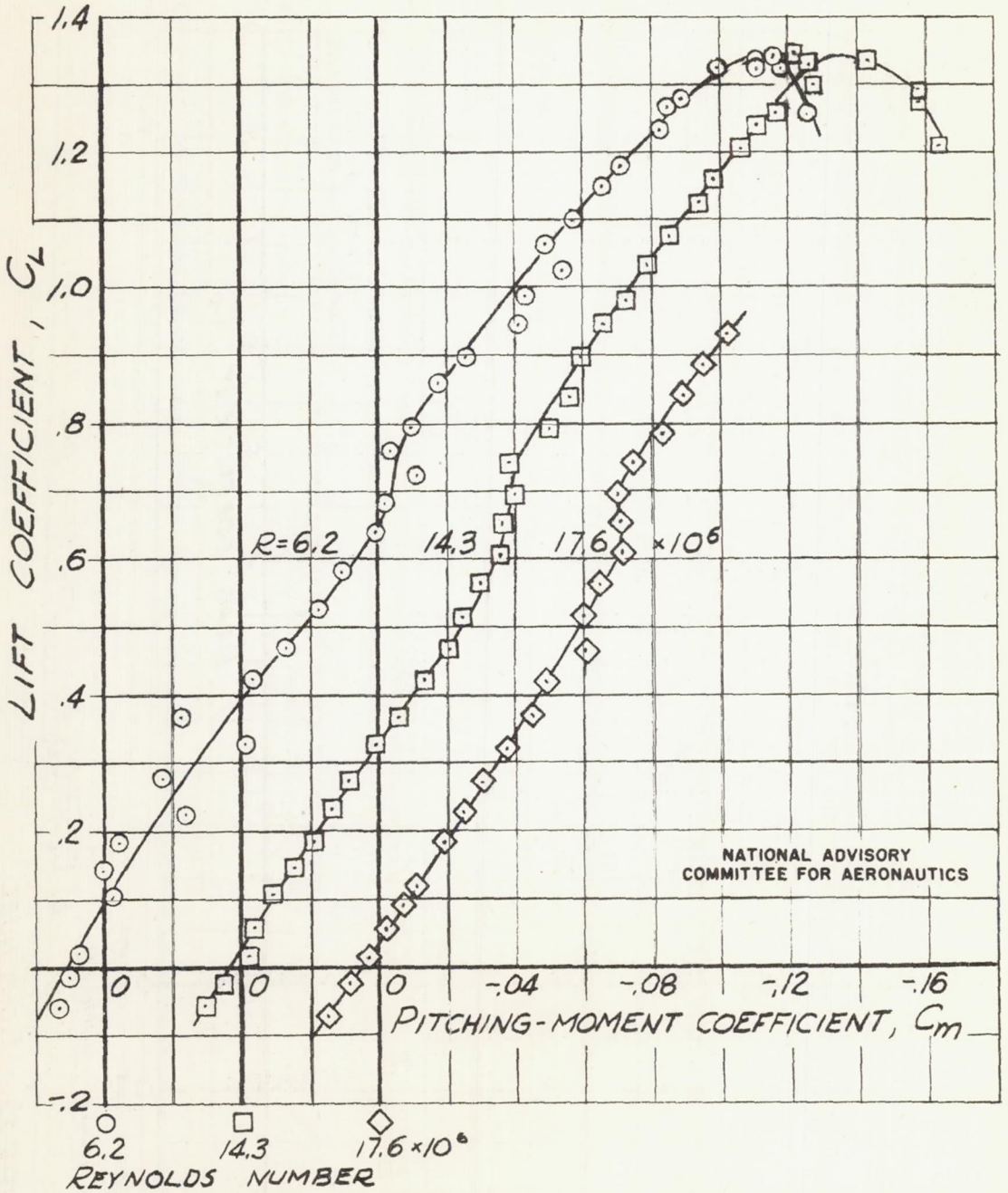
(a) C_L vs α

FIGURE 13.- AERODYNAMIC CHARACTERISTICS OF THE TRIANGULAR WING WITH 0.010c RADIUS (CHORDWISE) LEADING-EDGE PROFILE AT THREE REYNOLDS NUMBERS.



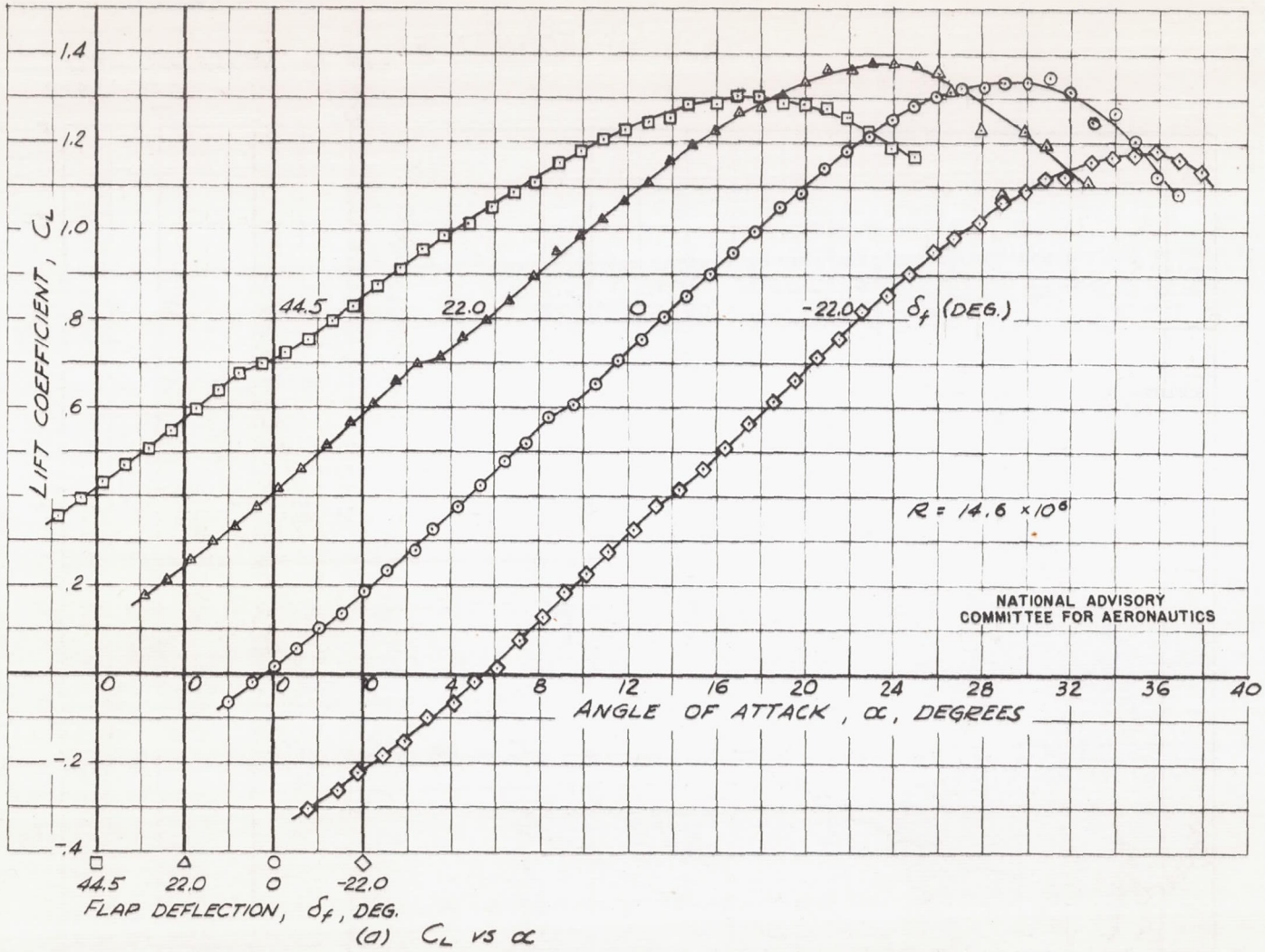
(b) C_L vs C_D

FIGURE 13.- CONTINUED.



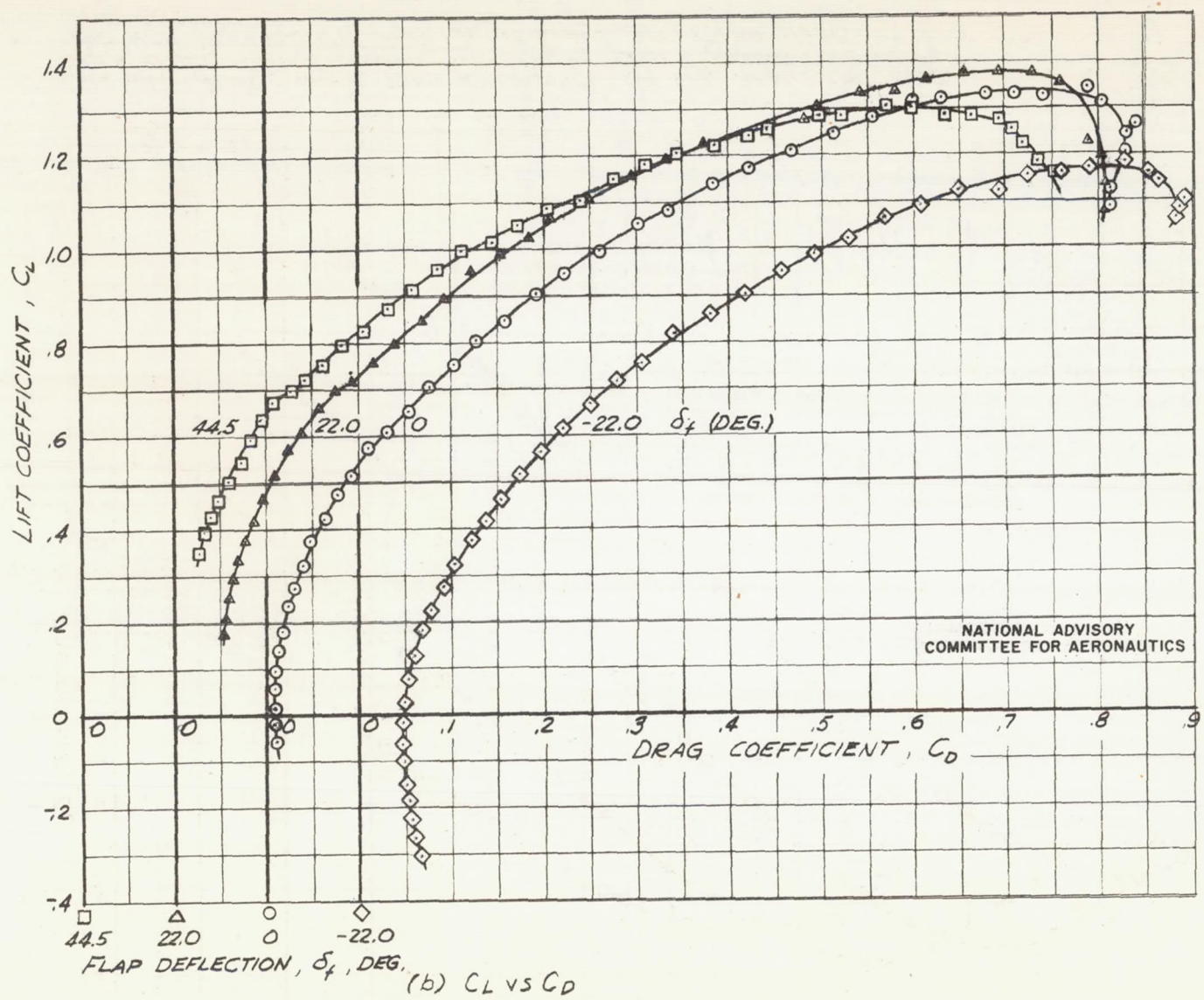
(c) C_L vs C_m

FIGURE 13.- CONCLUDED.



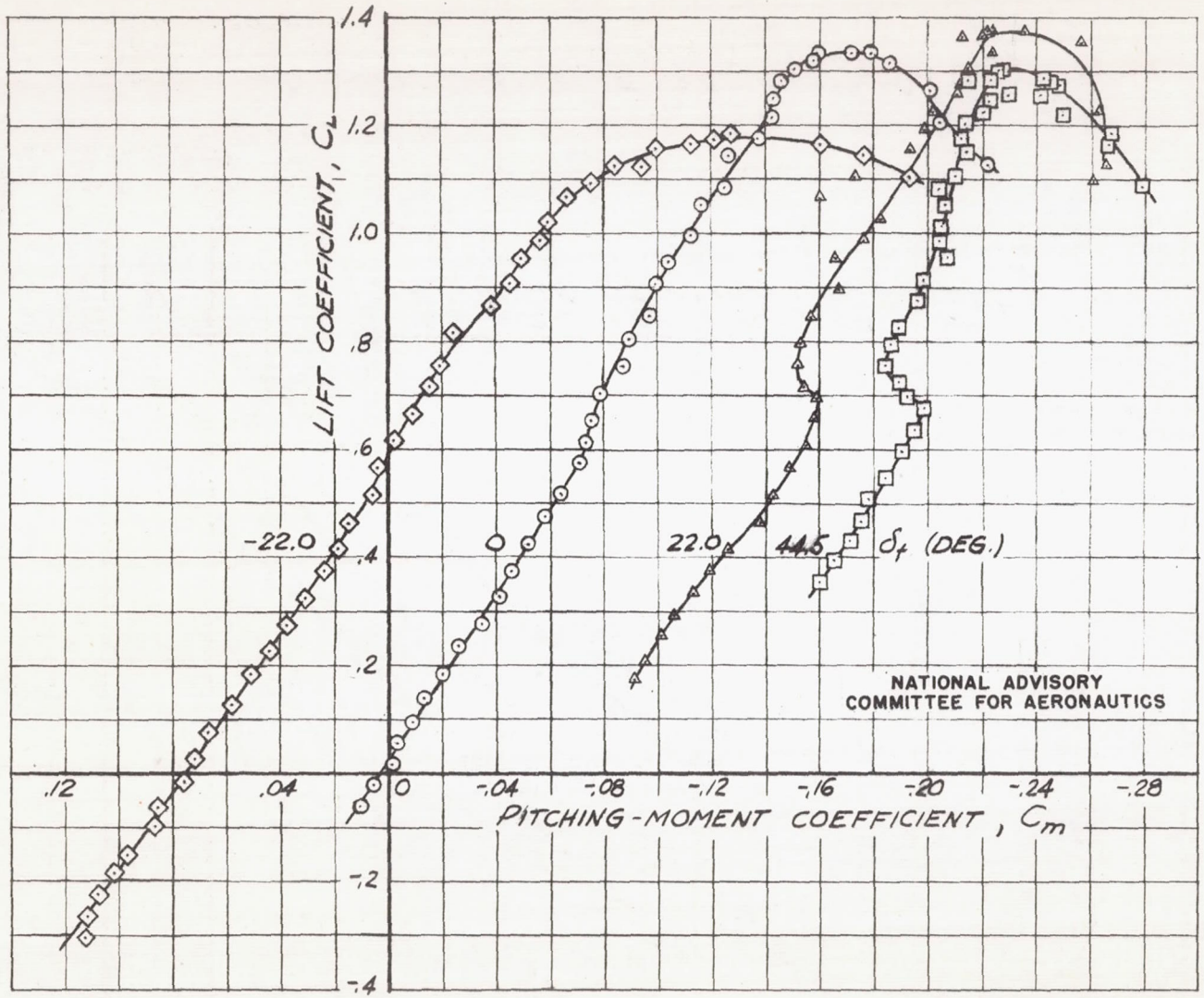
(a) C_L vs α

FIGURE 14.- AERODYNAMIC CHARACTERISTICS OF THE TRIANGULAR WING WITH 0.011C RADIUS (NORMAL TO LEADING EDGE) LEADING-EDGE PROFILE AND WITH 18.5-PERCENT AREA SPLIT FLAPS DEFLECTED -22.0°, 0°, 22.0° AND 44.5°.



(b) C_L vs C_D

FIGURE 14.- CONTINUED.



(c) C_L vs C_m

FIGURE 14.- CONCLUDED.

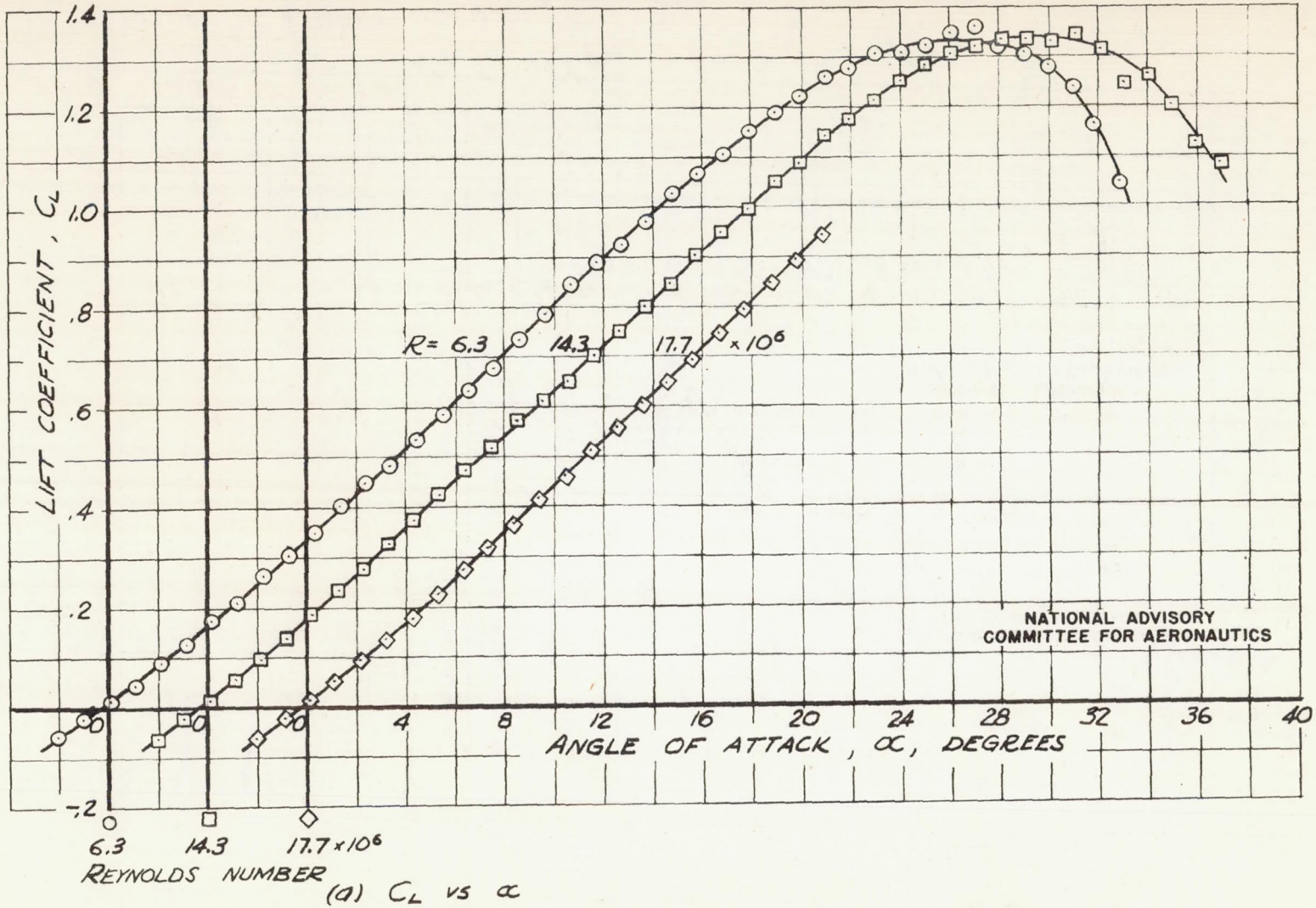
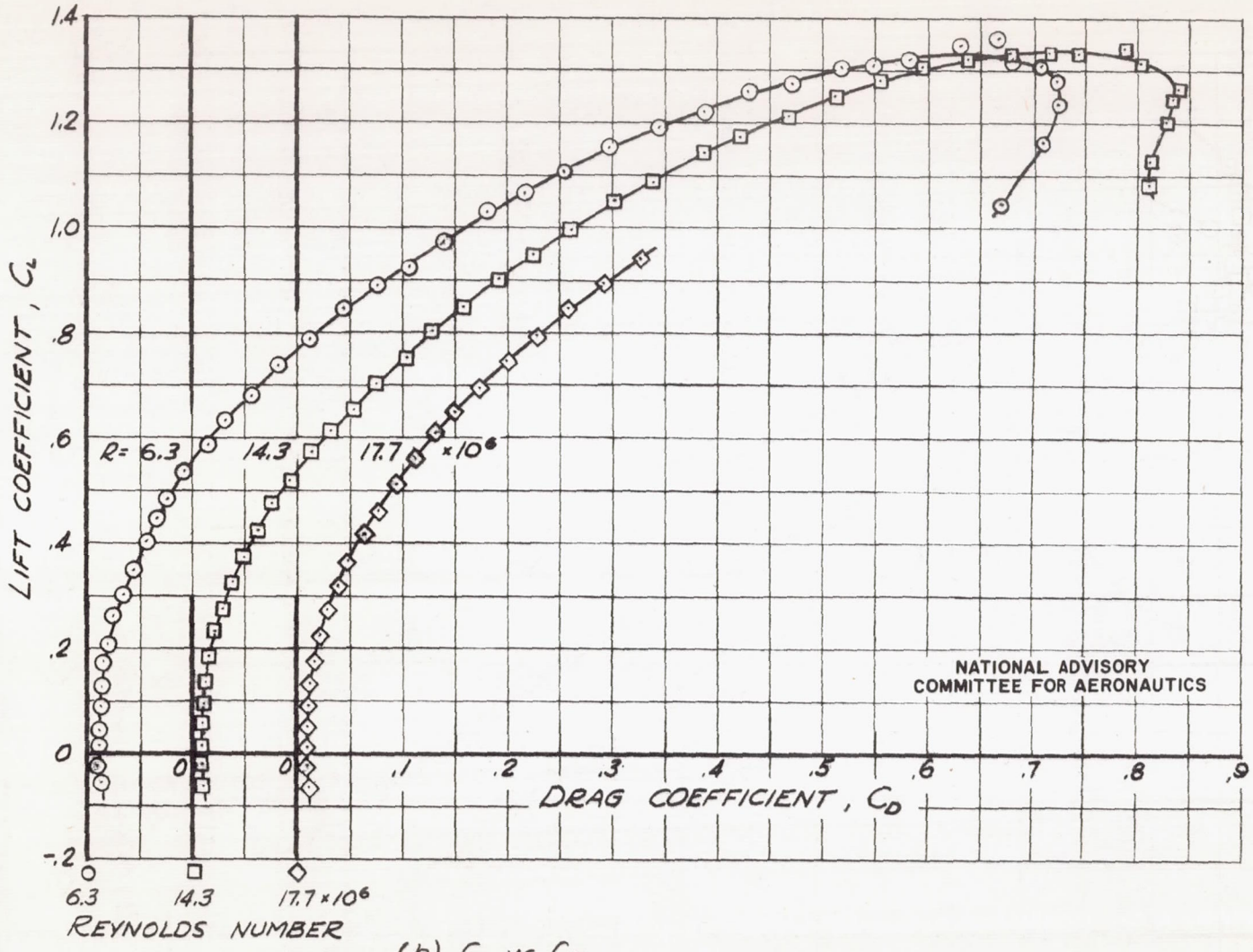
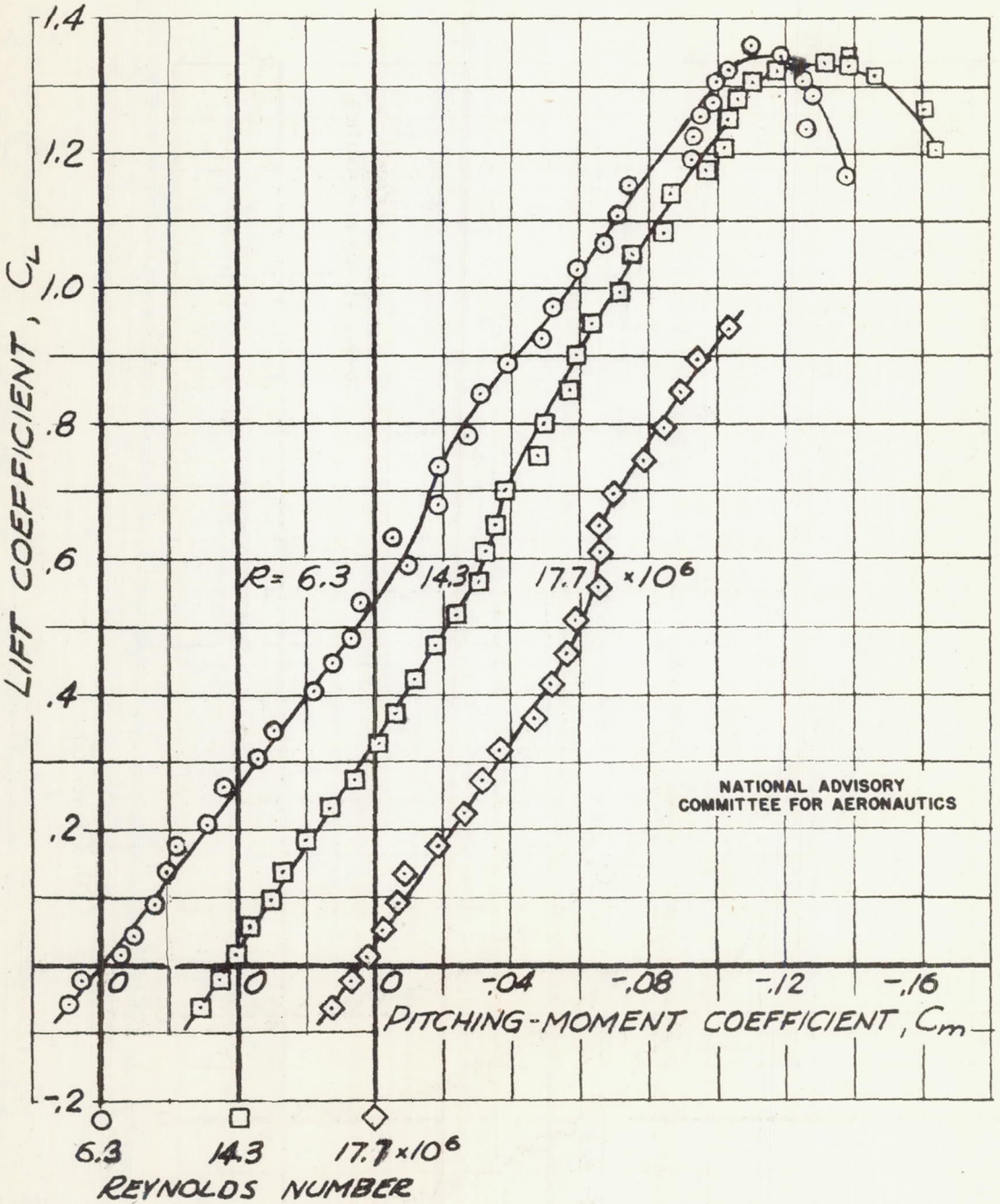


FIGURE 15.- AERODYNAMIC CHARACTERISTICS OF THE TRIANGULAR WING AT THREE REYNOLDS NUMBERS WITH 0.011C RADIUS (NORMAL TO LEADING EDGE) LEADING-EDGE PROFILE.



(b) C_L vs C_D

FIGURE 15.- CONTINUED.



(c) C_L vs C_m

FIGURE 15.- CONCLUDED.

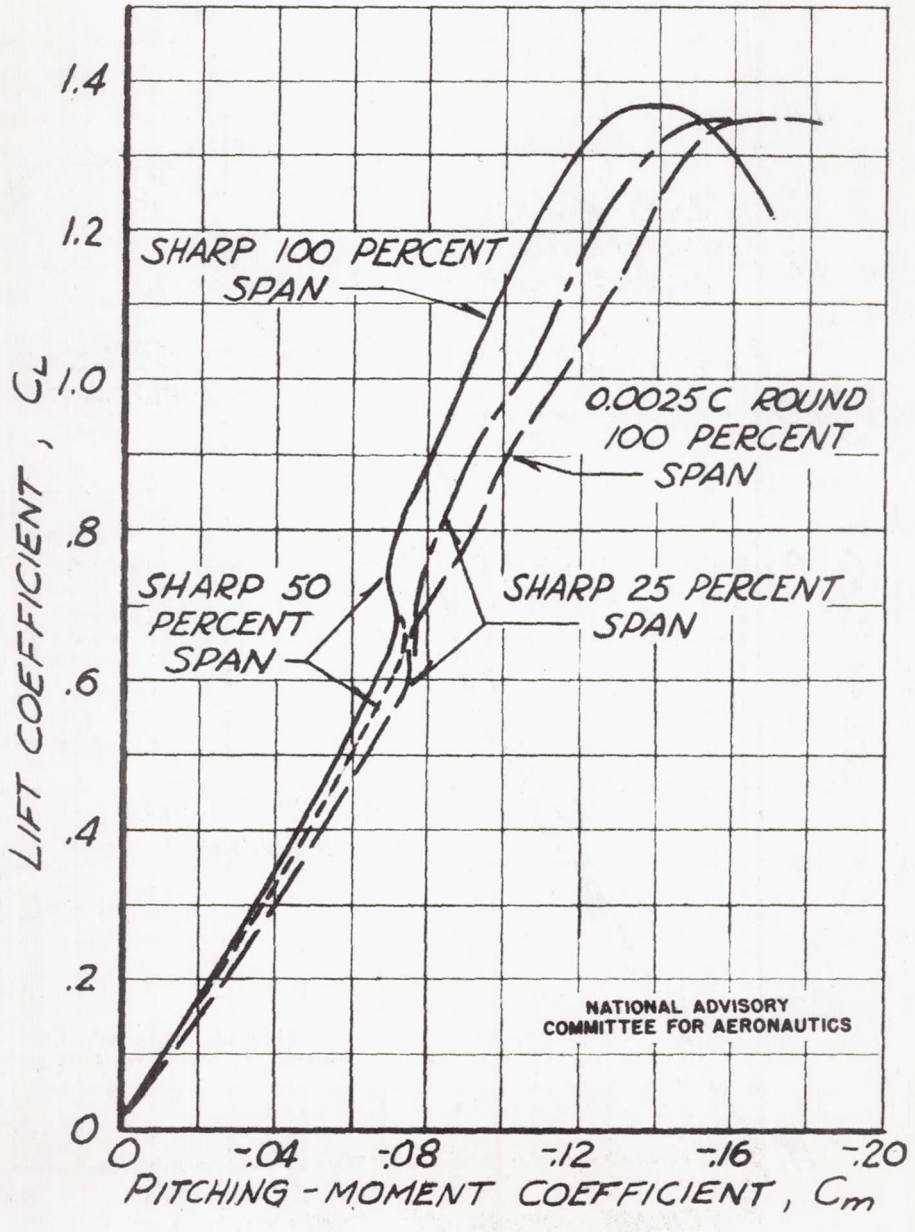
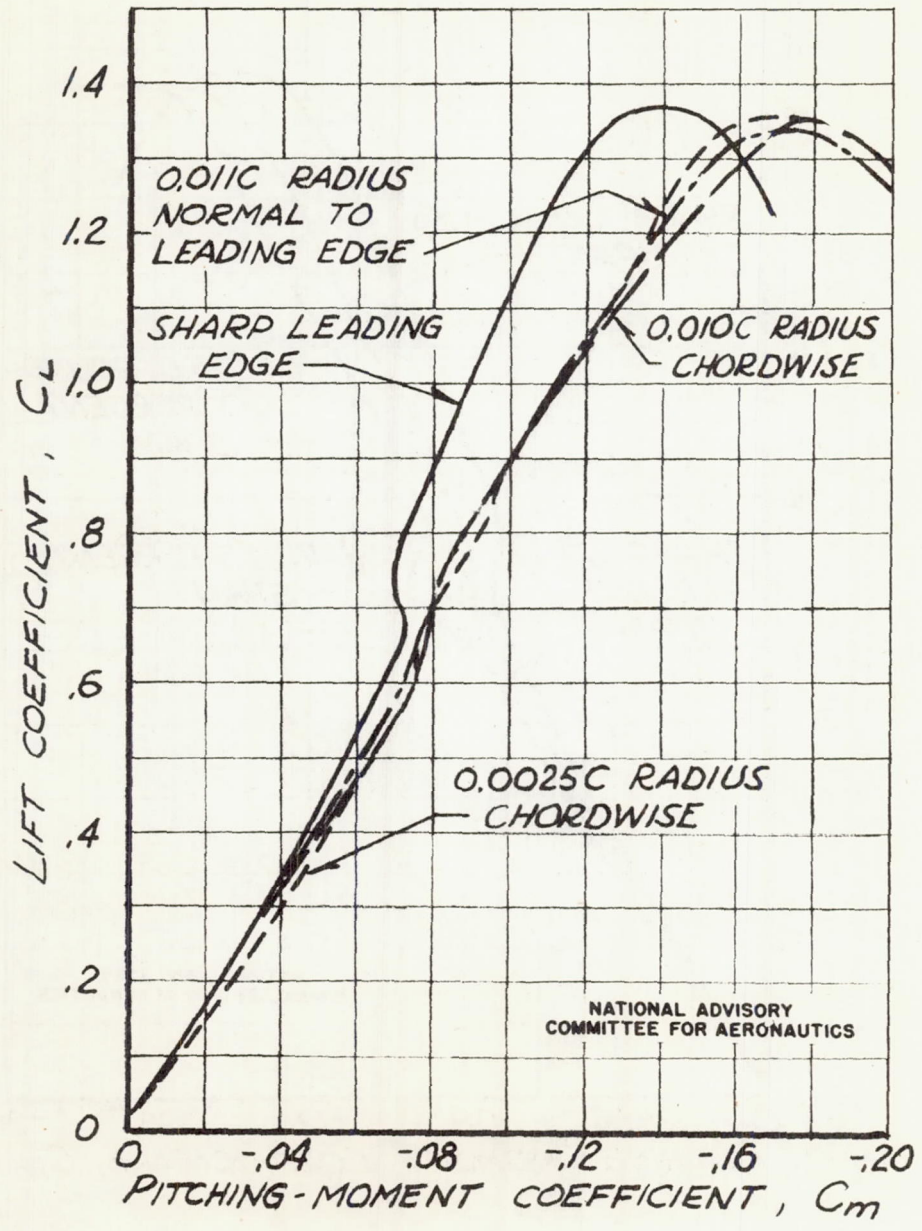
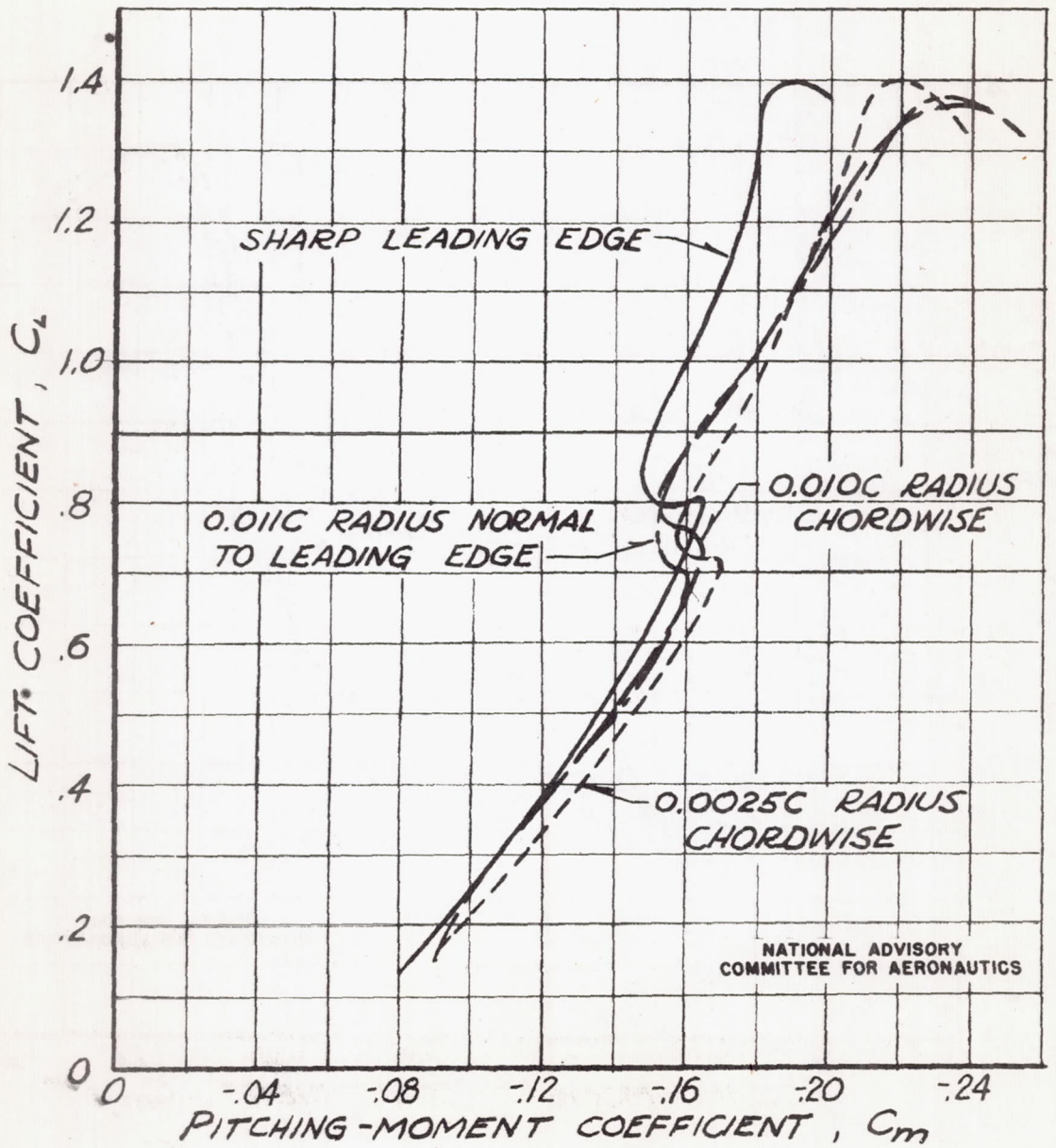


FIGURE 16.- EFFECT OF SPANWISE DISTRIBUTION OF LEADING-EDGE SHARPNESS ON PITCHING-MOMENT CHARACTERISTICS.



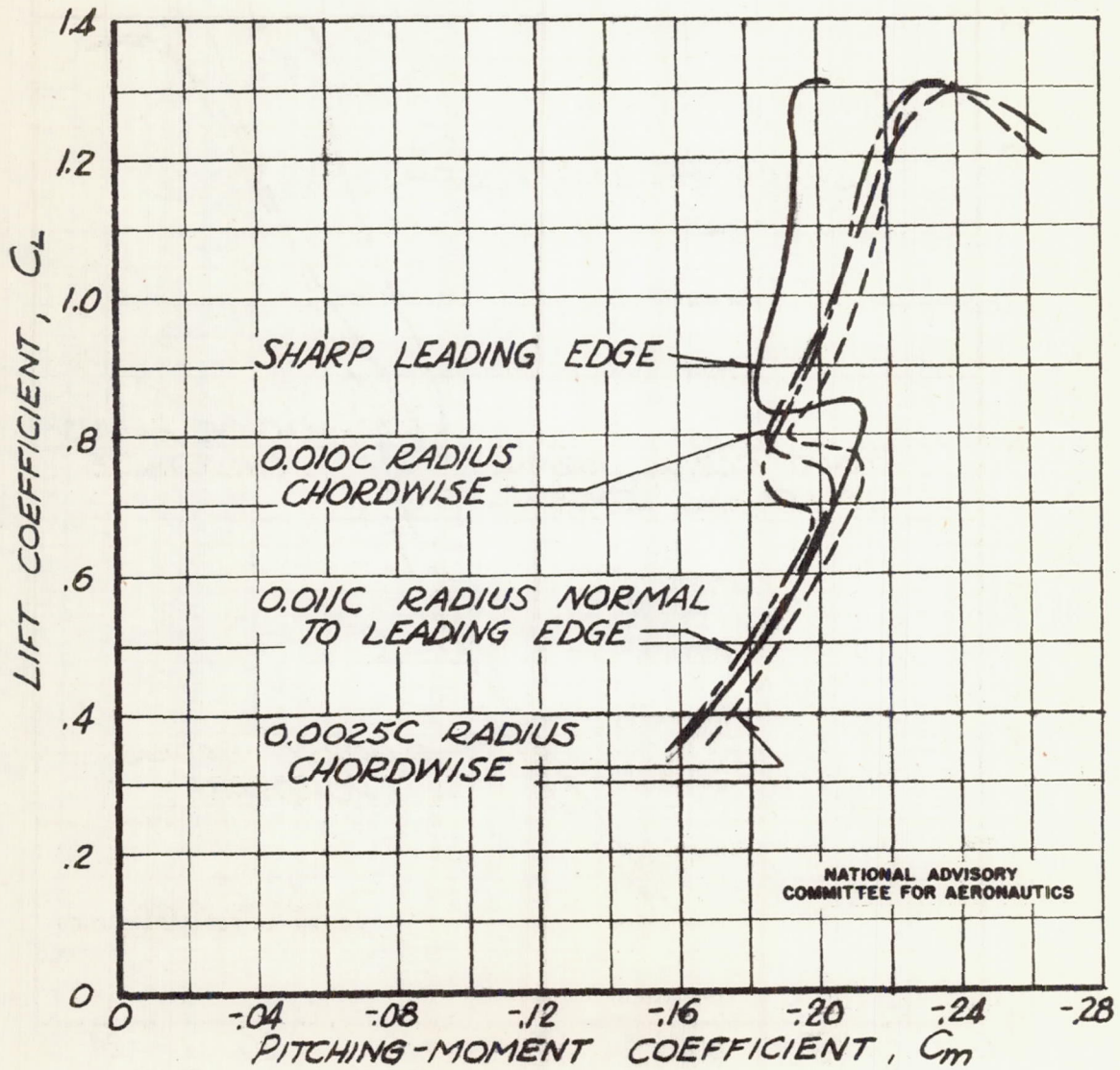
(a) $\delta_f = 0°$

FIGURE 17.- EFFECT OF LEADING-EDGE RADIUS ON PITCHING-MOMENT CHARACTERISTIC.



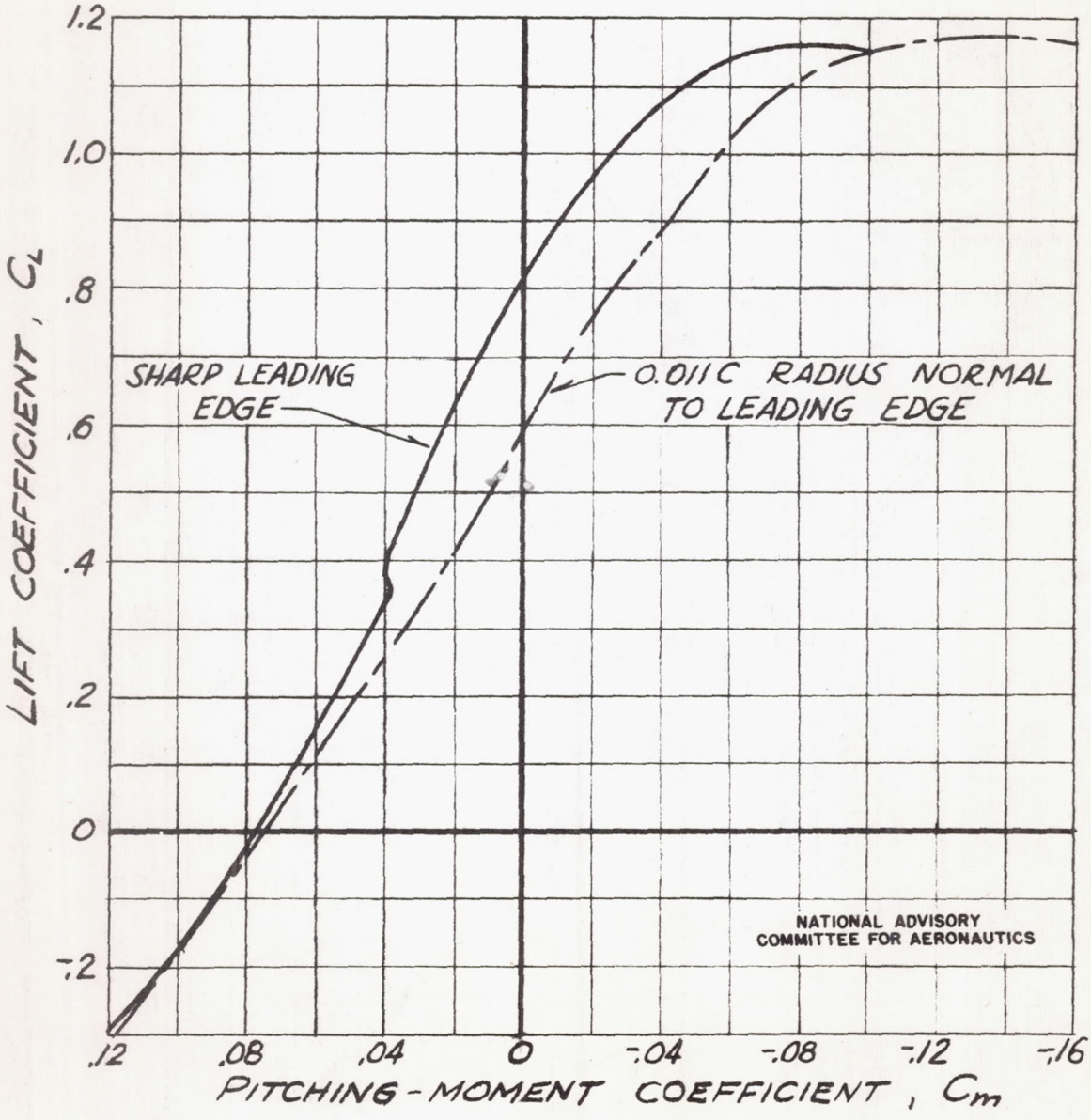
(b) $\delta_f = 22.0°$

FIGURE 17.- CONTINUED.



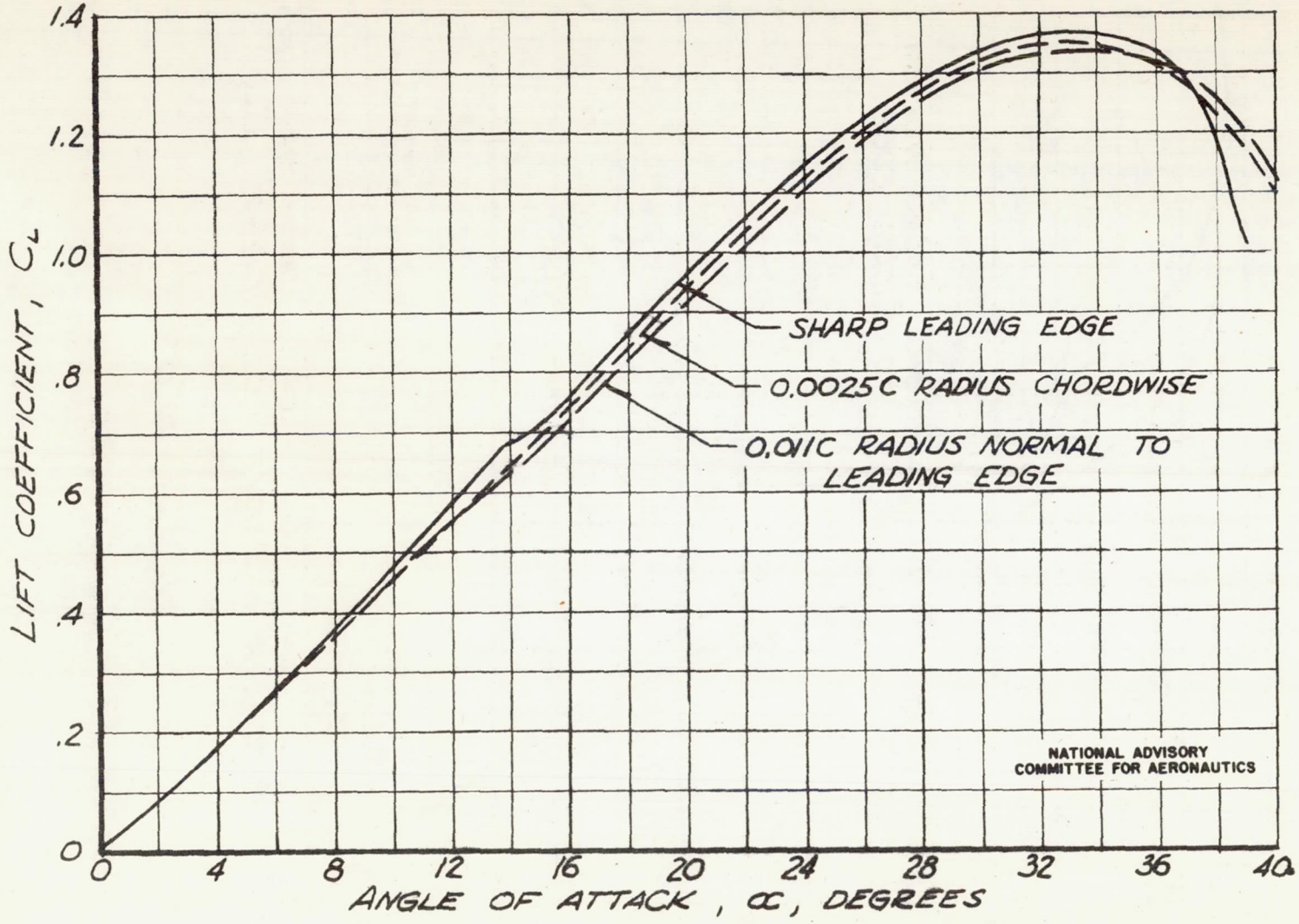
(c) $\delta_f = 44.5°$

FIGURE 17.- CONTINUED.



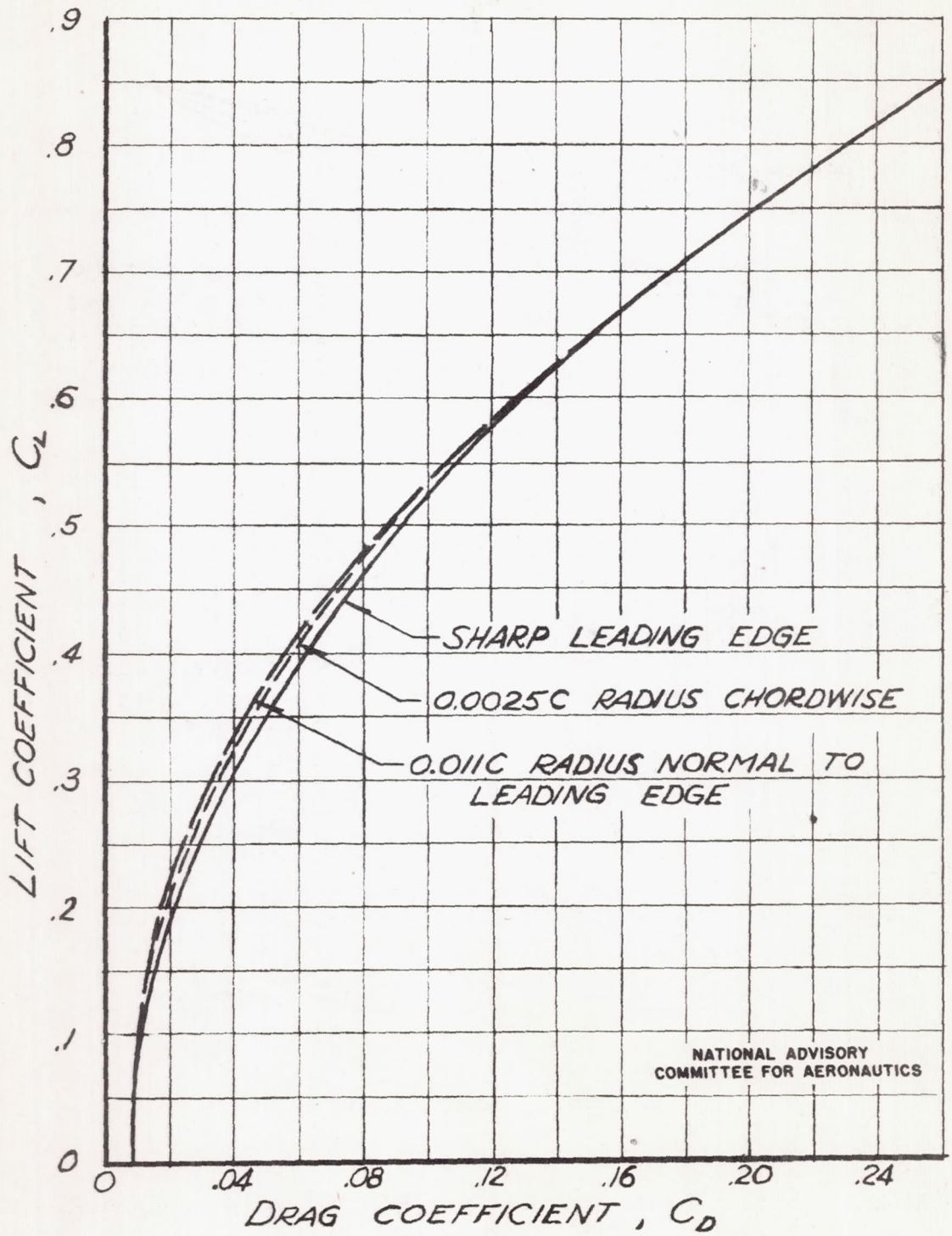
(d) $\delta_f = -22.0°$

FIGURE 17.- CONCLUDED.



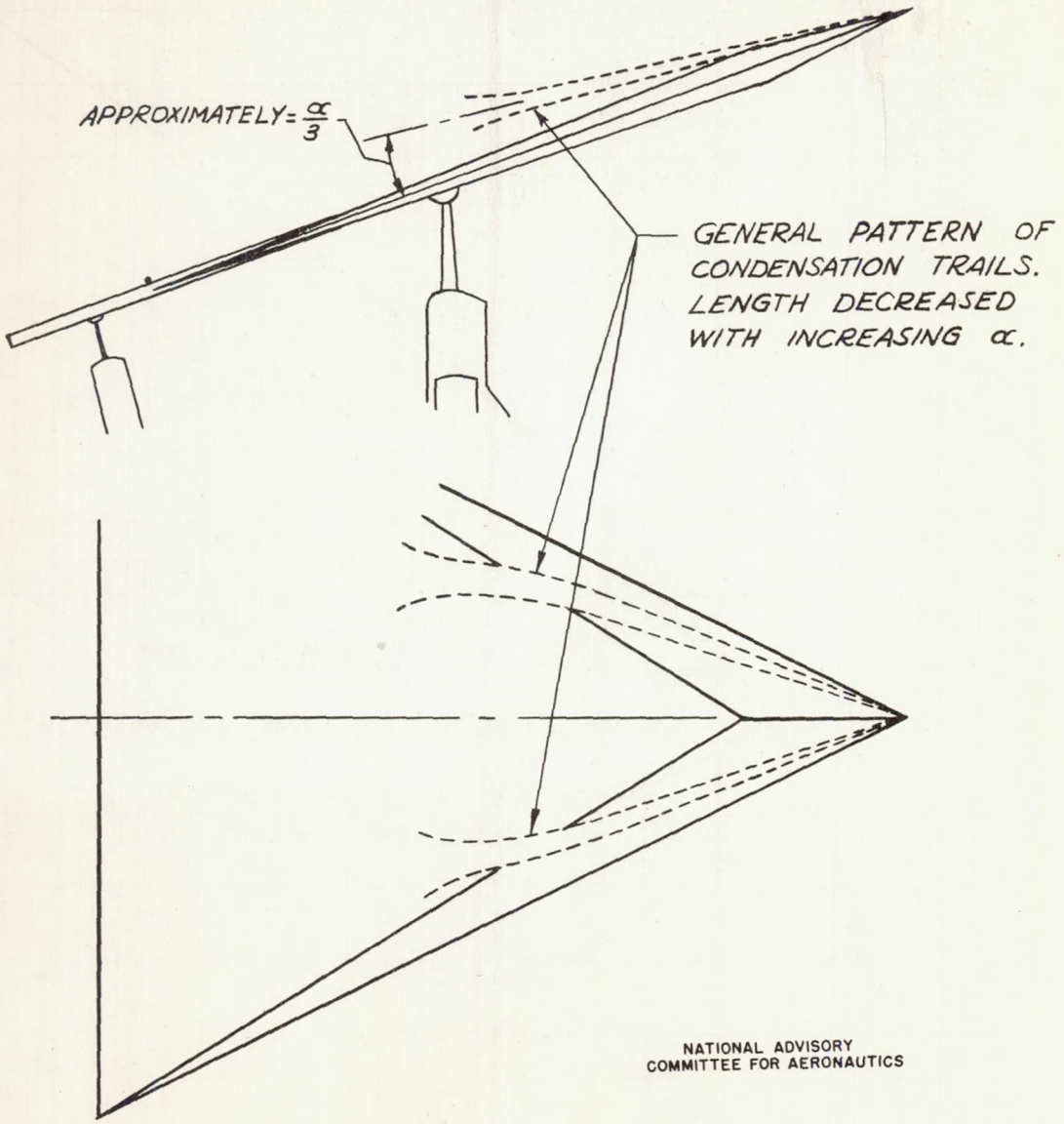
(a) C_L vs α

FIGURE 18.- EFFECT OF LEADING-EDGE RADIUS ON FORCE CHARACTERISTICS.



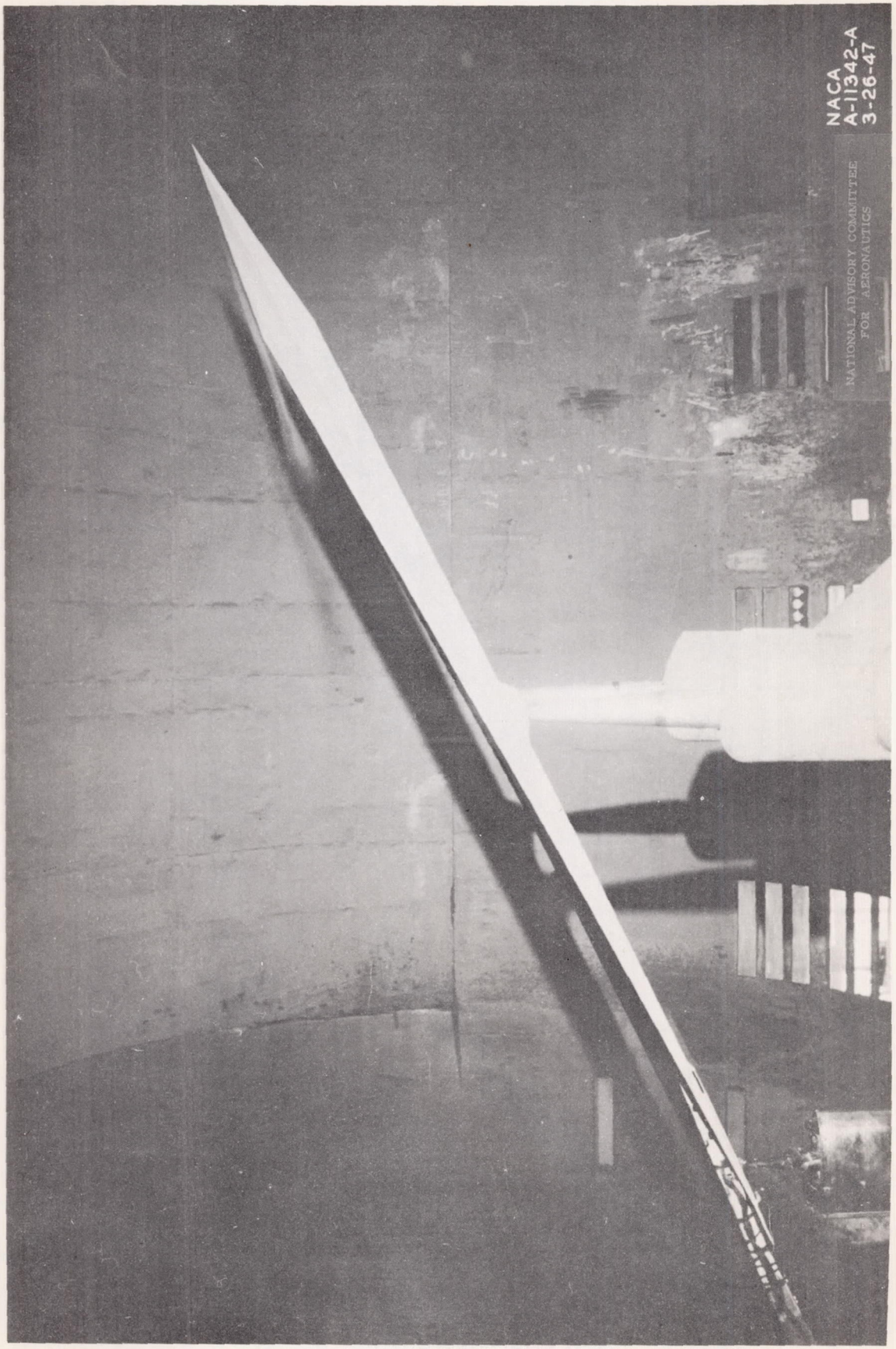
(b) C_L vs C_D

FIGURE 18.- CONCLUDED.



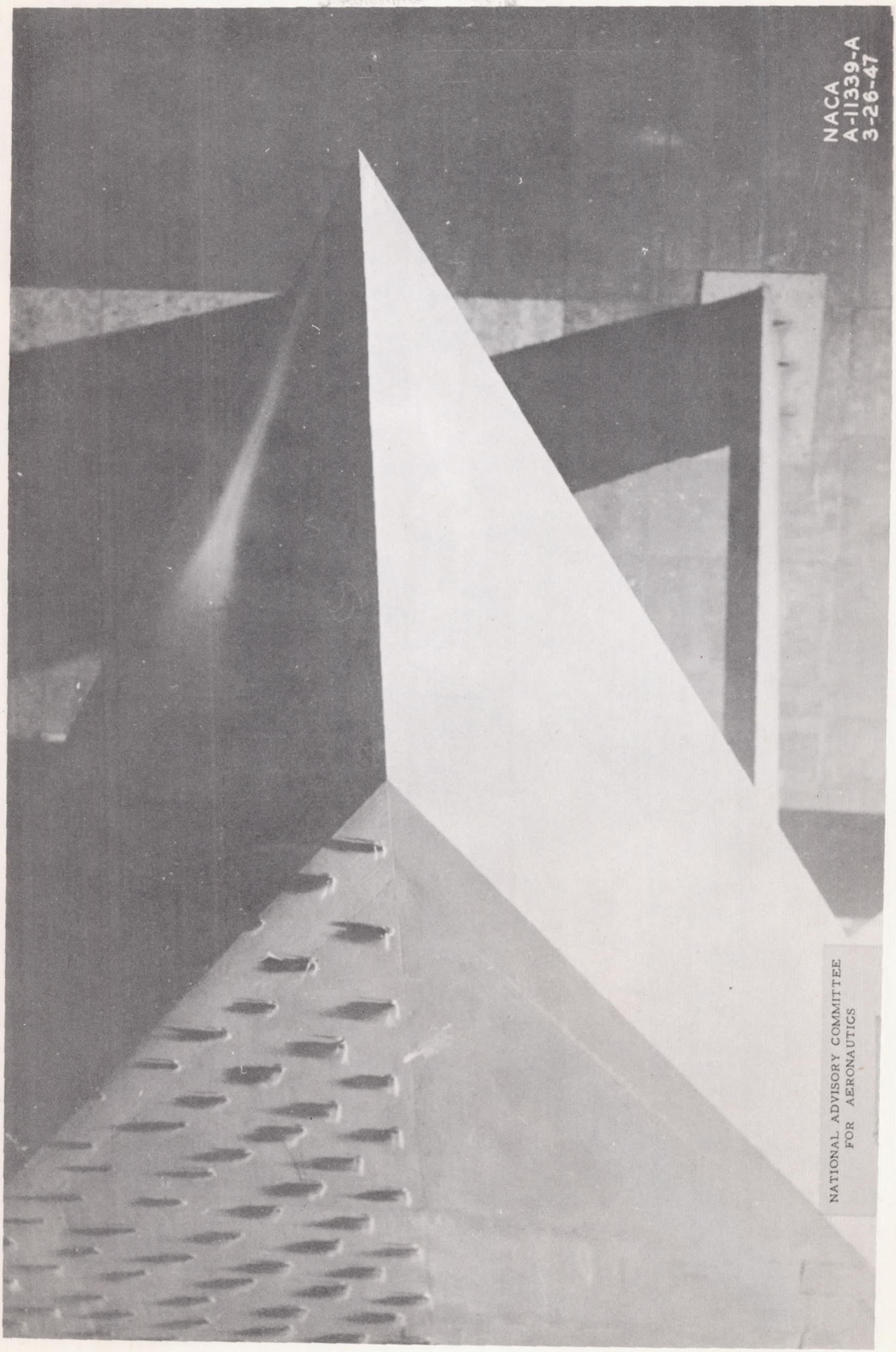
(a) General pattern.

Figure 19.- Visual study of the vortices forming at the apex of the triangular wing.



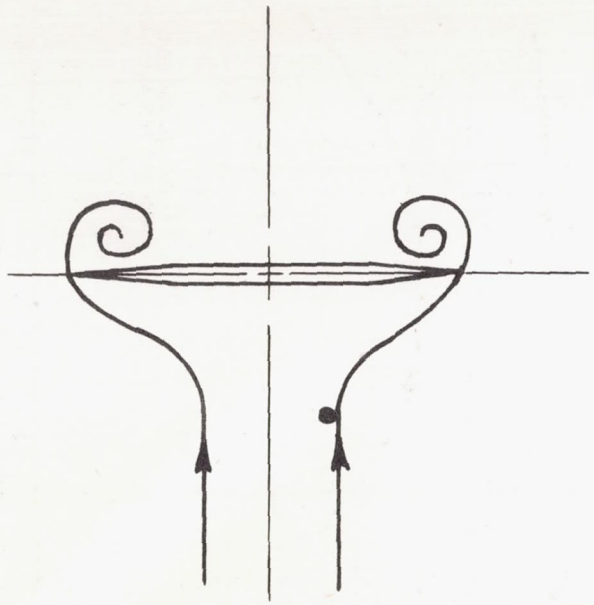
(b) $\alpha = 26.9^{\circ}$.

Figure 19.- Continued.



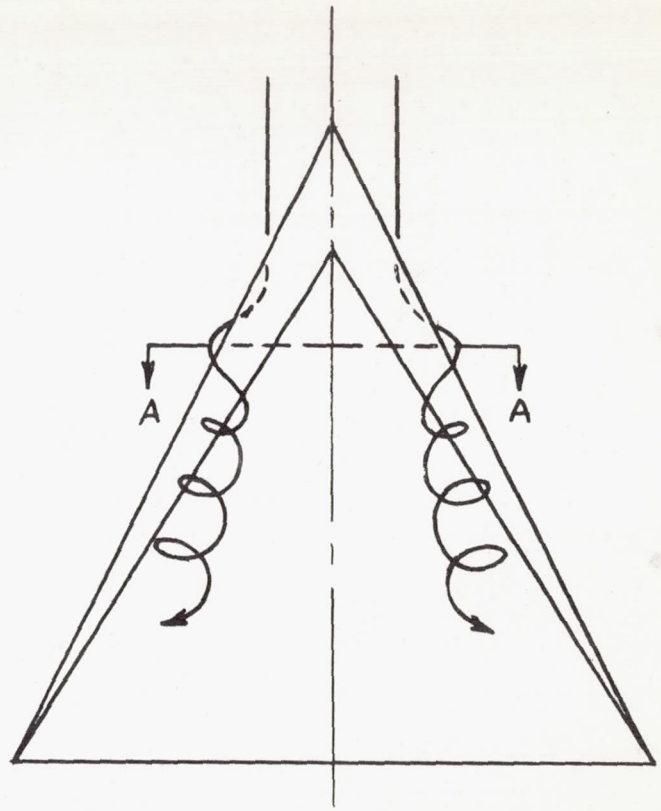
(c) $\alpha = 34.0^{\circ}$.

Figure 19.- Continued.



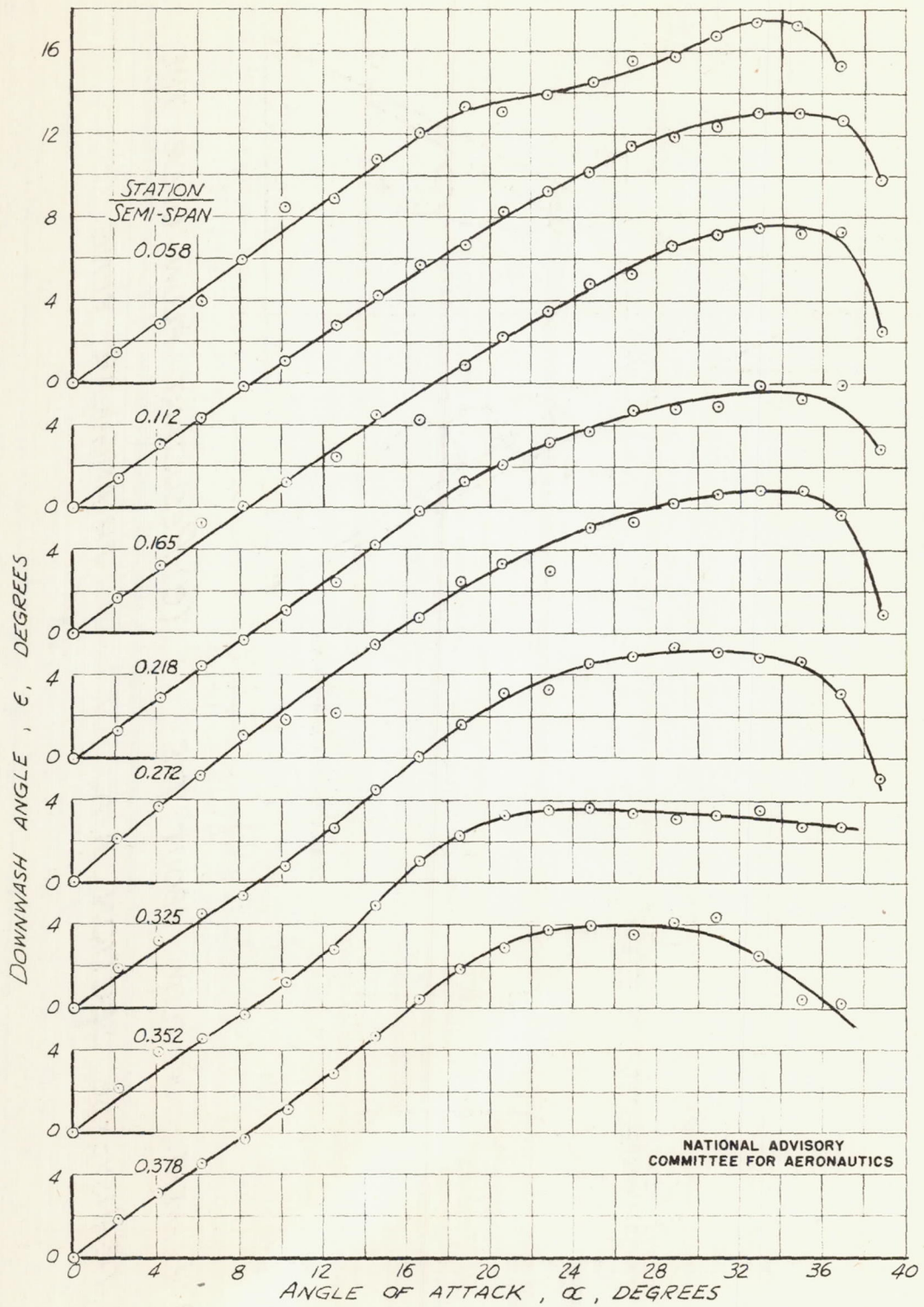
NATIONAL ADVISORY
COMMITTEE FOR AERONAUTICS

(d) Elements of flow about the transverse section A-A.



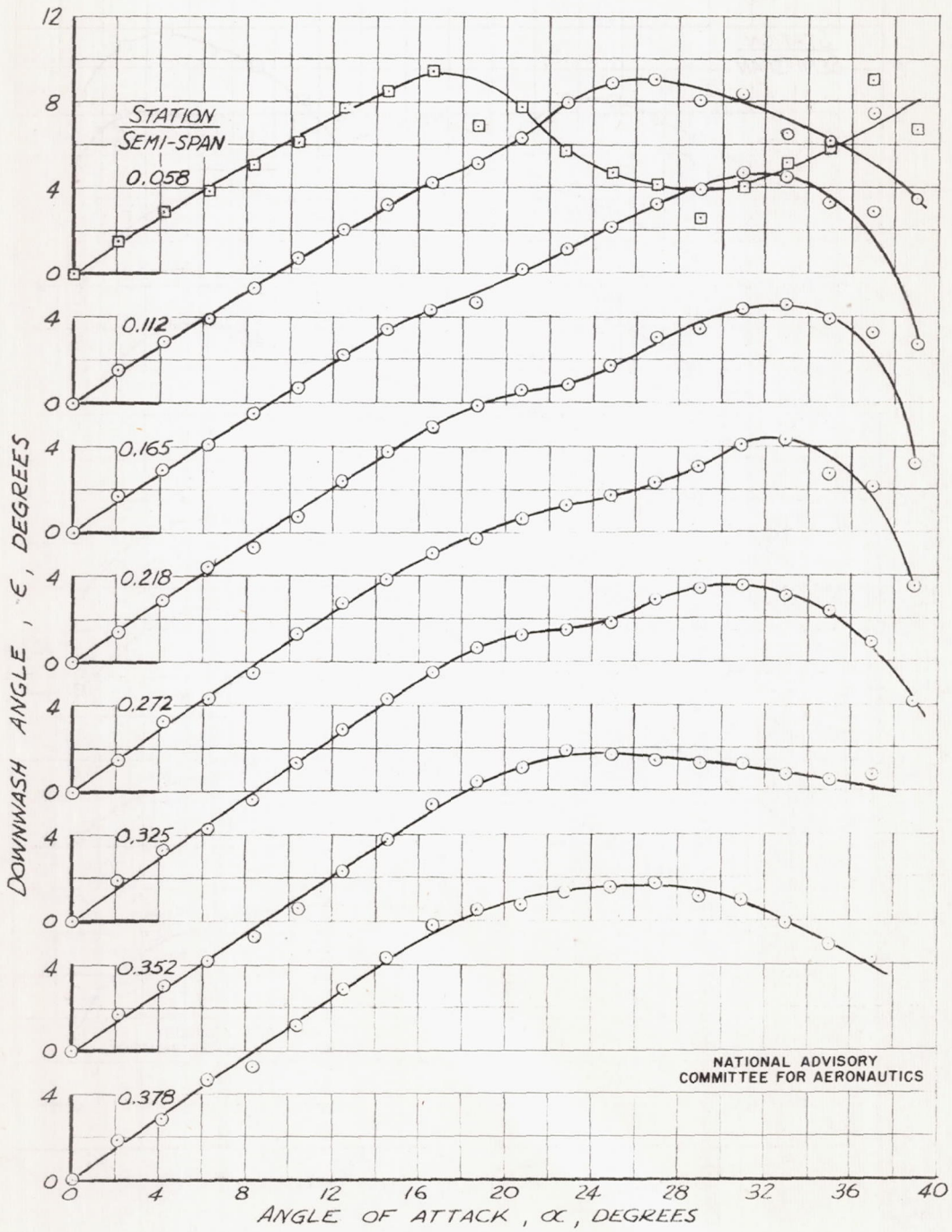
(e) Resultant flow over the triangular wing.

Figure 19.- Concluded.



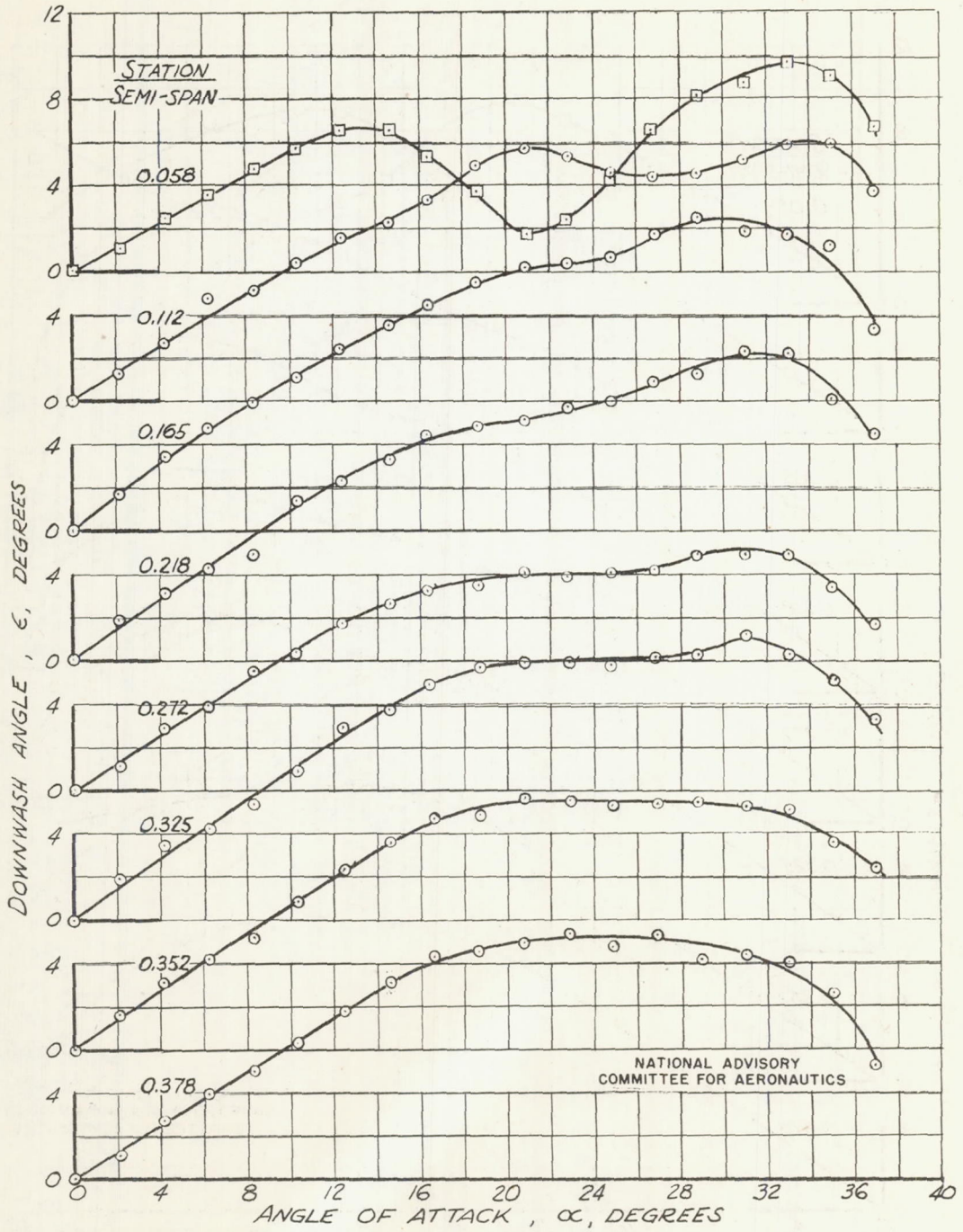
(a) 0.48 M.A.C. BEHIND WING , $\delta_f = 0°$

FIGURE 20.- VARIATION OF DOWNWASH ANGLE WITH ANGLE OF ATTACK FOR TRIANGULAR PLAN FORM WING WITH SYMMETRICAL DOUBLE-WEDGE AIRFOIL SECTION.



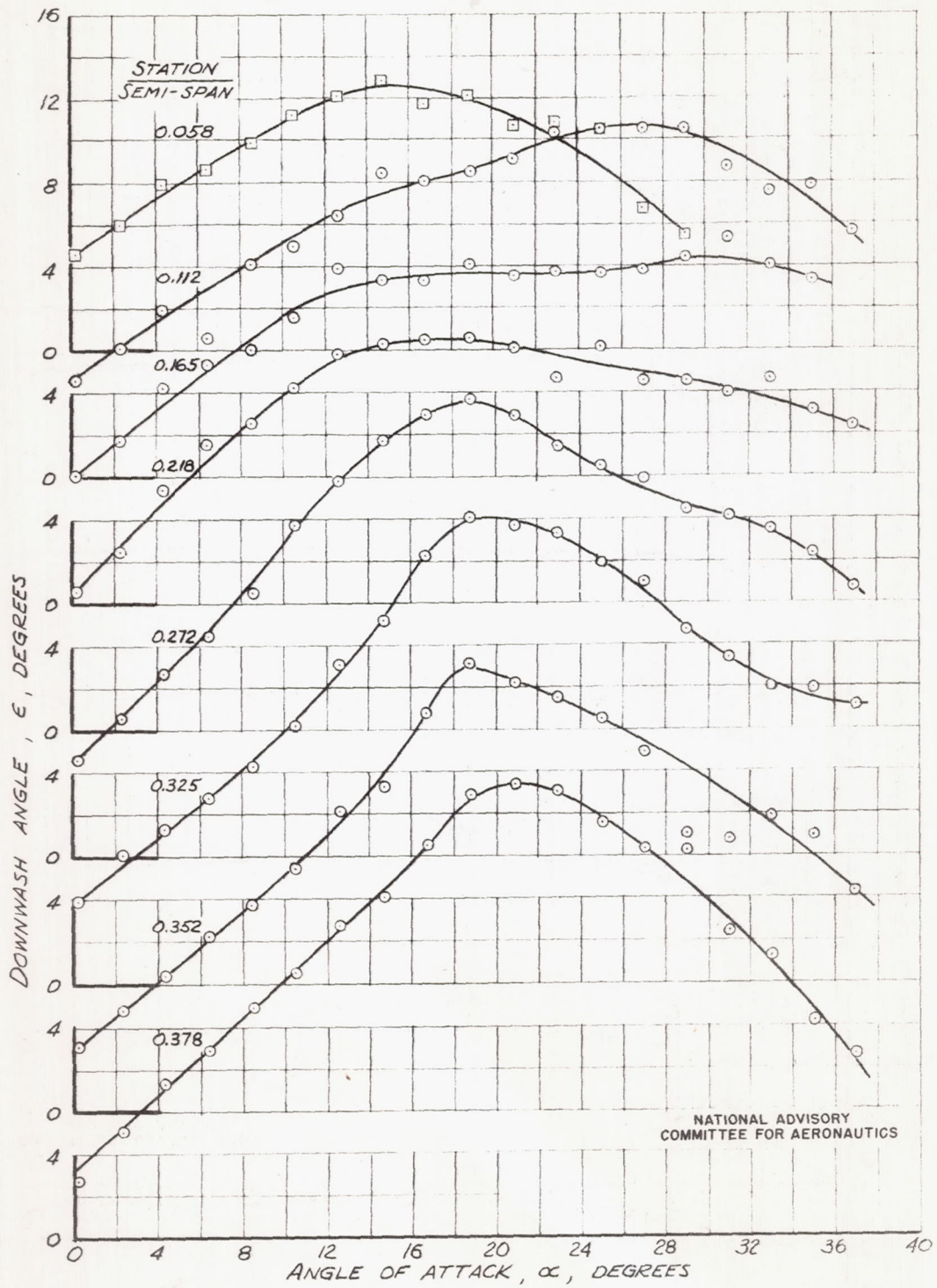
(b) 0.72 M.A.C. BEHIND WING , $\delta_f = 0°$

FIGURE 20. - CONTINUED.



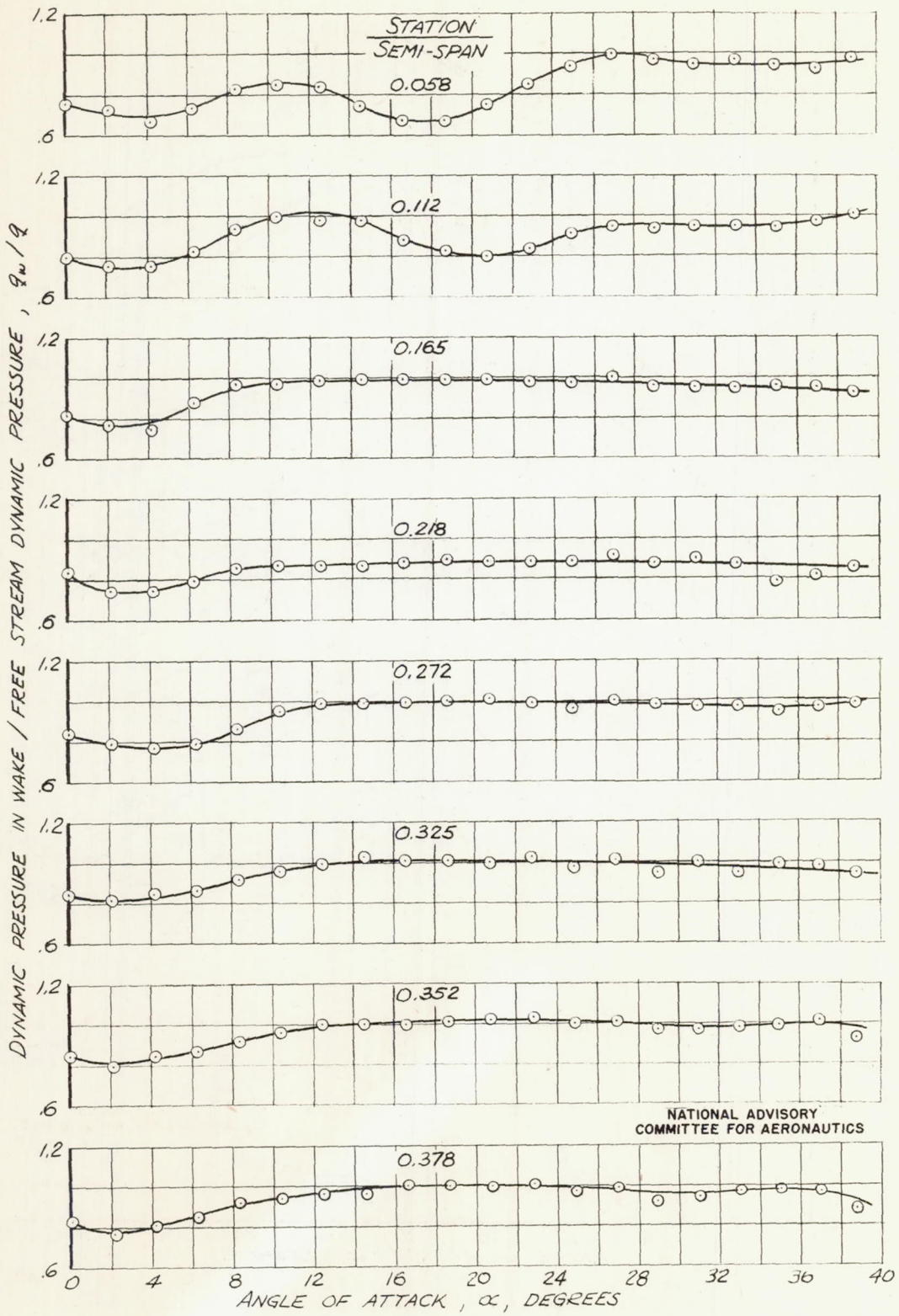
(c) 0.96 M.A.C. BEHIND WING , $\delta_f = 0°$

FIGURE 20. - CONTINUED.



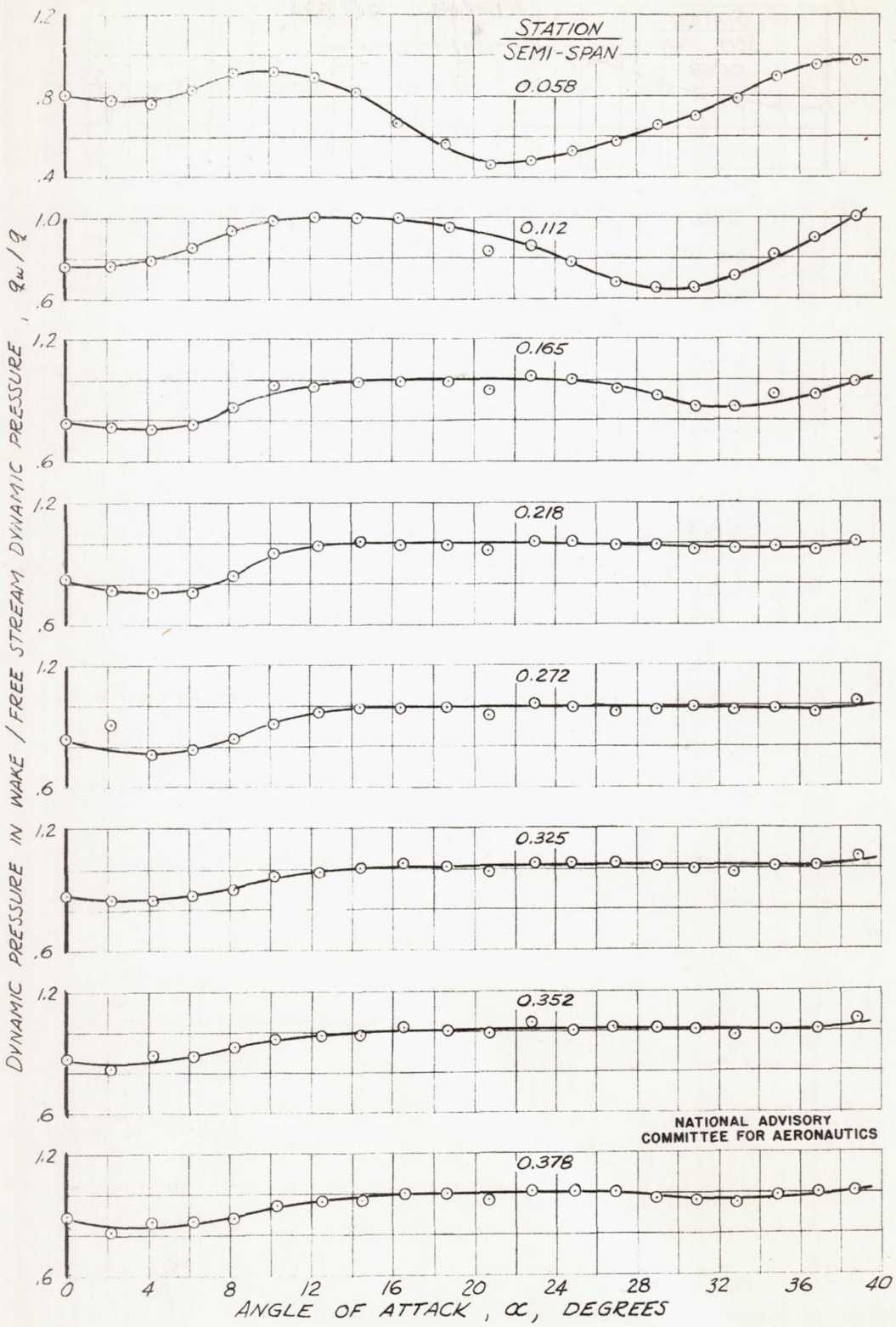
(d) 0.72 M.A.C. BEHIND WING , $\delta_f = 22.0°$

FIGURE 20. - CONCLUDED.



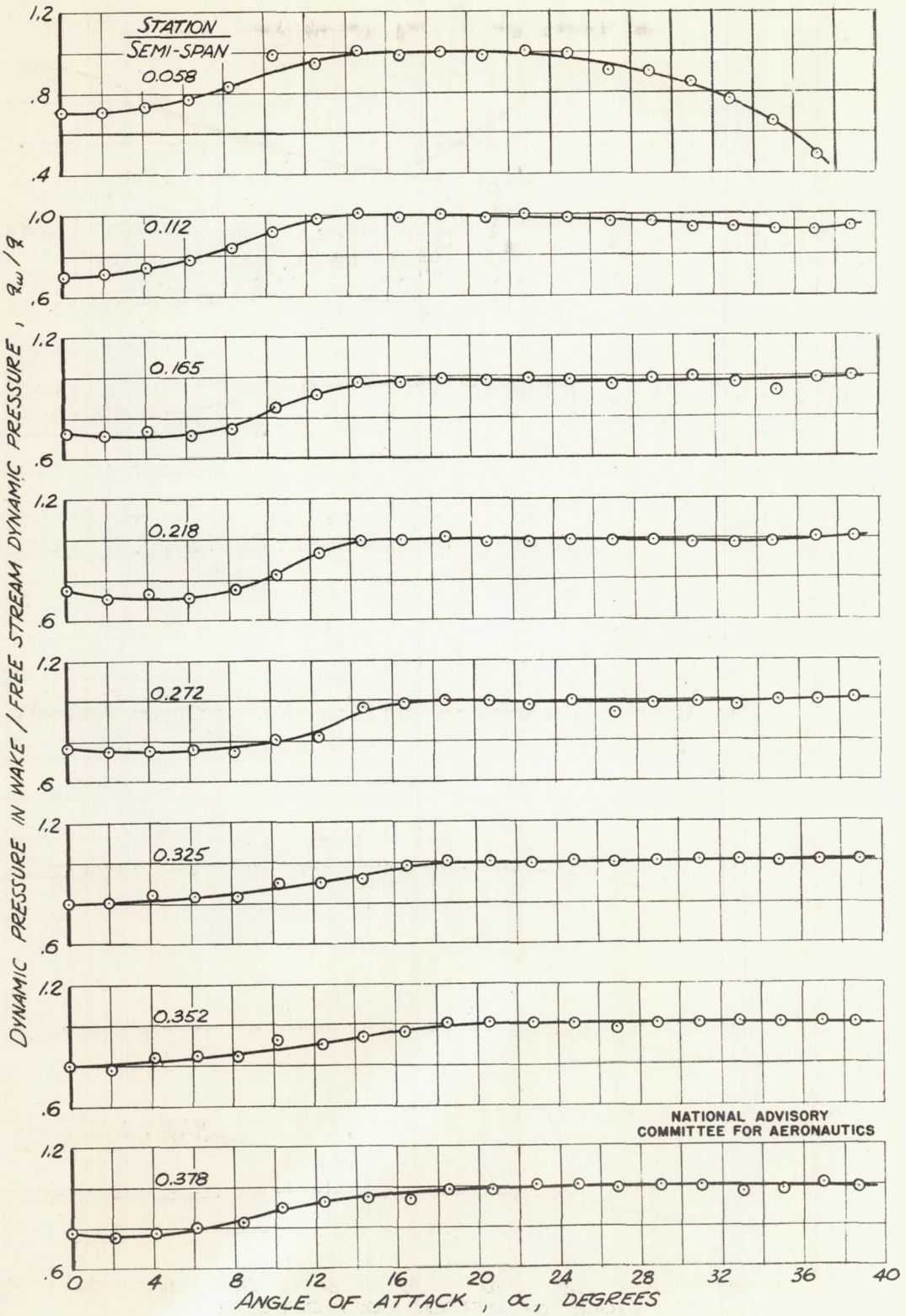
(a) 0.48 M.A.C. BEHIND WING, $\delta_f = 0°$

FIGURE 21.- DYNAMIC PRESSURE IN THE WAKE OF A TRIANGULAR PLAN FORM WING WITH SYMMETRICAL DOUBLE-WEDGE AIRFOIL SECTION.



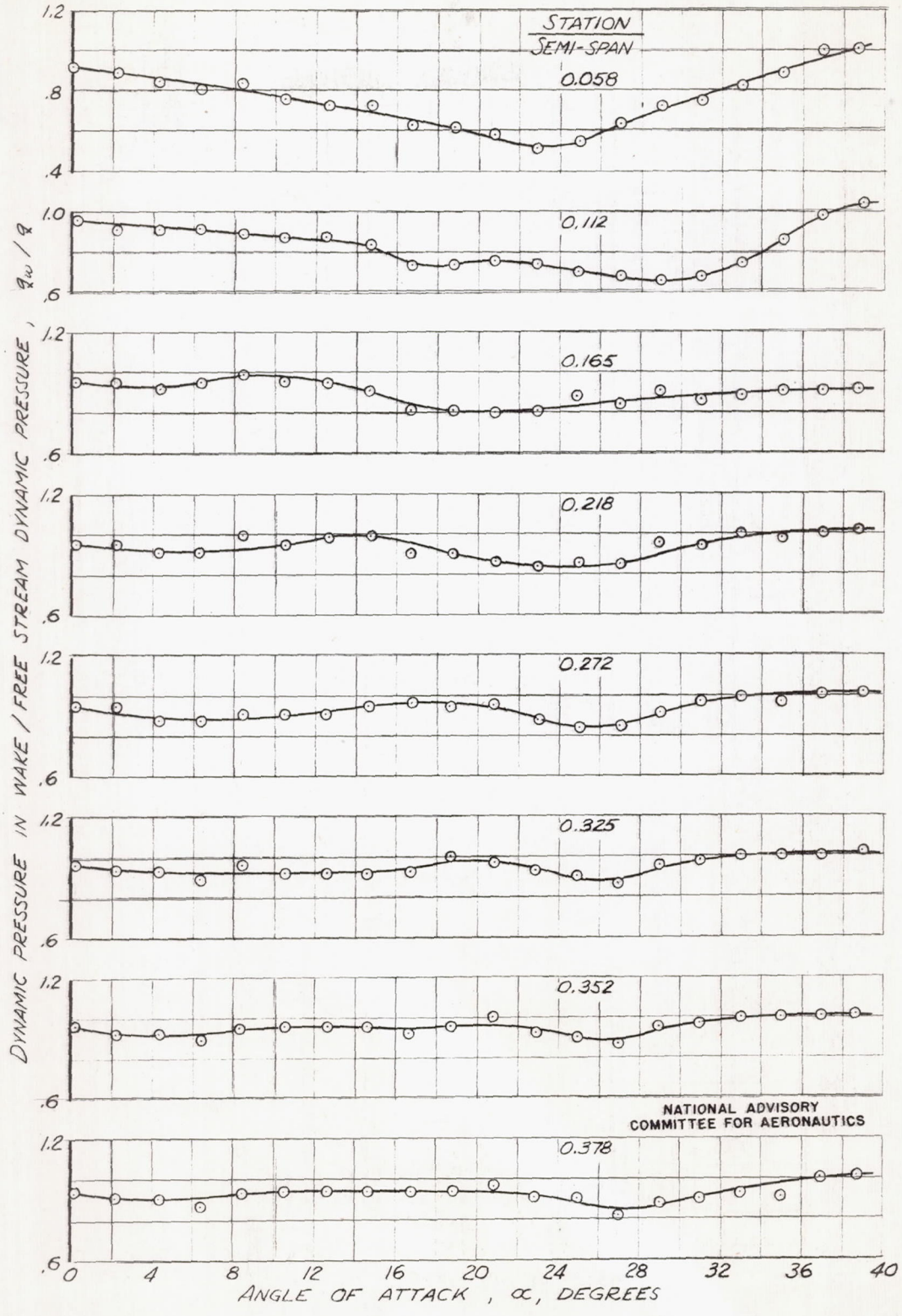
(b) 0.72 M.A.C. BEHIND WING, $\delta_f = 0°$.

FIGURE 21. - CONTINUED.



(c) 0.96 M.A.C. BEHIND WING, $\delta_f = 0°$

FIGURE 21 - CONTINUED.



(d) 0.72 M.A.C. BEHIND WING, $\delta_f = 22.0°$.

FIGURE 21.- CONCLUDED.

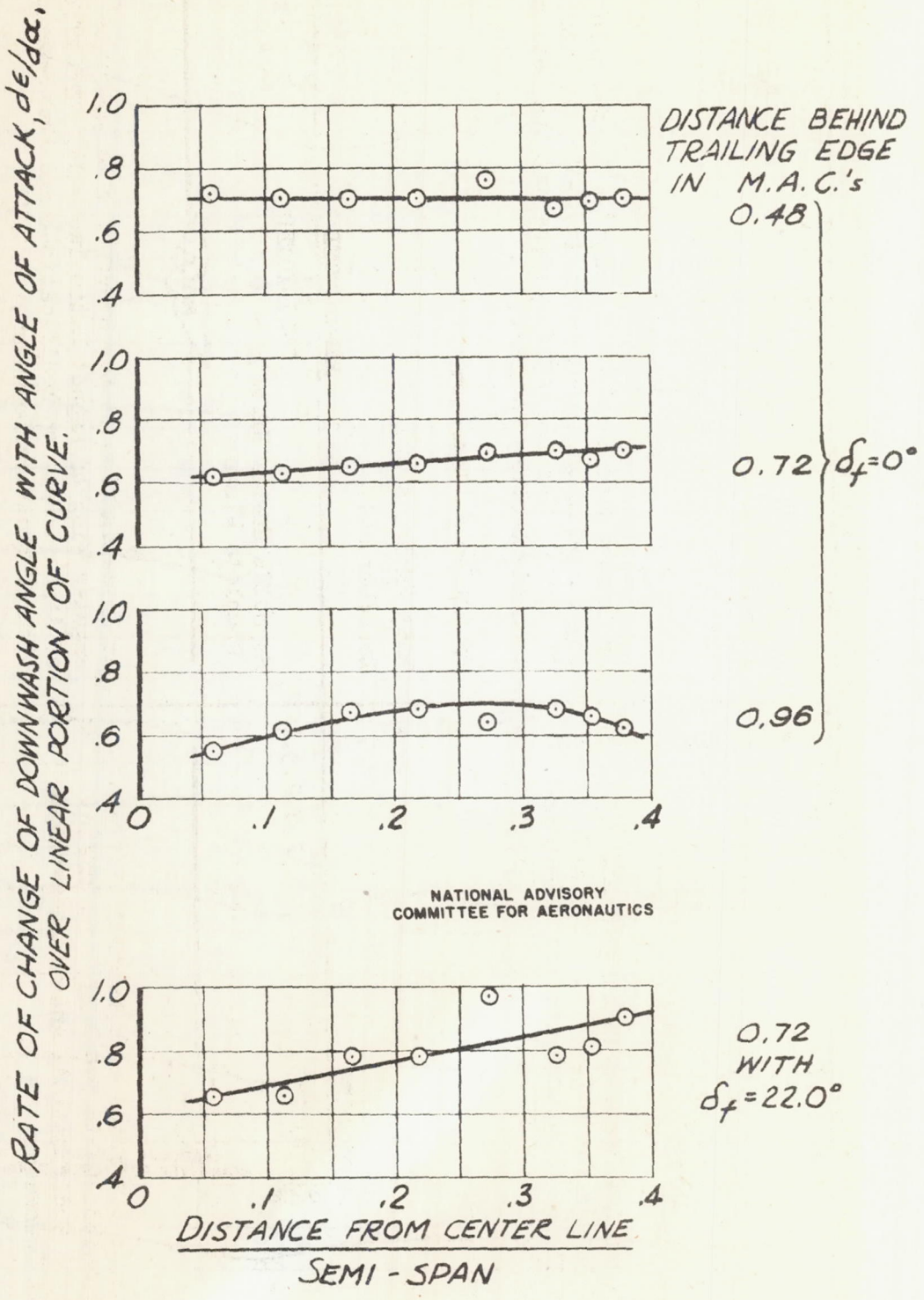


FIGURE 22.- RATE OF CHANGE OF DOWNWASH ANGLE WITH ANGLE OF ATTACK ALONG THE SPAN. VALUES OBTAINED FROM CURVES OF FIGURE 20.